

RECEIVED: September 19, 2019

REVISED: April 2, 2020

ACCEPTED: May 11, 2020

PUBLISHED: June 4, 2020

Search for squarks and gluinos in final states with same-sign leptons and jets using 139 fb^{-1} of data collected with the ATLAS detector



The ATLAS collaboration

E-mail: atlas.publications@cern.ch

ABSTRACT: A search for supersymmetric partners of gluons and quarks is presented, involving signatures with jets and either two isolated leptons (electrons or muons) with the same electric charge, or at least three isolated leptons. A data sample of proton-proton collisions at $\sqrt{s} = 13 \text{ TeV}$ recorded with the ATLAS detector at the Large Hadron Collider between 2015 and 2018, corresponding to a total integrated luminosity of 139 fb^{-1} , is used for the search. No significant excess over the Standard Model expectation is observed. The results are interpreted in simplified supersymmetric models featuring both R -parity conservation and R -parity violation, raising the exclusion limits beyond those of previous ATLAS searches to 1600 GeV for gluino masses and 750 GeV for bottom and top squark masses in these scenarios.

KEYWORDS: Hadron-Hadron scattering (experiments), Supersymmetry

ARXIV EPRINT: [1909.08457](https://arxiv.org/abs/1909.08457)

Contents

| | | |
|----------|---|-----------|
| 1 | Introduction | 1 |
| 2 | ATLAS detector | 3 |
| 3 | Event reconstruction | 3 |
| 4 | Event selection | 5 |
| 5 | Standard Model backgrounds | 7 |
| 6 | Backgrounds with non-prompt, fake or charge-flip leptons | 11 |
| 7 | Results | 15 |
| 8 | Exclusion limits on SUSY scenarios | 18 |
| 9 | Conclusion | 20 |
| | The ATLAS collaboration | 27 |

1 Introduction

Experimental searches for manifestations of physics beyond the Standard Model (BSM physics) at hadron colliders have long exploited the signature of final states comprising a pair of isolated light leptons (electrons, muons) with the same electric charge (‘same-sign leptons’). In the Standard Model (SM), production of prompt same-sign lepton pairs from weak-boson decays is rare. In the context of $\sqrt{s} = 13$ TeV pp collisions, the inclusive cross-section is of the order of 1 pb [1, 2], thus suppressed by more than three orders of magnitude relative to the production of opposite-sign lepton pairs. By contrast, in many scenarios heavy BSM particles, which may be produced in proton-proton (pp) collisions, decay into multiple massive SM bosons or top quarks. The subsequent decays of these heavy SM particles into same-sign leptons and jets may then occur with significant branching ratios. Pair production of heavy BSM Majorana fermions can be another abundant source of events with same-sign leptons [3].

At the Large Hadron Collider (LHC) [4], signatures with same-sign prompt leptons have been used by the ATLAS [5] and CMS [6] experiments to explore the landscape of possible SM extensions and their phenomenology. Among these proposed extensions, supersymmetry (SUSY) [7–12] stands out as a particularly compelling framework. It was shown [13–16] to favourably impact the scale evolution of perturbative gauge couplings needed for the unification of strong and electroweak interactions, and can address the SM

gauge hierarchy problem. In its minimal realisation, the MSSM [17, 18], each fundamental SM fermion is associated with a pair of new scalar partners — in the case of quarks q , the squarks \tilde{q}_L and \tilde{q}_R . Similarly, each SM bosonic degree of freedom is partnered with a new fermion. Mixing between the partners of SM electroweak and Higgs bosons¹ results in four massive Majorana fermions and two massive charged fermions (neutralinos $\tilde{\chi}_1^0$ to $\tilde{\chi}_4^0$ and charginos $\tilde{\chi}_1^\pm$ and $\tilde{\chi}_2^\pm$, indexed by increasing mass). The gluinos \tilde{g} , partners of the SM gluons, do not mix due to their colour charge.

SUSY can provide a massive dark-matter candidate [19, 20], the lightest supersymmetric particle (LSP), if an additional ad hoc discrete symmetry, called R -parity [21], is invoked. When this symmetry is conserved, supersymmetric partners can only be produced in pairs and decay into the LSP and SM particles, possibly in several steps via superpartners of intermediate masses. The LSP, stable and weakly interacting, escapes the detector, leaving a striking experimental signature of large missing transverse momentum. When R -parity is not conserved, the final states contain only SM particles; decay channels for squarks include e.g. $\tilde{q}_i \rightarrow q_j q_k$ or $\tilde{q}_i \rightarrow q_j \ell_k$, if the corresponding coupling strengths [22] λ''_{ijk} or λ'_{ijk} are non-zero.

Naturalness arguments [23, 24] suggest that the top squark mass may not exceed ≈ 1 TeV [25, 26]. Significant mixing between the scalar top partners \tilde{t}_L and \tilde{t}_R , enhanced relative to other quark flavours, can also lower the mass of the lightest eigenstate \tilde{t}_1 below that of other squarks. These constraints indirectly affect gluinos and bottom squark masses as well. Gluinos and third-generation squarks may therefore be among the superpartners with low mass and copiously produced at the LHC. Typical pair-production cross-sections [27] for interesting scenarios in the context of this paper are 9 fb for a 1.6 TeV gluino mass, or 33 fb for the lightest top \tilde{t}_1 or bottom \tilde{b}_1 squark mass of 800 GeV.

This paper presents a search for gluinos and squarks in final states with two same-sign leptons and jets. The events may include additional leptons. In addition, large missing transverse momentum is required in the case of R -parity-conserving models. The event selection also relies on the number of b -tagged jets. Signal regions (SRs) are built (section 4) from a set of requirements on the kinematic properties of the selected events, in order to isolate the signature of supersymmetric processes from SM backgrounds. The latter are estimated with Monte Carlo simulation for processes such as $t\bar{t}V$ or VV ($V = W, Z$) leading to prompt same-sign leptons (section 5), while sources of same-sign leptons arising from jets misidentified as leptons or non-prompt leptons from decays of hadrons, as well as other reducible backgrounds, are estimated with data (section 6). Event yields in data are then compared with the estimated contributions from SM processes. The results are presented in section 7 for 139 fb^{-1} of 13 TeV pp collision data recorded by the ATLAS experiment. They are interpreted in terms of exclusion limits (section 8) on the parameters of four benchmark supersymmetric signal scenarios, which are shown in figure 1.

A similar, earlier analysis, realised on a subset of the data for these results, was reported in ref. [28] and found no deviation from SM expectations. Searches based on these event topologies were also performed in the same context with the CMS experiment with the same outcome [29, 30].

¹The Higgs sector is also enriched by the presence of an additional complex doublet.

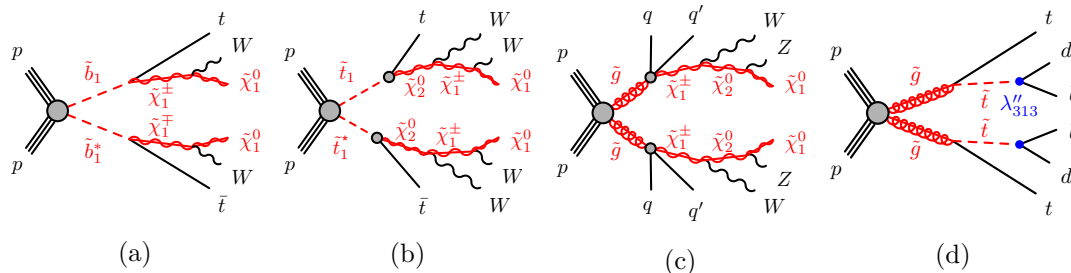


Figure 1. Examples of processes allowed in the MSSM, involving the pair production and cascade decays of squarks and gluinos into final states with leptons and jets.

2 ATLAS detector

The ATLAS experiment [5] at the LHC is a multipurpose particle detector with a forward-backward symmetric cylindrical geometry and a near 4π coverage in solid angle.² It consists of an inner tracking detector (ID) surrounded by a thin superconducting solenoid providing a 2 T axial magnetic field, electromagnetic (EM) and hadron calorimeters, and a muon spectrometer (MS). The ID covers the pseudorapidity range $|\eta| < 2.5$. It consists of silicon pixel, silicon microstrip, and transition radiation tracking detectors, completed by the insertable B-layer (IBL) installed before Run 2 [31, 32]. Lead/liquid-argon (LAr) sampling calorimeters provide EM energy measurements with high granularity. A steel/scintillator-tile hadron calorimeter covers the central pseudorapidity range $|\eta| < 1.7$. The endcap and forward regions are instrumented with LAr calorimeters for EM and hadronic energy measurements up to $|\eta| = 4.9$. The MS surrounds the calorimeters and is based on three large air-core toroidal superconducting magnets with eight coils each. The field integral of the toroids ranges between 2.0 and 6.0 T·m across most of the detector. The MS includes a system of precision tracking chambers and fast detectors for triggering. A two-level trigger system [33] is used to select events. The first-level trigger is implemented in hardware and uses a subset of the detector information to reduce the accepted rate to at most 100 kHz. This is followed by a software-based trigger that reduces the accepted event rate to 1 kHz on average depending on the data-taking conditions.

3 Event reconstruction

The analysis is performed on a set of pp collision data recorded by the ATLAS detector between 2015 and 2018. In this period, the LHC delivered colliding beams with a peak instantaneous luminosity up to $L = 2.1 \times 10^{34} \text{ cm}^{-2}\text{s}^{-1}$ achieved in 2018, and an average

²ATLAS uses a right-handed coordinate system with its origin at the nominal interaction point (IP) in the centre of the detector and the z -axis along the beam pipe. The x -axis points from the IP to the centre of the LHC ring, and the y -axis points upwards. Cylindrical coordinates r, ϕ are used in the transverse plane, ϕ being the azimuthal angle around the z -axis. The pseudorapidity is defined in terms of the polar angle θ as $\eta = -\ln \tan(\theta/2)$. The rapidity is defined relative to the beam axis as a function of the velocity β : $y = 0.5 \times \ln\{(1 + \beta \cos \theta)/(1 - \beta \cos \theta)\}$. The magnitude of the momentum in the plane transverse to the beam axis is denoted by p_T .

number of pp interactions per bunch crossing (‘pile-up’) of 33.7. After requirements on the stability of the beams, the operational status of all ATLAS detector components, and the quality of the recorded data, the total integrated luminosity of the dataset corresponds to 139 fb^{-1} with an uncertainty of 1.7%. It is obtained [34] using the LUCID-2 detector [35] for the primary luminosity measurements.

Proton-proton interaction vertices are reconstructed from charged-particle tracks in the ID with $p_{\text{T}} > 500\text{ MeV}$ [36, 37]. The presence of at least one such vertex with a minimum of two associated tracks is required, and the primary vertex is chosen as the vertex with the largest sum of p_{T}^2 of associated tracks.

The anti- k_t algorithm [38] with radius parameter $R = 0.4$ implemented in the **FastJet** library [39] is used to reconstruct jets up to $|\eta| = 4.9$, relying on topological energy clusters in the calorimeter [40] at the EM scale. Jets are then calibrated as described in ref. [41]. Only jets with $p_{\text{T}} > 20\text{ GeV}$ are further considered. Events are vetoed when containing jets induced by calorimeter noise or non-collision background, according to criteria similar to those described in ref. [42]. As decay products of heavy particles tend to be more central, this analysis only considers jets with $|\eta| < 2.8$ in multiplicity-based requirements. An additional discriminant referred to as the **Jet Vertex Tagger (JVT)** is used to exclude jets produced in pile-up processes [43], based on classifying the tracks associated with the jet as pointing or not pointing to the primary vertex.

Jets containing b -flavoured hadrons are identified in the region $|\eta| < 2.5$ by the MV2c10 b -tagging algorithm [44], which makes use of the impact parameters of tracks associated with the candidate jet, the position of reconstructed secondary vertices and their consistency with the decay chains of such hadrons. For the working point chosen for this analysis, such jets are tagged with an efficiency of 70% in simulated $t\bar{t}$ events, with mis-tag rates of 9% and 0.3% for jets initiated by charm quarks or light quarks/gluons, respectively.

Baseline muon candidates are reconstructed [45] in the region $|\eta| < 2.5$ from MS tracks matching ID tracks. The analysis only considers muons with $p_{\text{T}} > 10\text{ GeV}$ satisfying the set of requirements on the quality of the tracks which is defined as **Medium** in ref. [45]. The longitudinal impact parameter z_0 of the muon track must satisfy $|z_0 \sin \theta| < 0.5\text{ mm}$. Signal muons are defined as the baseline candidates sufficiently distant from jets (see below) and other leptons, which satisfy further requirements: the transverse impact parameter d_0 of the track must be sufficiently small relative to its uncertainty from the track reconstruction, $|d_0| < 3\sigma(d_0)$, and the candidate must satisfy a track-based isolation criterion. The latter requires the summed scalar p_{T} of nearby ID tracks not to exceed 6% of the muon p_{T} , for selected tracks in a p_{T} -dependent $\Delta R_{\eta} = \sqrt{(\Delta\eta)^2 + (\Delta\phi)^2}$ cone of maximal size 0.3 around the muon, excluding its own track, similarly to the isolation variables defined in ref. [45]; these tracks must be associated with the primary vertex to limit sensitivity to pile-up.

Baseline electron candidates are reconstructed [46] from energy depositions in the EM calorimeter matched to an ID track and are required to have $p_{\text{T}} > 10\text{ GeV}$ and $|\eta| < 2.47$, excluding the transition region $1.37 < |\eta| < 1.52$ between the barrel and endcap EM calorimeters. They must satisfy the **LooseAndBLayerLLH** identification discriminant defined in ref. [46], as well as requirements on the track impact parameters $|z_0 \sin \theta| < 0.5\text{ mm}$ and $|d_0| < 5\sigma(d_0)$. Signal electrons, which must be distant from jets and other leptons, are

required to satisfy the tighter **MediumLLH** identification and **FCTight** isolation requirements defined in ref. [46]. The latter are similar to the muon isolation requirement, with a maximal cone size of 0.2, but with an additional calorimeter-based isolation requirement using nearby topological clusters instead of tracks. Only signal electrons with $|\eta| < 2.0$ are considered in order to reduce the rate of electrons with wrongly reconstructed charge (‘charge-flip’); the latter are further rejected by the application of the **ECIDS** discriminant described in ref. [46], which exploits further information related to the electron track reconstruction and its compatibility with the primary vertex and the electron cluster.

The missing transverse momentum (whose magnitude is denoted E_T^{miss}) is defined as the negative vector sum of the transverse momenta of all identified objects (baseline electrons, photons [46], baseline muons and jets) and an additional soft term. The soft term is constructed from all tracks associated with the primary vertex but not with any physics object. In this way, the E_T^{miss} is adjusted for the best calibration of the jets and the other identified physics objects listed above, while maintaining approximate pile-up independence in the soft term [47, 48]. Overlaps between objects in the E_T^{miss} calculation are resolved as described in ref. [47].

To exclude non-prompt leptons produced inside jets, baseline leptons close to jets are discarded according to the angular distance $\Delta R = \sqrt{(\Delta y)^2 + (\Delta\phi)^2}$ between the two reconstructed objects. A requirement of $\Delta R > \min\{0.4, 0.1 + 9.6 \text{ GeV}/p_T(\ell)\}$ is used.

4 Event selection

Events are selected if they contain at least two signal leptons with $p_T > 20 \text{ GeV}$. In addition, there must be at least one pair of leptons with identical electric charges among the ensemble of signal leptons with $p_T > 10 \text{ GeV}$.

Data events were recorded via a combination of triggers based on the presence of missing transverse momentum or pairs of leptons [49–52]. For events with $E_T^{\text{miss}} < 250 \text{ GeV}$, only lepton-based triggers without isolation requirements are used, with lepton p_T thresholds which vary over the data collected in Run 2 up to a maximum of 24 GeV for triggers requiring two electrons, 22 GeV for the leading- p_T muon in triggers requiring two muons, and 17 GeV (14 GeV) for the electron (muon) in mixed dilepton triggers. For events with $E_T^{\text{miss}} > 250 \text{ GeV}$, triggers based on E_T^{miss} are also used. For events that are only accepted by lepton triggers with p_T requirements above 20 GeV, the analysis-level lepton p_T requirement is raised to be 1 GeV above the trigger threshold. This results in a relative reduction of the total fiducial acceptance by at most 2% for the benchmark signal scenarios of figure 1. For signal events selected in the SRs presented below, the trigger efficiency is above 95% for R -parity-conserving models, and above 93% otherwise. For signal events with $E_T^{\text{miss}} > 250 \text{ GeV}$, the trigger efficiency is above 99%.

Five SRs are built to isolate signatures of hypothetical supersymmetric signal processes from backgrounds; their definitions are summarised in table 1. They rely on the multiplicities of different reconstructed objects such as the number of leptons n_ℓ and their relative electric charges, the number of jets n_j with $p_T > 25$ or 40 GeV, and the number of b -tagged jets n_b with $p_T > 20 \text{ GeV}$. Several kinematic variables are also used: the effective

| SR | n_ℓ | n_b | n_j | E_T^{miss} [GeV] | m_{eff} [GeV] | $E_T^{\text{miss}}/m_{\text{eff}}$ | SUSY |
|-----------|---|----------|--|---------------------------|------------------------|------------------------------------|--|
| Rpv2L | ≥ 2 ($\ell^\pm \ell^\pm$) | ≥ 0 | ≥ 6 ($p_T > 40$ GeV) | – | > 2600 | – | $\tilde{g} \rightarrow t\tilde{t}_1^*, \tilde{t}_1^* \rightarrow qq'$ ($\lambda'' \neq 0$) $\tilde{g} \rightarrow t\tilde{t}\tilde{\chi}_1^0, \tilde{\chi}_1^0 \rightarrow 3q$ ($\lambda'' \neq 0$) $\tilde{g} \rightarrow q\tilde{q}\tilde{\chi}_1^0, \tilde{\chi}_1^0 \rightarrow qq'\ell$ ($\lambda' \neq 0$) |
| Rpc2L0b | ≥ 2 ($\ell^\pm \ell^\pm$) | $= 0$ | ≥ 6 ($p_T > 40$ GeV) | > 200 | > 1000 | > 0.2 | $\tilde{g} \rightarrow q\tilde{q}'WZ\tilde{\chi}_1^0$ |
| Rpc2L1b | ≥ 2 ($\ell^\pm \ell^\pm$) | ≥ 1 | ≥ 6 ($p_T > 40$ GeV) | – | – | > 0.25 | $\tilde{b}_1 \rightarrow tW\tilde{\chi}_1^0$ |
| Rpc2L2b | ≥ 2 ($\ell^\pm \ell^\pm$) | ≥ 2 | ≥ 6 ($p_T > 25$ GeV) | > 300 | > 1400 | > 0.14 | $\tilde{b}_1 \rightarrow tW\tilde{\chi}_1^0$ $\tilde{g} \rightarrow t\tilde{t}\tilde{\chi}_1^0$ |
| Rpc3LSS1b | ≥ 3 ($\ell^\pm \ell^\pm \ell^\pm$) | ≥ 1 | no cut but veto $81 \text{ GeV} < m_{e^\pm e^\pm} < 101 \text{ GeV}$ | | | > 0.14 | $\tilde{t}_1 \rightarrow tW^\pm(W^*)\tilde{\chi}_1^0$ |

Table 1. Definition of the signal regions used by the analysis, based on the variables defined in section 4. The last column provides examples of SUSY processes which may contribute to these signal regions.

mass m_{eff} consisting of the scalar p_T sum of all jets and leptons added to E_T^{miss} , the E_T^{miss} itself and its ratio to m_{eff} , and the invariant mass of same-sign electron pairs, $m_{e^\pm e^\pm}$. The latter helps to reduce the backgrounds featuring a $Z \rightarrow e^+e^-$ decay where the charge of one electron is mismeasured. The SR requirements were chosen loosely so as to provide sensitivity to non-excluded regions of the parameter space for the processes illustrated in figure 1, while preserving sensitivity to other SUSY processes with possibly different final states, as in table 1.

The SR Rpv2L targets gluino pair production in R -parity-violating scenarios, hence without any E_T^{miss} requirement. It is inclusive in terms of b -tagged jets to be sensitive to various decay modes of gluinos leading to final states with leptons and jets, such as the scenario illustrated in figure 1(d) or the few other examples mentioned in table 1. In this SR, a tight requirement on the effective mass $m_{\text{eff}} > 2.6 \text{ TeV}$ is used to reduce SM backgrounds.

The SR Rpc2L0b provides sensitivity to R -parity-conserving scenarios not involving third-generation squarks, as in figure 1(c), which are less likely to contain bottom quarks in the final state. A veto on b -tagged jets is imposed in order to reduce SM backgrounds with top quarks. Requiring a large number of jets strongly reduces the level of WZ and other multiboson backgrounds.

The SRs Rpc2L1b and Rpc2L2b provide sensitivity to scenarios involving third-generation squarks, such as $\tilde{b}_1 \rightarrow t\tilde{\chi}_1^-$ with a subsequent $\tilde{\chi}_1^\pm \rightarrow W^\pm\tilde{\chi}_1^0$ decay as in figure 1(a). Rpc2L2b uses tighter requirements on E_T^{miss} and m_{eff} than Rpc2L1b in order to complement it at low $\tilde{\chi}_1^0$ mass, as well as to provide good sensitivity to scenarios with heavier superpartners such as pair-produced gluinos decaying via $\tilde{g} \rightarrow t\tilde{t}\tilde{\chi}_1^0$.

Finally, the SR Rpc3LSS1b probes scenarios with long decay chains but compressed mass spectra leading to final states with softer decay products, such as the $\tilde{t}_1 \rightarrow t\tilde{\chi}_2^0 \rightarrow tW(W^*)\tilde{\chi}_1^0$ cascade decay shown in figure 1(b) and proposed in ref. [53]. This SR selects events with at least three leptons of identical charge, leading to a huge reduction of the expected SM background yields. Loose requirements on the $E_T^{\text{miss}}/m_{\text{eff}}$ ratio and the presence of at least one b -tagged jet, as well as the rejection of events containing any pair of

| Physics process | Event generator | Computation order | Parton shower | Cross-section normalisation | PDF set | Set of tuned parameters |
|---|-----------------------|---------------------------|-----------------------|-----------------------------|--------------------|-------------------------|
| $t\bar{t}W$ [55] | MG5_aMC@NLO 2.3.3 [1] | NLO | PYTHIA 8.210 [56] | NLO [57] | NNPDF2.3LO [58] | A14 [59] |
| $t\bar{t}Z/\gamma^*$ [55] | MG5_aMC@NLO 2.3.3 [1] | NLO | PYTHIA 8.210-212 [56] | NLO [57] | NNPDF2.3LO [58] | A14 [59] |
| $t\bar{t}WW$ | MG5_aMC@NLO 2.2.2 [1] | LO | PYTHIA 8.186 [60] | NLO [1] | NNPDF2.3LO [58] | A14 [59] |
| $t\bar{t}WZ$ | MG5_aMC@NLO 2.2.2 [1] | LO | PYTHIA 8.212 [56] | NLO [1] | NNPDF2.3LO [58] | A14 [59] |
| tWZ, tZ | MG5_aMC@NLO 2.3.3 [1] | LO | PYTHIA 8.212 [56] | NLO [1] | NNPDF2.3LO [58] | A14 [59] |
| $t\bar{t}H$ [55] | POWHEG 2 [61, 62] | NLO | PYTHIA 8.230 [56] | NLO [57] | NNPDF2.3LO [58] | A14 [59] |
| $3t, 4t$ | MG5_aMC@NLO 2.2.2 [1] | LO | PYTHIA 8.186 [60] | NLO [1] | NNPDF2.3LO [58] | A14 [59] |
| $pp \rightarrow 4\ell, 3\ell\nu$ [63] | SHERPA 2.2.2 [64] | NLO (0-1j) + LO (2-3j) | SHERPA | NLO | NNPDF3.0NNLO [65] | SHERPA |
| $gg \rightarrow 4\ell$ [63] | SHERPA 2.2.2 [64] | LO (0-1j) | SHERPA | NLO | NNPDF3.0 NNLO [65] | SHERPA |
| $pp \rightarrow (2\ell 2\nu/3\ell\nu/4\ell)jj$ [54, 63] | SHERPA 2.2.2 [64] | LO | SHERPA | LO | NNPDF3.0NNLO [65] | SHERPA |
| WH, ZH | PYTHIA 8.186 [60] | LO | PYTHIA | LO | NNPDF2.3LO [58] | A14 [59] |
| $VVV^{(*)}$ | SHERPA 2.2.1 [64] | LO (0-1j) | SHERPA | LO | NNPDF3.0NNLO [65] | SHERPA |
| $VVVjj$ [63] | SHERPA 2.2.2 [64] | LO (0-1j) | SHERPA | LO | NNPDF3.0NNLO [65] | SHERPA |

Table 2. List of Monte Carlo event generators and their settings used to predict the contributions from SM processes to the various regions of interest in the analysis. When no reference is provided for the cross-section normalisation, the one computed by the generator is used. The LO and NLO acronyms are defined in section 5.

same-sign electrons with $m_{e^\pm e^\pm}$ close to the Z boson mass, help to diminish the residual reducible background to low levels.

A simple cut-and-count analysis is performed in each SR. The number of events in data is reported in section 7 together with the expected contributions from SM processes and the reducible background, the estimations of which are described in the following sections.

5 Standard Model backgrounds

Major contributions from SM processes to the SRs arise from WZ +jets (with minor contributions from ZZ and $W^\pm W^\pm jj$ ³), $t\bar{t}W$ and $t\bar{t}Z$. The summed contributions of other processes involving associated production of top quarks and massive bosons, with smaller production cross-sections, can also amount to significant fractions of the expected SR event yields. SRs with at least one b -tagged jet are populated mainly by processes involving top quarks, while multiboson processes dominate in regions vetoing b -jets. In the case of the Rpc3LSS1b SR, only processes such as $WZZ, ZZZ, t\bar{t}WZ$ and $VH/t\bar{t}H$ where the Higgs boson H decays via $H \rightarrow 4\ell$ are genuine sources of events with three same-sign prompt leptons.

The contributions of these processes to the SRs are evaluated with Monte Carlo simulations to determine the fiducial acceptance of the various regions as well as the efficiencies of the detector and reconstruction software. Table 2 provides a complete list of the relevant processes considered in this analysis, the event generators used for the predictions and their settings. For the processes with the largest production cross-sections, the scattering amplitudes evaluated for the event generation rely on terms up to the next-to-leading order (NLO) in the perturbative expansion, while for other processes only leading-order

³This process corresponds to the production of two same-sign W bosons [54] which at the lowest order of the perturbative expansion are accompanied by two forward jets.

(LO) terms are accounted for. For most processes, the generated events are normalised to the inclusive cross-section computed with NLO accuracy, either taken from the references indicated in table 2, or directly from the generator. The generated events for the $t\bar{t}Z$, tZ , tWZ , VZ and VVZ processes include matrix elements for non-resonant $Z/\gamma^* \rightarrow \ell\ell$ contributions; the same is true for non-resonant $W^* \rightarrow \ell\nu$ in events from VV and VVV processes. For the **Rpc3LSS1b** SR, only contributions from processes with three same-sign prompt leptons are evaluated with Monte Carlo simulations, while the others (VV , $t\bar{t}V\dots$) are included in the estimation of the reducible background, which is described in section 6.

The generated events were processed through a detailed simulation of the ATLAS detector [66] based on GEANT4 [67]. To simulate the effects of additional pp collisions in the same and nearby bunch crossings, inelastic interactions were generated using the soft strong-interaction processes of PYTHIA 8.1.86 [56] with a set of tuned parameters referred to as the A3 tune [68] and the NNPDF23LO parton distribution function (PDF) set [58]. These inelastic interactions were overlaid onto the simulated hard-scatter events, which were then reweighted to match the pile-up conditions observed in the data. In all Monte Carlo samples, except those produced by the SHERPA event generator, the EVTGEN 1.2.0 program [69] was used to model the properties of bottom and charm hadron decays.

Simulated events are weighted by scale factors to correct for the mismodelling of inefficiencies associated with the reconstruction of leptons, the application of lepton identification and isolation requirements, the lepton-based trigger chains, and the application of pile-up rejection (JVT) and b -tagging requirements to jets that do or do not contain genuine b -flavoured hadrons.

Various sources of systematic uncertainties in the predicted event yields are accounted for. Experimental sources, evaluated for all processes, include uncertainties in the calibration of the momentum scale and resolution for jets, leptons and the soft term of the missing transverse momentum, as well as uncertainties in the various scale factors mentioned above, in the measured integrated luminosity, and in the distribution of the number of additional pp interactions per event.

Uncertainties in the theoretical modelling of each process are also considered. Uncertainties in the inclusive production cross-sections of $t\bar{t}W$, $t\bar{t}Z$ and $t\bar{t}H$ are taken as 12%, 13% and 8% [57], respectively, while a 6% uncertainty is assigned for VV processes [63]. The impact of the choice of factorisation and renormalisation scales on the estimated fiducial acceptance and reconstruction efficiencies of the SRs is assessed by considering the alternative event weights provided by the generators for up/down variations of these scales (see e.g. appendix B.3 in ref. [1]). The impact of PDF uncertainties is also taken into account by following the prescription in ref. [70] using the sets of eigenvectors provided for each PDF [58, 65].

For $t\bar{t}V$ and $t\bar{t}H$ processes, the modelling of initial- and final-state radiation by the parton shower algorithm is assessed by comparing five related variations of the PYTHIA 8 A14 event tune [59]. For $t\bar{t}W$ the modelling of extra jets is further compared with the prediction of the SHERPA 2.2.2 generator including LO matrix elements with two extra final-state partons; the difference is found to be smaller than the tune-based parton shower uncertainties.

| | n_ℓ | n_b | n_j | m_{eff} [GeV] | Other requirements |
|---------|---|----------|----------------------------|------------------------|---|
| VRWZ4j | = 3, | = 0 | ≥ 4 ($p_T > 25$ GeV) | > 600 | 81 GeV < $m_{\text{SFOS}} < 101$ GeV, $E_T^{\text{miss}} > 50$ GeV, no fourth baseline lepton |
| VRWZ5j | = 1 SFOS pair | = 0 | ≥ 5 ($p_T > 25$ GeV) | > 400 | |
| VRttV | ≥ 2 ($\ell^\pm \ell^\pm$) | ≥ 1 | ≥ 3 ($p_T > 40$ GeV) | > 600 | $p_T > 30$ GeV for the same-sign leptons, $\sum p_T^b > 0.4 \sum p_T^j$, $E_T^{\text{miss}} > 0.1 m_{\text{eff}}$, $\Delta R_\eta(\ell_1, j) > 1.1$ |
| All VRs | $m_{\text{eff}} < 1.5$ TeV, $E_T^{\text{miss}} < 250$ GeV; veto Rpc2L1b, Rpc2L2b, Rpc2L0b and Rpv2L signal regions. | | | | |

Table 3. Event selection defining the three validation regions enriched in WZ +jets and $t\bar{t}V$ SM processes, based on the variables defined in section 5.

For VV processes, the impact of the choice of resummation scale (QSF) and CKKW matching scale [71] is also evaluated by comparing the nominal prediction with alternatives obtained with variations of these scales. In addition, the modelling of high jet multiplicities is probed by switching between different parton shower recoil schemes implemented in the SHERPA generator [72, 73].

Overall, modelling uncertainties in the SRs where these processes have sizeable contributions are 35–45% for $t\bar{t}W$, 25–45% for $t\bar{t}Z$, 15–40% for $t\bar{t}H$, and 40–45% for WZ . For all other processes, uncertainties of 50% are assigned. The latter numbers are believed to be conservative as these processes produce a larger number of jets at the first order of the perturbative expansion, rendering them less sensitive to parton shower modelling uncertainties. For the largest contribution to the SRs among these rarer processes, namely from $4t$ production, the combined impact of factorisation and renormalisation scales as well as PDF uncertainties was checked and found to be indeed smaller than 50%. Modelling uncertainties are further assumed to be uncorrelated between processes shown in different categories in the tables and figures.

Three validation regions (VRs) enriched respectively in WZ +jets (VRWZ4j, VRWZ5j) and $t\bar{t}V$ (VRttV) are used to check the accuracy of the modelling of these processes by comparing event yields predicted in a signal-free environment with data. The definitions of these regions are provided in table 3, and are designed to minimise the level of reducible background. Requirements are set on some of the variables defined in section 4. The presence of a pair of same-flavour opposite-sign (SFOS) leptons is required in VRWZ4j and VRWZ5j, and its invariant mass m_{SFOS} must be close to m_Z . A minimum angular separation between the leading- p_T lepton and the jets ($\Delta R(\ell_1, j)$) is required in VRttV, together with a requirement on the ratio of the scalar p_T sum over all b -tagged jets to the sum over all jets. For all VRs, events belonging to any SR (except Rpc3LSS1b) are vetoed. Upper bounds on E_T^{miss} and m_{eff} are also imposed to minimise contributions from the benchmark SUSY scenarios of figure 1. Modelling uncertainties are evaluated with the same procedure as described above for the SRs, and lead to uncertainties of around 20% for $t\bar{t}V$ and 35% for WZ processes.

The number of events observed in each of the three VRs and the corresponding predictions for SM processes are shown in table 4, including the reducible background described in the next section, accounting for the systematic and statistical uncertainties. The predicted

| | VRt \bar{t} V | VRWZ4j | VRWZ5j |
|-------------------------------|------------------------|------------------------|------------------------|
| Observed | 127 | 355 | 190 |
| Total SM background | 106^{+16}_{-19} | 390^{+120}_{-100} | 209^{+68}_{-54} |
| $t\bar{t}W$ | $25.8^{+5.5}_{-5.6}$ | $0.40^{+0.17}_{-0.15}$ | $0.32^{+0.14}_{-0.15}$ |
| $t\bar{t}Z$ | $34.4^{+8.1}_{-8.2}$ | $37.2^{+8.6}_{-8.8}$ | $27.3^{+7.2}_{-7.4}$ |
| WZ | $5.8^{+2.5}_{-2.2}$ | 310^{+120}_{-90} | 153^{+64}_{-50} |
| $ZZ, W^{\pm}W^{\pm}, VH, VVV$ | $1.03^{+0.40}_{-0.39}$ | $12.0^{+3.4}_{-2.9}$ | $7.5^{+2.8}_{-2.1}$ |
| $t\bar{t}H$ | $7.3^{+1.1}_{-1.2}$ | $0.90^{+0.18}_{-0.18}$ | $0.81^{+0.18}_{-0.17}$ |
| $t(W)Z, t\bar{t}VV, 3t, 4t$ | $10.4^{+5.2}_{-5.2}$ | $10.3^{+5.3}_{-5.3}$ | $5.8^{+3.1}_{-3.1}$ |
| Fake/non-prompt | 14^{+8}_{-12} | 15^{+7}_{-13} | $13.7^{+5.4}_{-8.0}$ |
| Charge-flip | $7.1^{+5.7}_{-5.7}$ | – | – |

Table 4. Observed yields in data compared with the expected contributions from relevant SM processes (section 5) and the reducible background (section 6), in the three VRs enriched in WZ +jets and $t\bar{t}V$ processes. The displayed numbers include all sources of statistical and systematic uncertainties; since some of the latter might be correlated between different processes, the numbers do not necessarily add up in quadrature to the uncertainty in the total expected background. Selections with three leptons are not affected by the charge-flip electron background, so such contributions are denoted by –.

event yields in all VRs are consistent with the data. In the VRWZ4j and VRWZ5j regions, the large systematic uncertainties include contributions from theoretical modelling and from experimental sources (dominated by the jet energy scale) due to the large required number of jets.

Other potential sources of same-sign leptons in the SRs are not included, as they were estimated to be negligible. These include simultaneous production of massive bosons or top quarks via either double parton scattering (DPS) or pile-up interactions. Simple estimations of the inclusive production cross-sections were performed for several processes. For DPS the approach from ref. [74] was used, relying on the DPS effective cross-section σ_{eff} [75]. Earlier experiments probed the reliability of this approach for different centre-of-mass energies and physics processes [76], including more recently for $W^{\pm}W^{\pm}$ production [77]. All these measurements display a level of consistency allowing to conclude that DPS processes would not contribute noticeably to the SRs. For pile-up interactions, the estimation was based on the longitudinal density of reconstructed vertices [78], as the impact parameter requirements in the selection of the leptons strongly affect the yields of such processes. The only process for which the pile-up induced contribution is estimated to be more than 1% of the corresponding SM process is $W^{\pm}W^{\pm}$ production, which has been highlighted [79] as a sensitive process for DPS measurements. But this process is in itself a minor source of background for this analysis.

Another source, notably highlighted in ref. [80], is the production of additional pairs of leptons in radiative top quark decays, $t \rightarrow lvbll$ or $t \rightarrow qqbll$, which are not included in the generator matrix elements for the $t\bar{t}Z$ process. These contributions were studied by running the PHOTOS++ QED shower program [81] on the tree-level decay products of top quarks generated with MADGRAPH 2.6 or PYTHIA 8. The fraction of events in which an additional lepton is produced drops sharply with the p_T requirement for that lepton; for a $p_T = 10$ GeV threshold⁴ this fraction was found to be $\sim 0.2\%$, a similar order of magnitude to that quoted in ref. [81]. An additional isolation requirement similar to that used in the analysis reduces this rate by a factor of three. This represents less than 2% (4%) of the inclusive contribution from $t\bar{t}V$ processes for final states with same-sign (three) leptons; furthermore, the smaller reconstruction and identification efficiencies for low- p_T leptons should further reduce the radiative top quark decay contribution relative to $t\bar{t}V$ processes. The expected contribution to the SRs is therefore small enough to be neglected.

6 Backgrounds with non-prompt, fake or charge-flip leptons

Other SM processes that do not lead to genuine production of same-sign prompt leptons, such as $t\bar{t}$ processes and to a much lesser extent production of W/Z +jets or single top quarks, might contaminate the SRs via secondary interactions, for example bremsstrahlung or non-prompt leptons in ensuing decays, or misidentification of the reconstructed objects (fakes).

The first source consists of ‘charge-flip’ electrons, where the charge of a prompt electron is mismeasured due to the emission of a bremsstrahlung photon which through interaction with detector material converts into a pair of secondary electron tracks, one of which happens to better match the position of the calorimeter cluster than the original electron track and has a charge opposite to that of the prompt electron. Thanks to the application of the ECIDS discriminant for signal electrons, charge-flip electrons are only a minor background in the SRs. Muon charge-flip is negligible in the p_T range relevant to this analysis.

Backgrounds with charge-flip electrons are estimated by selecting data events with two opposite-sign leptons, and weighting them by the probability of one electron charge to be mismeasured. This offers a large improvement in statistical accuracy over relying directly on the simulation for these backgrounds, as well as the elimination of associated experimental and theory uncertainties. The charge-flip probabilities are measured in simulated $t\bar{t}$ events, as a function of p_T and $|\eta|$. They are corrected by scale factors corresponding to the ratio of probabilities measured in data and simulation from the reconstructed charges of electrons produced in $Z \rightarrow e^+e^-$ decays and selected with a ‘tag and probe’ method [46]. The probabilities reach $\mathcal{O}(0.1\%)$ at $p_T = 100$ GeV for central electrons ($|\eta| < 1.4$), and are about five times larger at higher $|\eta|$ due to the larger amount of material traversed by electrons. Systematic uncertainties are assessed by propagating the measurement uncertainties, leading to a 70–90% uncertainty in the predicted SR yields for the charge-flip background.

⁴Dilepton $t\bar{t}$ events with an extra $p_T > 10$ GeV lepton satisfy the lepton selection requirements of this analysis.

The data weighting method described above neglects the differences in momentum scale and resolution between standard and charge-flip electrons. This approximation was validated by recomputing the expected SR yields after reducing the p_T of the electron with largest $|\eta|$ by 5 GeV — a value bounding from above the invariant mass resolution of same-sign ee pairs near the Z boson mass — in all weighted data events, which was found to have a negligible impact on the results. For the Rpc3LSS1b SR, the method is adapted by simply selecting data events with three or more leptons, which are weighted by the probability of one or more electron charges to be mismeasured such that the resulting event contains three same-sign leptons.

Another, more important, source of reducible background includes fake or non-prompt leptons, referred to in the following as ‘F/NP’ leptons. These may originate from electroweak-mediated decays of hadrons (in particular b - and c -flavoured hadrons in decays of top quarks and weak bosons), single pions stopped in the EM calorimeter that fake electron signatures, in-flight decays of kaons into muons, or the conversion of photons into pairs of electrons in the beam pipe or detector material. Lepton candidates reconstructed from these different sources share the properties of being generally not well isolated and being mostly rejected by the lepton identification criteria and impact parameter requirements. Therefore, all sources of background with F/NP leptons are estimated together, using a common method that exploits these properties.

Sources of F/NP leptons in the SRs are mostly semileptonic or dileptonic $t\bar{t}$ processes. To estimate their contributions to the SRs, a matrix method as described in ref. [82] is used, with a different parameterisation of efficiencies and uncertainties as detailed in the following. It relies on data events selected with the same criteria as in the region of interest, but with a loosened lepton selection corresponding to the baseline leptons defined in section 3 after the overlap removal procedure with a few extra adjustments: muons are required to satisfy a loosened transverse impact parameter requirement $|d_0| < 7\sigma(d_0)$, and electrons must both be within $|\eta| < 2.0$ and satisfy the ECIDS requirement against charge-flip. These adjustments align the selection with the fiducial acceptance of signal leptons, and eliminate irrelevant sources of reconstructed leptons. The matrix method, for the simplest situation where selected events contain a single lepton, relies on the following asymptotic equality for the observed proportion of events \mathcal{S} where the lepton satisfies the signal lepton requirements:

$$\mathcal{S} = \varepsilon(1 - \mathcal{F}) + \zeta\mathcal{F} \tag{6.1}$$

where \mathcal{F} is the unknown proportion of events with a F/NP lepton, while ε and ζ are respectively the probabilities for a prompt or F/NP lepton to satisfy the signal lepton requirements. If ε and ζ are known, eq. (6.1) can be used to determine \mathcal{F} and thus the number of events with a F/NP lepton in the region of interest. The approach can be generalised to events with arbitrary numbers of leptons, as well as the more realistic situation where ε and ζ depend on the flavour and kinematic properties of the leptons.

The probabilities ε are obtained directly from the $t\bar{t}$ simulation, as a function of p_T and $|\eta|$, accounting for the various lepton-related scale factors mentioned in section 5. For $p_T > 30$ GeV the probabilities are larger than 80% and 90% for electrons and muons,

respectively. As ε might be smaller in data events coming from signal scenarios with busy environments, such as boosted top quarks that decay semileptonically, uncertainties are taken into account as a function of p_T and the proximity to the closest jet and can be as large as 30% for $\Delta R < 0.4$.

The probabilities ζ are measured in regions of the data enriched in F/NP leptons produced by $t\bar{t}$ processes, defined by selecting events with two same-sign leptons or three leptons, at least one b -tagged jet, $E_T^{\text{miss}} > 30$ GeV and ≥ 2 –3 jets; upper bounds on E_T^{miss} and m_{eff} avoid contamination from supersymmetric processes. The probabilities are measured as a function of p_T , separately for events with exactly one or exactly two b -tagged jets, as the proportion of non-prompt leptons from b -flavoured hadron decays is much smaller in the latter case than in events with at most one b -tagged jet. They are also measured separately for electrons that were or were not used to accept the event via a lepton-based trigger, as the requirements for electrons reconstructed online differ from those for electrons reconstructed offline. The measured probabilities are $\sim 10\%$ for both electrons and muons up to $p_T \sim 35$ GeV, and increase to 20% and 35% for electrons and muons with $p_T > 60$ GeV. They can be up to twice as large in events with two b -tagged jets.

Systematic uncertainties in the measured ζ probabilities account for variations in the relative contributions of different sources of F/NP leptons or in the environment, and they are assessed in simulated $t\bar{t}$ events. For electrons the latter amount to a 30% additional uncertainty. For muons the probabilities become smaller in events with a larger amount of activity, where non-prompt muons tend to be less well isolated. This leads to extra uncertainties of 30% to 80% for $p_T > 50$ GeV, as this effect is not accounted for with the simple p_T -based parameterisation used for ζ .

Events with charge-flip electrons may bias the matrix method prediction, as the probability for such electrons to satisfy signal lepton requirements differ from both standard and F/NP electrons. For that reason, estimated charge-flip contributions are subtracted from the data event yields when the method is applied.

The data-driven methods employed to estimate the reducible background are validated by comparing the event yields in data with the combined predictions for these backgrounds, added to Monte Carlo predictions for SM processes as described in section 5. Figure 2 shows such a comparison for a loose event preselection requiring same-sign leptons, $E_T^{\text{miss}} > 50$ GeV and at least three jets with $p_T > 40$ GeV, binned in the different lepton flavour and b -tag multiplicity combinations. Simulation studies show that the sources of reducible background for such a preselection are dominated, as in the SRs, by $t\bar{t}$ processes. While the F/NP lepton background represents a major contribution to the total yields, the charge-flip background is always small. In all bins, the observed and predicted event yields agree within uncertainties. Figure 3 presents the distributions of E_T^{miss} and the number of jets in events with at least two jets and an otherwise identical preselection, for which good agreement is observed between data and predictions.

As $t\bar{t}$ processes with F/NP leptons produce a major background in this analysis, the estimated SR yields obtained with the matrix method are cross-checked against an alternative method based on a factorisation approach. In the latter, a control region CR is built for each SR by relaxing some of the E_T^{miss} or m_{eff} requirements. Another set of regions SR'

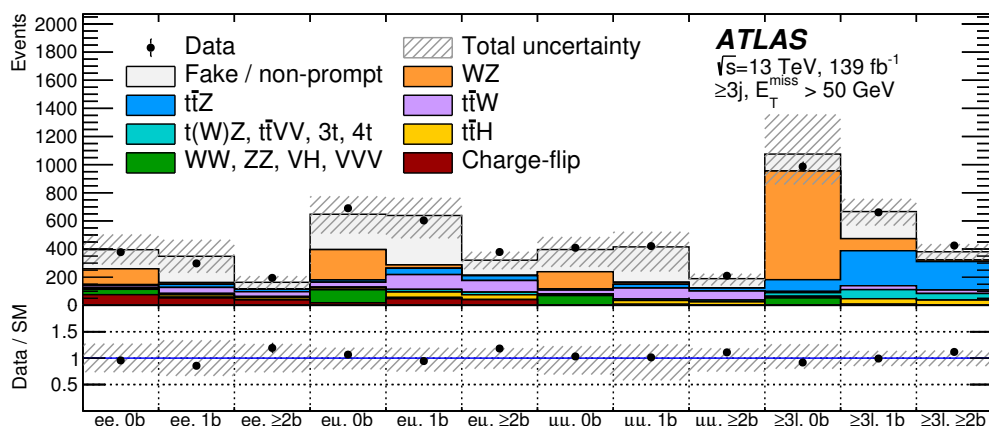


Figure 2. Data event yields compared with the expected contributions from relevant SM processes (section 5) and the reducible background (section 6), after a loose preselection requiring events with same-sign leptons, $E_T^{\text{miss}} > 50 \text{ GeV}$ and at least three jets with $p_T > 40 \text{ GeV}$. The observed and predicted event yields are classified as a function of the number and flavour of the leptons, as well as the number of b -tagged jets. The uncertainties, shown with hashed bands, include the total uncertainties in the reducible background, as well as the modelling and statistical uncertainties for the Monte Carlo simulations.

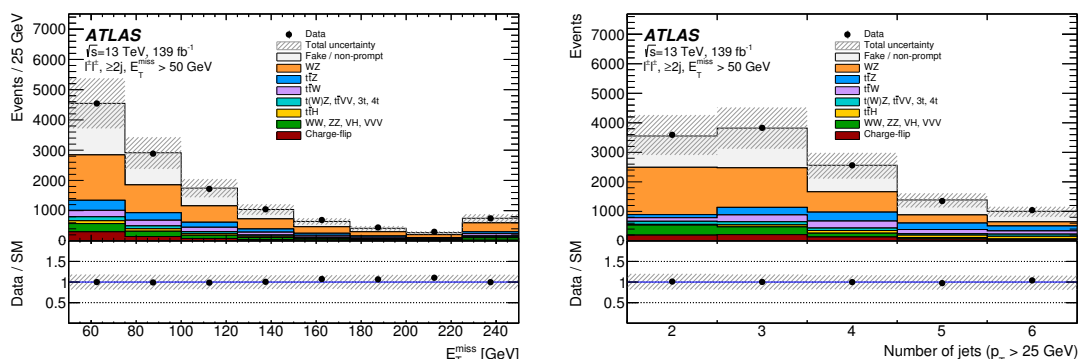


Figure 3. Distributions of (left) E_T^{miss} and (right) the number of jets with $p_T > 25 \text{ GeV}$, after a loose preselection requiring events with same-sign leptons, $E_T^{\text{miss}} > 50 \text{ GeV}$ and at least two jets with $p_T > 40 \text{ GeV}$. The uncertainties, shown with hashed bands, include the total uncertainties in the reducible background, as well as the modelling and statistical uncertainty for the Monte Carlo simulations. The last bin is inclusive.

and CR' is built with identical criteria but using events where a single lepton is selected instead of the same-sign pair, as well as an additional object (jet, b -tagged jet, photon) that might be a source of F/NP leptons. Each CR is chosen such that the kinematic properties of the additional object are similar in CR' and SR' . A ‘transfer factor’ is built as the ratio of the number of data events in SR' to the number in CR' . The transfer factor is then multiplied by the number of events with same-sign leptons in the CR to obtain an estimate of the F/NP lepton background yield in the SR. The estimated contributions to

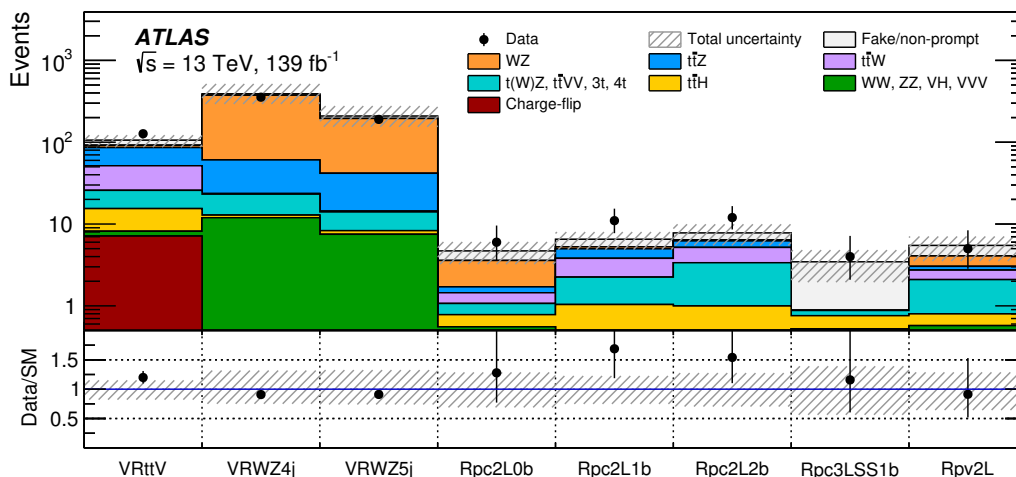


Figure 4. Data event yields compared with the expected contributions from relevant SM processes (section 5) and the reducible background (section 6), in the three VRs and the five SRs. The total uncertainties in the expected event yields are shown as the hashed bands.

the CR from SM processes with same-sign prompt leptons are subtracted, as is the charge-flip background. Differences between the transfer factors calculated using different choices for the additional object are treated as a source of systematic uncertainty. The estimated F/NP lepton background yields in the five SRs obtained with this alternative method are consistent with the matrix method prediction within uncertainties.

7 Results

The event yields in data in the five SRs, and the corresponding estimates for SM processes and the reducible background, are shown in figure 4 and detailed in table 5. No significant excess over the expected yields is observed in any of the SRs. The SRs `Rpc2L1b` and `Rpc2L2b` overlap by approximately 15% in terms of expected yields from SM processes, and two data events satisfy the requirements for both regions. Among SM processes with smaller cross-sections, the largest contributions originate from $t\bar{t}H$ (in `Rpc2L1b`) and $4t$ (in `Rpc2L2b`, `Rpv2L`). The distributions of E_T^{miss} , m_{eff} or the $E_T^{\text{miss}}/m_{\text{eff}}$ ratio are shown with the SR requirement relaxed for the displayed variable in figure 5 for four of the SRs. When E_T^{miss} is relaxed (`Rpc2L0b`, `Rpc2L2b`), the m_{eff} requirement is also loosened by the difference between the actual E_T^{miss} and the minimum E_T^{miss} required in the SR, to avoid selecting harder jets or leptons in the low- E_T^{miss} region. The $E_T^{\text{miss}}/m_{\text{eff}}$ requirement is loosened similarly. For `Rpc2L0b`, the small number of events in the low- E_T^{miss} region, compared with the SR, is due to the combined effects of the m_{eff} and $E_T^{\text{miss}}/m_{\text{eff}}$ requirements, preventing high- m_{eff} events from being selected.

Figure 6 presents a summary of the contributions from different sources of systematic uncertainty to the total uncertainties in the predicted total background yields. These range from 23% to 41%, and are always smaller than the statistical uncertainties in the observed event yields.

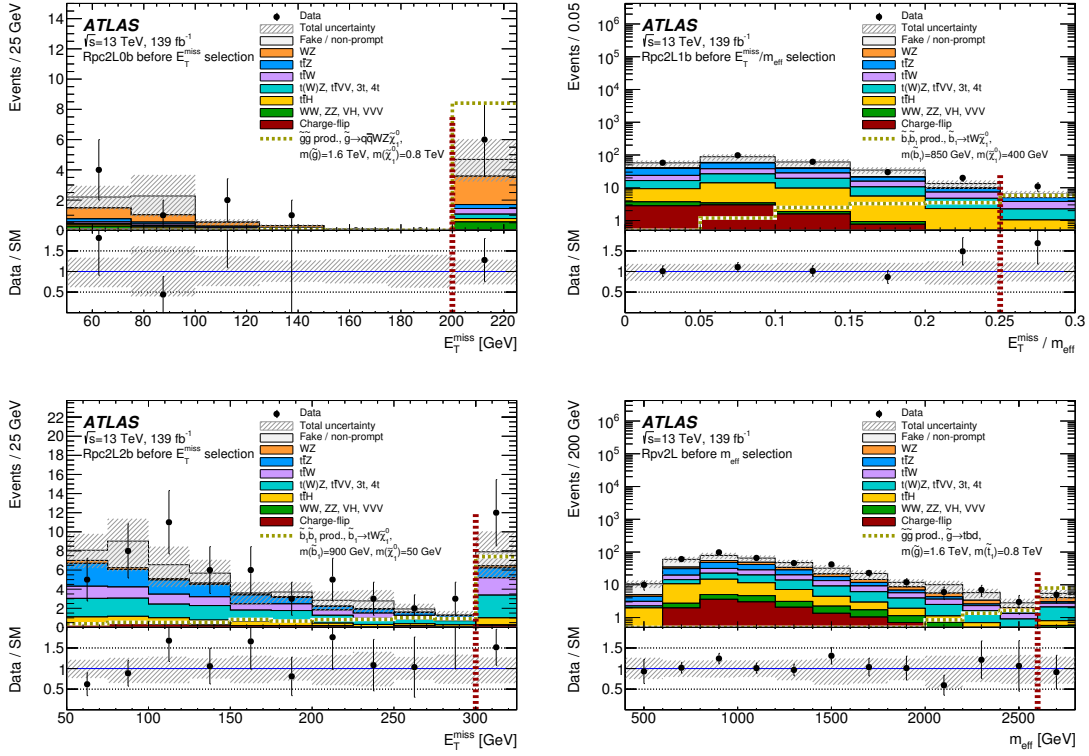


Figure 5. Distributions of E_T^{miss} , m_{eff} or the $E_T^{\text{miss}}/m_{\text{eff}}$ ratio near the SRs (top left) Rpc2L0b, (top right) Rpc2L1b, (bottom left) Rpc2L2b and (bottom right) Rpv2L. The total uncertainties in the expected event yields are shown as the hashed bands. The last bin, isolated by a vertical red dashed line, is inclusive and corresponds to the SR. Hypothetical contributions from representative SUSY scenarios are displayed by the dashed-line overlaid histograms.

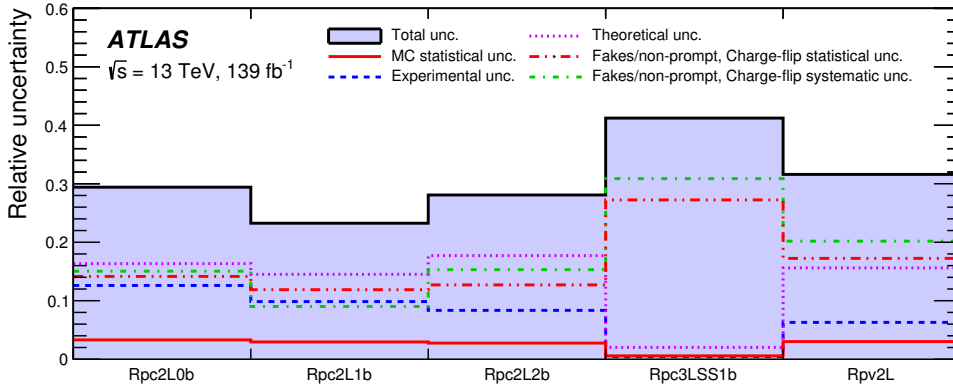


Figure 6. Contributions of different categories of uncertainties relative to the expected background yields in the five SRs. The statistical uncertainties originate from the limited number of preselected or opposite-sign data events used in the matrix method and the charge-flip electron background estimate, respectively, as well as the effect of limited numbers of simulated events for SM processes.

| | Rpc2L0b | Rpc2L1b | Rpc2L2b | Rpc3LSS1b | Rpv2L |
|-----------------------------|------------------------|------------------------|------------------------|------------------------|------------------------|
| Observed | 6 | 11 | 12 | 4 | 5 |
| Total SM background | $4.7^{+1.3}_{-1.5}$ | $6.5^{+1.5}_{-1.6}$ | $7.8^{+2.1}_{-2.3}$ | $3.5^{+1.4}_{-1.5}$ | $5.5^{+1.6}_{-2.0}$ |
| $t\bar{t}W$ | $0.38^{+0.21}_{-0.22}$ | $1.56^{+0.64}_{-0.63}$ | $1.81^{+0.74}_{-0.62}$ | – | $0.64^{+0.30}_{-0.29}$ |
| $t\bar{t}Z$ | $0.26^{+0.13}_{-0.11}$ | $1.17^{+0.43}_{-0.43}$ | $1.04^{+0.34}_{-0.33}$ | – | $0.30^{+0.18}_{-0.17}$ |
| WZ | $1.88^{+0.85}_{-0.76}$ | $0.29^{+0.15}_{-0.15}$ | $0.21^{+0.10}_{-0.11}$ | – | $1.03^{+0.48}_{-0.45}$ |
| $ZZ, W^\pm W^\pm, VH, VVV$ | $0.50^{+0.18}_{-0.16}$ | $0.04^{+0.02}_{-0.02}$ | $0.03^{+0.01}_{-0.01}$ | < 0.02 | $0.43^{+0.13}_{-0.13}$ |
| $t\bar{t}H$ | $0.23^{+0.09}_{-0.08}$ | $0.90^{+0.27}_{-0.26}$ | $0.75^{+0.25}_{-0.20}$ | $0.24^{+0.05}_{-0.05}$ | $0.22^{+0.10}_{-0.09}$ |
| $t(W)Z, t\bar{t}VV, 3t, 4t$ | $0.29^{+0.17}_{-0.16}$ | $1.21^{+0.63}_{-0.63}$ | $2.4^{+1.2}_{-1.2}$ | $0.12^{+0.06}_{-0.06}$ | $1.29^{+0.67}_{-0.67}$ |
| Fake/non-prompt | $1.1^{+0.8}_{-1.1}$ | $1.3^{+0.9}_{-1.1}$ | $1.4^{+1.4}_{-1.4}$ | $2.6^{+1.3}_{-1.5}$ | $1.4^{+1.2}_{-1.4}$ |
| Charge-flip | $0.05^{+0.04}_{-0.04}$ | $0.11^{+0.11}_{-0.11}$ | $0.22^{+0.22}_{-0.22}$ | $0.52^{+0.39}_{-0.39}$ | $0.14^{+0.14}_{-0.14}$ |

Table 5. Observed yields in data and expected contributions from SM processes (section 5) and the reducible background (section 6) to the five SRs. The displayed numbers include all sources of statistical and systematic uncertainty; since some of the latter might be correlated between different processes, the numbers do not necessarily add up in quadrature to the uncertainty in the total expected background. The WZ and $t\bar{t}V$ processes cannot genuinely result in final states with three same-sign leptons, so their contributions to the Rpc3LSS1b signal region are denoted by –. Contributions to Rpc3LSS1b only include those from processes producing final states with three genuine same-sign leptons, such as $t\bar{t}WZ$ or WZZ .

| Signal region | σ_{vis} [fb] | S_{obs}^{95} | S_{exp}^{95} | $p(s = 0)$ |
|---------------|----------------------------|-----------------------|-----------------------|------------|
| Rpc2L0b | 0.05 | 7.6 | $6.4^{+3.2}_{-2.0}$ | 0.33 |
| Rpc2L1b | 0.08 | 11.6 | $7.3^{+3.6}_{-2.3}$ | 0.09 |
| Rpc2L2b | 0.09 | 12.4 | $8.7^{+4.0}_{-2.7}$ | 0.14 |
| Rpc3LSS1b | 0.04 | 6.2 | $5.7^{+2.9}_{-1.8}$ | 0.41 |
| Rpv2L | 0.05 | 6.7 | $6.9^{+3.2}_{-2.0}$ | 0.50 |

Table 6. Computed 95% CL upper limits on the numbers of BSM events S^{95} , as well as the $\pm 1\sigma$ expected fluctuations around the mean expected limit. These are also translated into upper limits on the visible cross-section σ_{vis} . The p -values $p(s = 0)$ give the probabilities to observe a deviation from the predicted background at least as large as that in the data. They are capped at 0.50.

Upper limits at 95% confidence level (CL) on possible BSM contributions to the SRs are computed with the HistFitter framework [83], relying on a profile-likelihood-ratio test [84] and following the CL_s prescription [85]. The hypothesis tests are performed for each of the SRs independently. The likelihood is built as the product of a Poisson probability distribution describing the observed number of events in the SR and the probability distri-

butions of the nuisance parameters encoding the systematic uncertainties. The latter are Gaussian distributions for all sources, including statistical uncertainties arising from the limited number of preselected or opposite-sign data events in the estimation of the reducible background, or the limited number of simulated events. Correlations of a given nuisance parameter between the backgrounds and the signal are taken into account when relevant.

Table 6 presents 95% CL upper limits on the number of BSM events, S^{95} , that may contribute to the SRs. Normalising these by the integrated luminosity L of the data sample, they can be interpreted as upper limits on the visible BSM cross-section (σ_{vis}), defined as $\sigma_{\text{vis}} = \sigma_{\text{prod}} \times \mathcal{A} \times \epsilon = S^{95}/L$, where σ_{prod} is the production cross-section of an arbitrary BSM signal process, and \mathcal{A} and ϵ are the corresponding fiducial acceptance and reconstruction efficiencies for the relevant SR. These limits are computed with asymptotic approximations of the probability distributions of the test statistic under the different hypotheses [84]. They were confirmed to be within 10% of an alternative computation based on pseudo-experiments. The probability of the observations being compatible with the SM-only hypothesis is quantified by the p -values displayed in table 6; the smallest, for Rpc2L1b, corresponds to about 1.3 standard deviations.

8 Exclusion limits on SUSY scenarios

Exclusion limits are computed for the masses of superpartners involved in the benchmark SUSY signal scenarios shown in figure 1, using the same statistical tools as those described in section 7. The limits are obtained in the context of simplified models [86–88] assuming a single production process with 100% branching ratio into the chosen decay mode, and where superpartners not involved in the process are treated as decoupled. All superpartners are assumed to decay promptly. The expected signal contributions to the SRs are estimated from simulated Monte Carlo samples produced with the MADGRAPH5_aMC@NLO 2.2.1 generator using LO matrix elements for the signal process with up to two extra partons. Parton shower, hadronisation and modelling of the underlying event were performed using the PYTHIA 8.230 generator [56] with the A14 tune [59], using the CKKW-L matching prescription [89] with a matching scale set to one quarter of the mass of the gluinos or squarks produced in the interaction. The samples were processed through a fast simulation of the ATLAS detector using a parameterisation of the calorimeter response but GEANT4 for the ID and MS [66, 90]. Such an approach is known to be appropriate for the standard reconstruction techniques described in section 3, and alternative corrections and scale factors to those evoked in sections 3 and 5 are employed. The samples are normalised to the ‘NNLO_{approx}+NNLL’ reference cross-sections [27], which combine near-threshold approximate next-to-next-to-leading-order corrections [91] to the NLO cross-section with a resummation of soft gluon divergences at next-to-next-to-leading-logarithm accuracy [27]. Corresponding uncertainties are taken from envelopes of cross-section predictions using different PDF sets and factorisation and renormalisation scales, as described in ref. [70]. They range from 12% to 20% for gluino masses from 1 to 2 TeV, and from 7% to 11% for top or bottom squark masses from 400 GeV to 1 TeV.

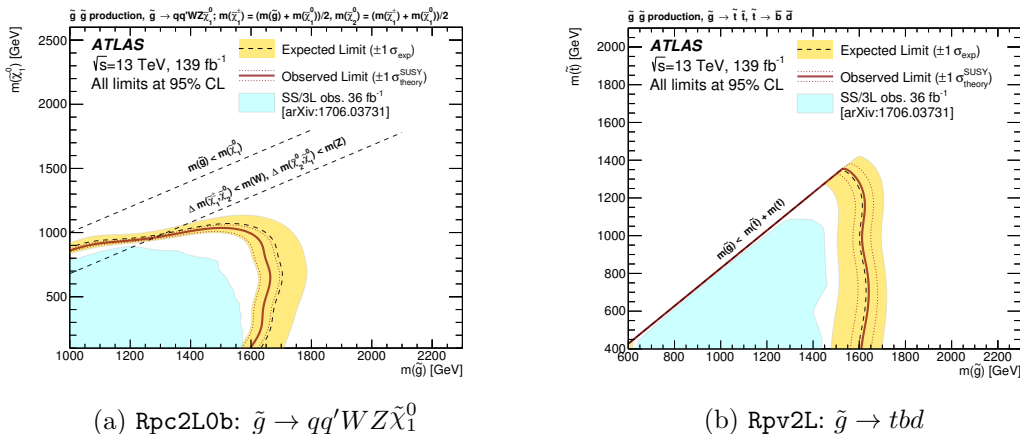


Figure 7. 95% CL exclusion limits on the production of pairs of gluinos, assuming production cross-sections as in ref. [27] and 100% branching ratios into the decay modes illustrated in figures 1(c) and 1(d) for the left and right plots, respectively. The limits are determined from the expected contributions of these processes to the Rpc2L0b (left) and Rpv2L (right) SRs. The coloured bands display the $\pm 1\sigma$ ranges of the expected fluctuations around the mean expected limit, in the absence of contributions from the sought-for signals. They do not account for uncertainties in the signal process cross-sections, the impact of which is illustrated by the dashed lines around the observed limits. The figures show for reference the reach of the previous analysis [28].

Exclusion limits on the masses of gluinos are shown in figure 7. The limits in figure 7(a) are set for pair production of gluinos in an R -parity-conserving scenario (figure 1(c)) with decoupled squarks and gluinos decaying in two steps with intermediate $\tilde{\chi}_1^\pm$ and $\tilde{\chi}_2^0$ into jets, weak bosons and the LSP $\tilde{\chi}_1^0$. The $\tilde{\chi}_1^\pm$ mass is assumed to be $0.5 \times \{m(\tilde{g}) + m(\tilde{\chi}_1^0)\}$, while the $\tilde{\chi}_2^0$ mass is similarly $0.5 \times \{m(\tilde{\chi}_1^\pm) + m(\tilde{\chi}_1^0)\}$. The weak bosons produced in the cascade decays might be off shell, if $\Delta m(\tilde{\chi}_1^\pm, \tilde{\chi}_2^0) < m_W$ or $\Delta m(\tilde{\chi}_2^0, \tilde{\chi}_1^0) < m_Z$. The limits in figure 7(b) are set for pair production of gluinos in an R -parity-violating scenario (figure 1(d)) where gluinos decay via top squarks into $t b d$ or $t b s$ final states (experimentally indistinguishable) when λ''_{313} or λ''_{323} couplings are non-zero. Sensitivity to these two scenarios is provided by the SRs Rpc2L0b and Rpv2L, and allows exclusion of gluino masses below 1.6 TeV for $\tilde{\chi}_1^0$ masses up to 1 TeV or \tilde{t}_1 masses up to 1.2 TeV. For gluino masses around the exclusion limits, the signal $\mathcal{A} \times \epsilon$ is as large as 0.9% for Rpc2L0b and 0.7% for Rpv2L.

Exclusion limits on the masses of third-generation squarks are shown in figure 8. The limits in figure 8(a) are set for pair production of bottom squarks in an R -parity-conserving scenario (figure 1(a)) with decoupled gluinos and squarks of other flavours, with \tilde{b}_1 squarks decaying via an intermediate $\tilde{\chi}_1^\pm$ into a top quark, a W boson and the LSP $\tilde{\chi}_1^0$. The mass of the charginos $\tilde{\chi}_1^\pm$ are assumed equal to $m(\tilde{\chi}_1^0) + 100$ GeV. For each point of the $\{m(\tilde{b}_1), m(\tilde{\chi}_1^0)\}$ parameter space, Rpc2L1b and Rpc2L2b is chosen according to which provides better expected sensitivity. The former provides sensitivity over most of the plane, while the latter provides some complementarity in the low- $m(\tilde{\chi}_1^0)$ region. The transition between the two regions corresponds to the breaking of the exclusion limits smoothness

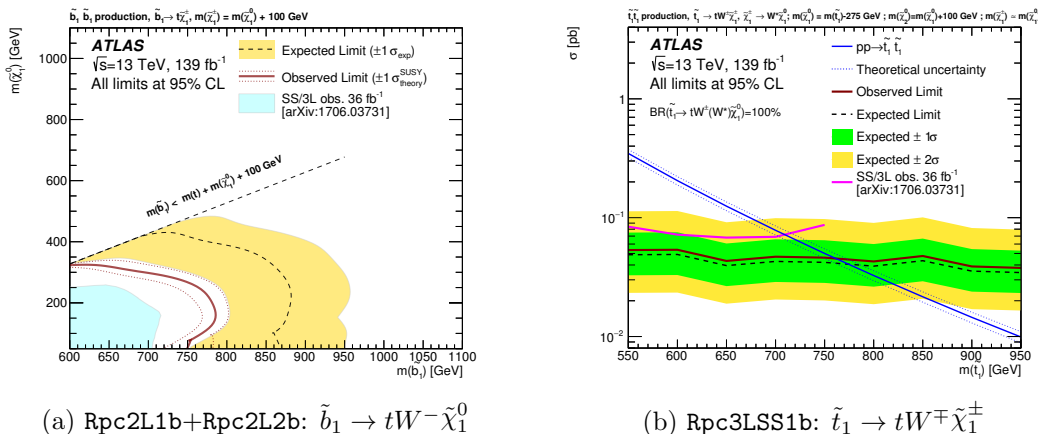


Figure 8. 95% CL exclusion limits on the production of pairs of third-generation squarks, assuming production cross-sections as in ref. [27] (for the left plot) and 100% branching ratios into the decay modes illustrated in figures 1(a) and 1(b) for the left and right plots, respectively. The limits are determined from the expected contributions of these processes to the Rpc2L1b and Rpc2L2b (left) and Rpc3LSS1b (right) SRs. The coloured bands display the $\pm 1\sigma$ ranges (as well as $\pm 2\sigma$ for the right figure) of the expected fluctuations around the mean expected limit, in the absence of contributions from the sought-for signals. They do not account for uncertainties in the signal process cross-sections, the impact of which is illustrated by the dashed lines around the observed limits. The figures show for reference the reach of the previous analysis [28].

at $m(\tilde{\chi}_1^0) \approx 100$ GeV. The limits in figure 8(b) are set for pair production of top squarks (figure 1(b)) decaying into a top quark, a chargino and a W boson via a neutralino $\tilde{\chi}_2^0$. The masses are chosen similarly to ref. [53] such that $m(\tilde{t}_1) = m(\tilde{\chi}_2^0) + m_t = m(\tilde{\chi}_1^0) + 275$ GeV to suppress $\tilde{\chi}_2^0 \rightarrow H\tilde{\chi}_1^0$ and have $\tilde{\chi}_2^0 \rightarrow W^\mp \tilde{\chi}_1^\pm$ as the dominant decay mode, and $m(\tilde{\chi}_1^\pm) \approx m(\tilde{\chi}_1^0)$ such that products of the former's decay into the LSP $\tilde{\chi}_1^0$ are invisible. Upper limits on the production cross-section are provided as a function of the \tilde{t}_1 mass; top squarks with masses up to 750 GeV are excluded. For squark masses around the exclusion limit, the signal $\mathcal{A} \times \epsilon$ is as large as 0.2% for Rpc2L1b and Rpc2L2b, and close to 0.1% for Rpc3LSS1b.

9 Conclusion

A search for supersymmetry in events with same-sign leptons and jets is presented. The analysis is performed with pp collision data collected at a centre-of-mass energy of $\sqrt{s} = 13$ TeV between 2015 and 2018 with the ATLAS detector at the LHC, corresponding to an integrated luminosity of 139 fb^{-1} . Five signal regions are defined to provide sensitivity to a broad range of supersymmetric processes. No significant excess over the yields expected from SM processes is observed, and model-independent limits on the cross-section of possible BSM signal contributions to the signal regions are reported.

The results are interpreted in the framework of four simplified models featuring pair production of gluinos or third-generation squarks. Lower limits on particle masses are derived at 95% confidence level for these models, reaching up to 1.6 TeV for gluinos and

750 GeV for bottom and top squarks, raising the exclusion limits beyond those from a previous similar search made by ATLAS on a smaller 13 TeV dataset.

Acknowledgments

We thank CERN for the very successful operation of the LHC, as well as the support staff from our institutions without whom ATLAS could not be operated efficiently.

We acknowledge the support of ANPCyT, Argentina; YerPhI, Armenia; ARC, Australia; BMWFW and FWF, Austria; ANAS, Azerbaijan; SSTC, Belarus; CNPq and FAPESP, Brazil; NSERC, NRC and CFI, Canada; CERN; CONICYT, Chile; CAS, MOST and NSFC, China; COLCIENCIAS, Colombia; MSMT CR, MPO CR and VSC CR, Czech Republic; DNRF and DNSRC, Denmark; IN2P3-CNRS and CEA-DRF/IRFU, France; SRNSFG, Georgia; BMBF, HGF and MPG, Germany; GSRT, Greece; RGC and Hong Kong SAR, China; ISF and Benozziyo Center, Israel; INFN, Italy; MEXT and JSPS, Japan; CNRST, Morocco; NWO, Netherlands; RCN, Norway; MNiSW and NCN, Poland; FCT, Portugal; MNE/IFA, Romania; MES of Russia and NRC KI, Russia Federation; JINR; MESTD, Serbia; MSSR, Slovakia; ARRS and MIZŠ, Slovenia; DST/NRF, South Africa; MINECO, Spain; SRC and Wallenberg Foundation, Sweden; SERI, SNSF and Cantons of Bern and Geneva, Switzerland; MOST, Taiwan; TAEK, Turkey; STFC, United Kingdom; DOE and NSF, United States of America. In addition, individual groups and members have received support from BCKDF, CANARIE, Compute Canada and CRC, Canada; ERC, ERDF, Horizon 2020, Marie Skłodowska-Curie Actions and COST, European Union; Investissements d’Avenir Labex, Investissements d’Avenir Idex and ANR, France; DFG and AvH Foundation, Germany; Herakleitos, Thales and Aristeia programmes co-financed by EU-ESF and the Greek NSRF, Greece; BSF-NSF and GIF, Israel; CERCA Programme Generalitat de Catalunya and PROMETEO Programme Generalitat Valenciana, Spain; Göran Gustafssons Stiftelse, Sweden; The Royal Society and Leverhulme Trust, United Kingdom.

The crucial computing support from all WLCG partners is acknowledged gratefully, in particular from CERN, the ATLAS Tier-1 facilities at TRIUMF (Canada), NDGF (Denmark, Norway, Sweden), CC-IN2P3 (France), KIT/GridKA (Germany), INFN-CNAF (Italy), NL-T1 (Netherlands), PIC (Spain), ASGC (Taiwan), RAL (U.K.) and BNL (U.S.A.), the Tier-2 facilities worldwide and large non-WLCG resource providers. Major contributors of computing resources are listed in ref. [92].

Open Access. This article is distributed under the terms of the Creative Commons Attribution License ([CC-BY 4.0](https://creativecommons.org/licenses/by/4.0/)), which permits any use, distribution and reproduction in any medium, provided the original author(s) and source are credited.

References

- [1] J. Alwall et al., *The automated computation of tree-level and next-to-leading order differential cross sections and their matching to parton shower simulations*, *JHEP* **07** (2014) 079 [[arXiv:1405.0301](https://arxiv.org/abs/1405.0301)] [[INSPIRE](https://inspirehep.net/literature/1200205)].

- [2] PARTICLE DATA GROUP collaboration, *Review of particle physics*, *Phys. Rev. D* **98** (2018) 030001 [INSPIRE].
- [3] R.M. Barnett, J.F. Gunion and H.E. Haber, *Discovering supersymmetry with like sign dileptons*, *Phys. Lett. B* **315** (1993) 349 [hep-ph/9306204] [INSPIRE].
- [4] L. Evans and P. Bryant, *LHC machine*, 2008 *JINST* **3** S08001 [INSPIRE].
- [5] ATLAS collaboration, *The ATLAS experiment at the CERN Large Hadron Collider*, 2008 *JINST* **3** S08003 [INSPIRE].
- [6] CMS collaboration, *The CMS experiment at the CERN LHC*, 2008 *JINST* **3** S08004 [INSPIRE].
- [7] Yu. A. Golfand and E.P. Likhtman, *Extension of the algebra of Poincaré group generators and violation of p invariance*, *JETP Lett.* **13** (1971) 323 [INSPIRE].
- [8] D.V. Volkov and V.P. Akulov, *Is the neutrino a Goldstone particle?*, *Phys. Lett.* **46B** (1973) 109 [INSPIRE].
- [9] J. Wess and B. Zumino, *Supergauge transformations in four-dimensions*, *Nucl. Phys. B* **70** (1974) 39 [INSPIRE].
- [10] J. Wess and B. Zumino, *Supergauge invariant extension of quantum electrodynamics*, *Nucl. Phys. B* **78** (1974) 1 [INSPIRE].
- [11] S. Ferrara and B. Zumino, *Supergauge invariant Yang-Mills Theories*, *Nucl. Phys. B* **79** (1974) 413 [INSPIRE].
- [12] A. Salam and J.A. Strathdee, *Supersymmetry and non-Abelian gauges*, *Phys. Lett.* **51B** (1974) 353 [INSPIRE].
- [13] N. Sakai, *Naturalness in supersymmetric guts*, *Z. Phys. C* **11** (1981) 153 [INSPIRE].
- [14] S. Dimopoulos, S. Raby and F. Wilczek, *Supersymmetry and the scale of unification*, *Phys. Rev. D* **24** (1981) 1681 [INSPIRE].
- [15] L.E. Ibáñez and G.G. Ross, *Low-energy predictions in supersymmetric grand unified theories*, *Phys. Lett.* **105B** (1981) 439 [INSPIRE].
- [16] S. Dimopoulos and H. Georgi, *Softly broken supersymmetry and SU(5)*, *Nucl. Phys. B* **193** (1981) 150 [INSPIRE].
- [17] P. Fayet, *Supersymmetry and weak, electromagnetic and strong interactions*, *Phys. Lett.* **64B** (1976) 159 [INSPIRE].
- [18] P. Fayet, *Spontaneously broken supersymmetric theories of weak, electromagnetic and strong interactions*, *Phys. Lett.* **69B** (1977) 489 [INSPIRE].
- [19] H. Goldberg, *Constraint on the photino mass from cosmology*, *Phys. Rev. Lett.* **50** (1983) 1419 [Erratum *ibid.* **103** (2009) 099905] [INSPIRE].
- [20] J.R. Ellis et al., *Supersymmetric relics from the Big Bang*, *Nucl. Phys. B* **238** (1984) 453 [INSPIRE].
- [21] G.R. Farrar and P. Fayet, *Phenomenology of the production, decay and detection of new hadronic states associated with supersymmetry*, *Phys. Lett.* **76B** (1978) 575 [INSPIRE].
- [22] S.P. Martin, *A Supersymmetry primer*, *Adv. Ser. Direct. High Energy Phys.* **18** (1998) 1 [hep-ph/9709356] [INSPIRE].

- [23] R. Barbieri and G.F. Giudice, *Upper bounds on supersymmetric particle masses*, *Nucl. Phys. B* **306** (1988) 63 [INSPIRE].
- [24] B. de Carlos and J.A. Casas, *One loop analysis of the electroweak breaking in supersymmetric models and the fine tuning problem*, *Phys. Lett. B* **309** (1993) 320 [hep-ph/9303291] [INSPIRE].
- [25] K. Inoue, A. Kakuto, H. Komatsu and S. Takeshita, *Aspects of grand unified models with softly broken supersymmetry*, *Prog. Theor. Phys.* **68** (1982) 927 [Erratum *ibid.* **70** (1983) 330] [INSPIRE].
- [26] J.R. Ellis and S. Rudaz, *Search for supersymmetry in toponium decays*, *Phys. Lett.* **128B** (1983) 248 [INSPIRE].
- [27] W. Beenakker et al., *NNLL-fast: predictions for coloured supersymmetric particle production at the LHC with threshold and Coulomb resummation*, *JHEP* **12** (2016) 133 [arXiv:1607.07741] [INSPIRE].
- [28] ATLAS collaboration, *Search for supersymmetry in final states with two same-sign or three leptons and jets using 36 fb^{-1} of $\sqrt{s} = 13 \text{ TeV}$ pp collision data with the ATLAS detector*, *JHEP* **09** (2017) 084 [Erratum *ibid.* **1908** (2019) 121] [arXiv:1706.03731] [INSPIRE].
- [29] CMS collaboration, *Search for physics beyond the standard model in events with two leptons of same sign, missing transverse momentum and jets in proton-proton collisions at $\sqrt{s} = 13 \text{ TeV}$* , *Eur. Phys. J. C* **77** (2017) 578 [arXiv:1704.07323] [INSPIRE].
- [30] CMS collaboration, *Search for supersymmetry in events with at least three electrons or muons, jets and missing transverse momentum in proton-proton collisions at $\sqrt{s} = 13 \text{ TeV}$* , *JHEP* **02** (2018) 067 [arXiv:1710.09154] [INSPIRE].
- [31] ATLAS collaboration, *ATLAS insertable B-layer technical design report*, *ATLAS-TDR-19* (2010) [ATLAS-TDR-19-ADD-1].
- [32] ATLAS IBL collaboration, *Production and Integration of the ATLAS Insertable B-Layer*, *2018 JINST* **13** T05008 [arXiv:1803.00844] [INSPIRE].
- [33] ATLAS collaboration, *Performance of the ATLAS trigger system in 2015*, *Eur. Phys. J. C* **77** (2017) 317 [arXiv:1611.09661] [INSPIRE].
- [34] ATLAS collaboration, *Luminosity determination in pp collisions at $\sqrt{s} = 13 \text{ TeV}$ using the ATLAS detector at the LHC*, *ATLAS-CONF-2019-021* (2019).
- [35] G. Avoni et al., *The new LUCID-2 detector for luminosity measurement and monitoring in ATLAS*, *2018 JINST* **13** P07017 [INSPIRE].
- [36] ATLAS collaboration, *Vertex reconstruction performance of the ATLAS detector at $\sqrt{s} = 13 \text{ TeV}$* , *ATL-PHYS-PUB-2015-026* (2015).
- [37] ATLAS collaboration, *Reconstruction of primary vertices at the ATLAS experiment in Run 1 proton-proton collisions at the LHC*, *Eur. Phys. J. C* **77** (2017) 332 [arXiv:1611.10235] [INSPIRE].
- [38] M. Cacciari, G.P. Salam and G. Soyez, *The anti- k_t jet clustering algorithm*, *JHEP* **04** (2008) 063 [arXiv:0802.1189] [INSPIRE].
- [39] M. Cacciari, G.P. Salam and G. Soyez, *FastJet user manual*, *Eur. Phys. J. C* **72** (2012) 1896 [arXiv:1111.6097] [INSPIRE].

- [40] ATLAS collaboration, *Topological cell clustering in the ATLAS calorimeters and its performance in LHC Run 1*, *Eur. Phys. J. C* **77** (2017) 490 [[arXiv:1603.02934](#)] [[INSPIRE](#)].
- [41] ATLAS collaboration, *Jet energy scale measurements and their systematic uncertainties in proton-proton collisions at $\sqrt{s} = 13$ TeV with the ATLAS detector*, *Phys. Rev. D* **96** (2017) 072002 [[arXiv:1703.09665](#)] [[INSPIRE](#)].
- [42] ATLAS collaboration, *Selection of jets produced in 13TeV proton-proton collisions with the ATLAS detector*, *ATLAS-CONF-2015-029* (2015).
- [43] ATLAS collaboration, *Performance of pile-up mitigation techniques for jets in pp collisions at $\sqrt{s} = 8$ TeV using the ATLAS detector*, *Eur. Phys. J. C* **76** (2016) 581 [[arXiv:1510.03823](#)] [[INSPIRE](#)].
- [44] ATLAS collaboration, *ATLAS b-jet identification performance and efficiency measurement with $t\bar{t}$ events in pp collisions at $\sqrt{s} = 13$ TeV*, *Eur. Phys. J. C* **79** (2019) 970 [[arXiv:1907.05120](#)] [[INSPIRE](#)].
- [45] ATLAS collaboration, *Muon reconstruction performance of the ATLAS detector in proton-proton collision data at $\sqrt{s} = 13$ TeV*, *Eur. Phys. J. C* **76** (2016) 292 [[arXiv:1603.05598](#)] [[INSPIRE](#)].
- [46] ATLAS collaboration, *Electron and photon performance measurements with the ATLAS detector using the 2015-2017 LHC proton-proton collision data*, *2019 JINST* **14** P12006 [[arXiv:1908.00005](#)] [[INSPIRE](#)].
- [47] ATLAS collaboration, *Performance of missing transverse momentum reconstruction with the ATLAS detector using proton-proton collisions at $\sqrt{s} = 13$ TeV*, *Eur. Phys. J. C* **78** (2018) 903 [[arXiv:1802.08168](#)] [[INSPIRE](#)].
- [48] ATLAS collaboration, *E_T^{miss} performance in the ATLAS detector using 2015-2016 LHC -p collisions*, *ATLAS-CONF-2018-023* (2018).
- [49] ATLAS collaboration, *2015 start-up trigger menu and initial performance assessment of the ATLAS trigger using Run-2 data*, *ATL-DAQ-PUB-2016-001* (2016).
- [50] ATLAS collaboration, *Trigger menu in 2016*, *ATL-DAQ-PUB-2017-001* (2017).
- [51] ATLAS collaboration, *Trigger menu in 2017*, *ATL-DAQ-PUB-2018-002* (2018).
- [52] ATLAS collaboration, *Performance of electron and photon triggers in ATLAS during LHC Run 2*, *Eur. Phys. J. C* **80** (2020) 47 [[arXiv:1909.00761](#)] [[INSPIRE](#)].
- [53] P. Huang, A. Ismail, I. Low and C.E.M. Wagner, *Same-sign dilepton excesses and light top squarks*, *Phys. Rev. D* **92** (2015) 075035 [[arXiv:1507.01601](#)] [[INSPIRE](#)].
- [54] ATLAS collaboration, *Modelling of the vector boson scattering process $pp \rightarrow W^\pm W^\pm jj$ in Monte Carlo generators in ATLAS*, *ATL-PHYS-PUB-2019-004* (2019).
- [55] ATLAS collaboration, *Modelling of the $t\bar{t}H$ and $t\bar{t}V$ ($V = W, Z$) processes for $\sqrt{s} = 13$ TeV ATLAS analyses*, *ATL-PHYS-PUB-2016-005* (2016).
- [56] T. Sjöstrand et al., *An introduction to PYTHIA 8.2*, *Comput. Phys. Commun.* **191** (2015) 159 [[arXiv:1410.3012](#)] [[INSPIRE](#)].
- [57] LHC HIGGS CROSS SECTION WORKING GROUP, D. de Florian et al., *Handbook of LHC Higgs Cross Sections: 4. Deciphering the Nature of the Higgs Sector*, CERN Yellow Reports: Monographs, Volume 2, *CERN-2017-002-M* (2017), [arXiv:1610.07922](#) [[INSPIRE](#)].

- [58] R.D. Ball et al., *Parton distributions with LHC data*, *Nucl. Phys. B* **867** (2013) 244 [[arXiv:1207.1303](#)] [[INSPIRE](#)].
- [59] ATLAS collaboration, *ATLAS PYTHIA 8 tunes to 7 TeV datas*, *ATL-PHYS-PUB-2014-021* (2014).
- [60] T. Sjöstrand, S. Mrenna and P.Z. Skands, *A brief introduction to PYTHIA 8.1*, *Comput. Phys. Commun.* **178** (2008) 852 [[arXiv:0710.3820](#)] [[INSPIRE](#)].
- [61] P. Nason, *A new method for combining NLO QCD with shower Monte Carlo algorithms*, *JHEP* **11** (2004) 040 [[hep-ph/0409146](#)] [[INSPIRE](#)].
- [62] H.B. Hartanto, B. Jager, L. Reina and D. Wackerroth, *Higgs boson production in association with top quarks in the POWHEG BOX*, *Phys. Rev. D* **91** (2015) 094003 [[arXiv:1501.04498](#)] [[INSPIRE](#)].
- [63] ATLAS collaboration, *Multi-boson simulation for 13 TeV ATLAS analyses*, *ATL-PHYS-PUB-2017-005* (2017).
- [64] T. Gleisberg et al., *Event generation with SHERPA 1.1*, *JHEP* **02** (2009) 007 [[arXiv:0811.4622](#)] [[INSPIRE](#)].
- [65] NNPDF collaboration, *Parton distributions for the LHC Run II*, *JHEP* **04** (2015) 040 [[arXiv:1410.8849](#)] [[INSPIRE](#)].
- [66] ATLAS collaboration, *The ATLAS simulation infrastructure*, *Eur. Phys. J. C* **70** (2010) 823 [[arXiv:1005.4568](#)] [[INSPIRE](#)].
- [67] GEANT4 collaboration, *GEANT4 — a simulation toolkit*, *Nucl. Instrum. Meth. A* **506** (2003) 250 [[INSPIRE](#)].
- [68] ATLAS collaboration, *The PYTHIA 8 A3 tune description of ATLAS minimum bias and inelastic measurements incorporating the Donnachie-Landshoff diffractive model*, *ATL-PHYS-PUB-2016-017* (2016).
- [69] D.J. Lange, *The EvtGen particle decay simulation package*, *Nucl. Instrum. Meth. A* **462** (2001) 152 [[INSPIRE](#)].
- [70] J. Butterworth et al., *PDF4LHC recommendations for LHC Run II*, *J. Phys. G* **43** (2016) 023001 [[arXiv:1510.03865](#)] [[INSPIRE](#)].
- [71] S. Höche, F. Krauss, S. Schumann and F. Siegert, *QCD matrix elements and truncated showers*, *JHEP* **05** (2009) 053 [[arXiv:0903.1219](#)] [[INSPIRE](#)].
- [72] S. Hoeche, S. Schumann and F. Siegert, *Hard photon production and matrix-element parton-shower merging*, *Phys. Rev. D* **81** (2010) 034026 [[arXiv:0912.3501](#)] [[INSPIRE](#)].
- [73] S. Schumann and F. Krauss, *A parton shower algorithm based on Catani-Seymour dipole factorisation*, *JHEP* **03** (2008) 038 [[arXiv:0709.1027](#)] [[INSPIRE](#)].
- [74] B. Humpert and R. Odorico, *Multiparton scattering and QCD radiation as sources of four jet events*, *Phys. Lett.* **154B** (1985) 211 [[INSPIRE](#)].
- [75] D. Treleani, *Double parton scattering, diffraction and effective cross section*, *Phys. Rev. D* **76** (2007) 076006 [[arXiv:0708.2603](#)] [[INSPIRE](#)].
- [76] ATLAS collaboration, *Study of the hard double-parton scattering contribution to inclusive four-lepton production in pp collisions at $\sqrt{s} = 8$ TeV with the ATLAS detector*, *Phys. Lett. B* **790** (2019) 595 [[arXiv:1811.11094](#)] [[INSPIRE](#)].

- [77] CMS collaboration, *Evidence for WW production from double-parton interactions in proton–proton collisions at $\sqrt{s} = 13$ TeV*, *Eur. Phys. J. C* **80** (2020) 41 [[arXiv:1909.06265](#)] [[INSPIRE](#)].
- [78] ATLAS collaboration, *Study of multiple hard-scatter processes from different $p p$ interactions in the same ATLAS event*, *ATL-PHYS-PUB-2018-007* (2018).
- [79] J.R. Gaunt, C.-H. Kom, A. Kulesza and W.J. Stirling, *Same-sign W pair production as a probe of double parton scattering at the LHC*, *Eur. Phys. J. C* **69** (2010) 53 [[arXiv:1003.3953](#)] [[INSPIRE](#)].
- [80] P. Onyisi and A. Webb, *Impact of rare decays $t \rightarrow \ell' \nu b \ell \ell$ and $t \rightarrow qq' b \ell \ell$ on searches for top-associated physics*, *JHEP* **02** (2018) 156 [[arXiv:1704.07343](#)] [[INSPIRE](#)].
- [81] N. Davidson, T. Przedzinski and Z. Was, *PHOTOS interface in C++: technical and physics documentation*, *Comput. Phys. Commun.* **199** (2016) 86 [[arXiv:1011.0937](#)] [[INSPIRE](#)].
- [82] ATLAS collaboration, *Search for supersymmetry at $\sqrt{s} = 8$ TeV in final states with jets and two same-sign leptons or three leptons with the ATLAS detector*, *JHEP* **06** (2014) 035 [[arXiv:1404.2500](#)] [[INSPIRE](#)].
- [83] M. Baak et al., *HistFitter software framework for statistical data analysis*, *Eur. Phys. J. C* **75** (2015) 153 [[arXiv:1410.1280](#)] [[INSPIRE](#)].
- [84] G. Cowan, K. Cranmer, E. Gross and O. Vitells, *Asymptotic formulae for likelihood-based tests of new physics*, *Eur. Phys. J. C* **71** (2011) 1554 [*Erratum ibid.* **C 73** (2013) 2501] [[arXiv:1007.1727](#)] [[INSPIRE](#)].
- [85] A.L. Read, *Presentation of search results: the CL_s technique*, *J. Phys. G* **28** (2002) 2693 [[INSPIRE](#)].
- [86] J. Alwall, M.-P. Le, M. Lisanti and J.G. Wacker, *Searching for directly decaying gluinos at the Tevatron*, *Phys. Lett. B* **666** (2008) 34 [[arXiv:0803.0019](#)] [[INSPIRE](#)].
- [87] J. Alwall, P. Schuster and N. Toro, *Simplified models for a first characterization of new physics at the LHC*, *Phys. Rev. D* **79** (2009) 075020 [[arXiv:0810.3921](#)] [[INSPIRE](#)].
- [88] LHC NEW PHYSICS WORKING GROUP collaboration, *Simplified models for LHC new physics searches*, *J. Phys. G* **39** (2012) 105005 [[arXiv:1105.2838](#)] [[INSPIRE](#)].
- [89] L. Lönnblad and S. Prestel, *Matching tree-level matrix elements with interleaved showers*, *JHEP* **03** (2012) 019 [[arXiv:1109.4829](#)] [[INSPIRE](#)].
- [90] ATLAS collaboration, *The simulation principle and performance of the ATLAS fast calorimeter simulation FastCaloSim*, *ATL-PHYS-PUB-2010-013* (2010).
- [91] M. Beneke, M. Czakon, P. Falgari, A. Mitov and C. Schwinn, *Threshold expansion of the $gg(q\bar{q}) \rightarrow Q\bar{Q} + X$ cross section at $O(\alpha_s^4)$* , *Phys. Lett. B* **690** (2010) 483 [[arXiv:0911.5166](#)] [[INSPIRE](#)].
- [92] ATLAS collaboration, *ATLAS computing acknowledgements*, *ATL-GEN-PUB-2016-002* (2016).

The ATLAS collaboration

G. Aad¹⁰², B. Abbott¹²⁹, D.C. Abbott¹⁰³, A. Abed Abud^{71a,71b}, K. Abeling⁵³,
D.K. Abhayasinghe⁹⁴, S.H. Abidi¹⁶⁷, O.S. AbouZeid⁴⁰, N.L. Abraham¹⁵⁶, H. Abramowicz¹⁶¹,
H. Abreu¹⁶⁰, Y. Abulaiti⁶, B.S. Acharya^{67a,67b,o}, B. Achkar⁵³, S. Adachi¹⁶³, L. Adam¹⁰⁰,
C. Adam Bourdarios⁵, L. Adamczyk^{84a}, L. Adamek¹⁶⁷, J. Adelman¹²¹, M. Adersberger¹¹⁴,
A. Adiguzel^{12c,ak}, S. Adorni⁵⁴, T. Adye¹⁴⁴, A.A. Affolder¹⁴⁶, Y. Afik¹⁶⁰, C. Agapopoulou⁶⁵,
M.N. Agaras³⁸, A. Aggarwal¹¹⁹, C. Agheorghiesei^{27c}, J.A. Aguilar-Saavedra^{140f,140a,aj},
F. Ahmadov⁸⁰, W.S. Ahmed¹⁰⁴, X. Ai¹⁸, G. Aielli^{74a,74b}, S. Akatsuka⁸⁶, T.P.A. Åkesson⁹⁷,
E. Akilli⁵⁴, A.V. Akimov¹¹¹, K. Al Khoury⁶⁵, G.L. Alberghi^{23b,23a}, J. Albert¹⁷⁶,
M.J. Alconada Verzini¹⁶¹, S. Alderweireldt³⁶, M. Aleksa³⁶, I.N. Aleksandrov⁸⁰, C. Alexa^{27b},
D. Alexandre¹⁹, T. Alexopoulos¹⁰, A. Alfonsi¹²⁰, F. Alfonsi^{23b,23a}, M. Alhroob¹²⁹, B. Ali¹⁴²,
G. Alimonti^{69a}, J. Alison³⁷, S.P. Alkire¹⁴⁸, C. Allaire⁶⁵, B.M.M. Allbrooke¹⁵⁶, B.W. Allen¹³²,
P.P. Allport²¹, A. Aloisio^{70a,70b}, A. Alonso⁴⁰, F. Alonso⁸⁹, C. Alpigiani¹⁴⁸, A.A. Alshehri⁵⁷,
M. Alvarez Estevez⁹⁹, D. Álvarez Piqueras¹⁷⁴, M.G. Alvigi^{70a,70b}, Y. Amaral Coutinho^{81b},
A. Ambler¹⁰⁴, L. Ambroz¹³⁵, C. Amelung²⁶, D. Amidei¹⁰⁶, S.P. Amor Dos Santos^{140a},
S. Amoroso⁴⁶, C.S. Amrouche⁵⁴, F. An⁷⁹, C. Anastopoulos¹⁴⁹, N. Andari¹⁴⁵, T. Andeen¹¹,
C.F. Anders^{61b}, J.K. Anders²⁰, A. Andreazza^{69a,69b}, V. Andrei^{61a}, C.R. Anelli¹⁷⁶,
S. Angelidakis³⁸, A. Angerami³⁹, A.V. Anisenkov^{122b,122a}, A. Annovi^{72a}, C. Antel^{61a},
M.T. Anthony¹⁴⁹, M. Antonelli⁵¹, D.J.A. Antrim¹⁷¹, F. Anulli^{73a}, M. Aoki⁸²,
J.A. Aparisi Pozo¹⁷⁴, L. Aperio Bella^{15a}, G. Arabidze¹⁰⁷, J.P. Araque^{140a}, V. Araujo Ferraz^{81b},
R. Araujo Pereira^{81b}, C. Arcangeletti⁵¹, A.T.H. Arce⁴⁹, F.A. Arduh⁸⁹, J-F. Arguin¹¹⁰,
S. Argyropoulos⁷⁸, J.-H. Arling⁴⁶, A.J. Armbruster³⁶, A. Armstrong¹⁷¹, O. Arnaez¹⁶⁷,
H. Arnold¹²⁰, Z.P. Arrubarrena Tame¹¹⁴, A. Artamonov^{124,*}, G. Artoni¹³⁵, S. Artz¹⁰⁰, S. Asai¹⁶³,
N. Asbah⁵⁹, E.M. Asimakopoulou¹⁷², L. Asquith¹⁵⁶, J. Assahsah^{35d}, K. Assamagan²⁹,
R. Astalos^{28a}, R.J. Atkin^{33a}, M. Atkinson¹⁷³, N.B. Atlay¹⁹, H. Atmani⁶⁵, K. Augsten¹⁴²,
G. Avolio³⁶, R. Avramidou^{60a}, M.K. Ayoub^{15a}, A.M. Azoulay^{168b}, G. Azuelos^{110,ax},
H. Bachacou¹⁴⁵, K. Bachas^{68a,68b}, M. Backes¹³⁵, F. Backman^{45a,45b}, P. Bagnaia^{73a,73b},
M. Bahmani⁸⁵, H. Bahrasemani¹⁵², A.J. Bailey¹⁷⁴, V.R. Bailey¹⁷³, J.T. Baines¹⁴⁴, M. Bajic⁴⁰,
C. Bakalis¹⁰, O.K. Baker¹⁸³, P.J. Bakker¹²⁰, D. Bakshi Gupta⁸, S. Balaji¹⁵⁷, E.M. Baldin^{122b,122a},
P. Balek¹⁸⁰, F. Balli¹⁴⁵, W.K. Balunas¹³⁵, J. Balz¹⁰⁰, E. Banas⁸⁵, A. Bandyopadhyay²⁴,
Sw. Banerjee^{181,j}, A.A.E. Bannoura¹⁸², L. Barak¹⁶¹, W.M. Barbe³⁸, E.L. Barberio¹⁰⁵,
D. Barberis^{55b,55a}, M. Barbero¹⁰², G. Barbour⁹⁵, T. Barillari¹¹⁵, M-S. Barisits³⁶, J. Barkeloo¹³²,
T. Barklow¹⁵³, R. Barnea¹⁶⁰, S.L. Barnes^{60c}, B.M. Barnett¹⁴⁴, R.M. Barnett¹⁸,
Z. Barnovska-Blenessy^{60a}, A. Baroncelli^{60a}, G. Barone²⁹, A.J. Barr¹³⁵, L. Barranco Navarro^{45a,45b},
F. Barreiro⁹⁹, J. Barreiro Guimarães da Costa^{15a}, S. Barsov¹³⁸, R. Bartoldus¹⁵³, G. Bartolini¹⁰²,
A.E. Barton⁹⁰, P. Bartos^{28a}, A. Basalae⁴⁶, A. Bassalat^{65,ar}, M.J. Basso¹⁶⁷, R.L. Bates⁵⁷,
S. Batlamous^{35e}, J.R. Batley³², B. Batool¹⁵¹, M. Battaglia¹⁴⁶, M. Bause^{73a,73b}, F. Bauer¹⁴⁵,
K.T. Bauer¹⁷¹, H.S. Bawa^{31,m}, J.B. Beacham⁴⁹, T. Beau¹³⁶, P.H. Beauchemin¹⁷⁰, F. Becherer⁵²,
P. Bechtel²⁴, H.C. Beck⁵³, H.P. Beck^{20,s}, K. Becker⁵², M. Becker¹⁰⁰, C. Becot⁴⁶, A. Beddall^{12d},
A.J. Beddall^{12a}, V.A. Bednyakov⁸⁰, M. Bedognetti¹²⁰, C.P. Bee¹⁵⁵, T.A. Beermann⁷⁷,
M. Begalli^{81b}, M. Begel²⁹, A. Behera¹⁵⁵, J.K. Behr⁴⁶, F. Beisiegel²⁴, A.S. Bell⁹⁵, G. Bella¹⁶¹,
L. Bellagamba^{23b}, A. Bellerive³⁴, P. Bellos⁹, K. Beloborodov^{122b,122a}, K. Belotskiy¹¹²,
N.L. Belyaev¹¹², D. Benckekroun^{35a}, N. Benekos¹⁰, Y. Benhammou¹⁶¹, D.P. Benjamin⁶,
M. Benoit⁵⁴, J.R. Bensinger²⁶, S. Bentvelsen¹²⁰, L. Beresford¹³⁵, M. Beretta⁵¹, D. Berge⁴⁶,
E. Bergeas Kuutmann¹⁷², N. Berger⁵, B. Bergmann¹⁴², L.J. Bergsten²⁶, J. Beringer¹⁸,
S. Berlendis⁷, N.R. Bernard¹⁰³, G. Bernardi¹³⁶, C. Bernius¹⁵³, F.U. Bernlochner²⁴, T. Berry⁹⁴,
P. Berta¹⁰⁰, C. Bertella^{15a}, I.A. Bertram⁹⁰, O. Bessidskaia Bylund¹⁸², N. Besson¹⁴⁵,

A. Bethani¹⁰¹, S. Bethke¹¹⁵, A. Betti²⁴, A.J. Bevan⁹³, J. Beyer¹¹⁵, D.S. Bhattacharya¹⁷⁷,
 R. Bi¹³⁹, R.M. Bianchi¹³⁹, O. Biebel¹¹⁴, D. Biedermann¹⁹, R. Bielski³⁶, K. Bierwagen¹⁰⁰,
 N.V. Biesuz^{72a,72b}, M. Biglietti^{75a}, T.R.V. Billoud¹¹⁰, M. Bindi⁵³, A. Bingul^{12d}, C. Bini^{73a,73b},
 S. Biondi^{23b,23a}, M. Birman¹⁸⁰, T. Bisanz⁵³, J.P. Biswal¹⁶¹, D. Biswas^{181,j}, A. Bitadze¹⁰¹,
 C. Bittrich⁴⁸, K. Bjørke¹³⁴, K.M. Black²⁵, T. Blazek^{28a}, I. Bloch⁴⁶, C. Blocker²⁶, A. Blue⁵⁷,
 U. Blumenschein⁹³, G.J. Bobbink¹²⁰, V.S. Bobrovnikov^{122b,122a}, S.S. Bocchetta⁹⁷, A. Bocci⁴⁹,
 D. Boerner⁴⁶, D. Bogavac¹⁴, A.G. Bogdanchikov^{122b,122a}, C. Boehm^{45a}, V. Boisvert⁹⁴,
 P. Bokan^{53,172}, T. Bold^{84a}, A.S. Boldyrev¹¹³, A.E. Bolz^{61b}, M. Bomben¹³⁶, M. Bona⁹³,
 J.S. Bonilla¹³², M. Boonekamp¹⁴⁵, H.M. Borecka-Bielska⁹¹, A. Borisov¹²³, G. Borissov⁹⁰,
 J. Bortfeldt³⁶, D. Bortoletto¹³⁵, D. Boscherini^{23b}, M. Bosman¹⁴, J.D. Bossio Sola¹⁰⁴,
 K. Bouaouda^{35a}, J. Boudreau¹³⁹, E.V. Bouhova-Thacker⁹⁰, D. Boumediene³⁸, S.K. Boutle⁵⁷,
 A. Boveia¹²⁷, J. Boyd³⁶, D. Boye^{33c,as}, I.R. Boyko⁸⁰, A.J. Bozson⁹⁴, J. Bracinik²¹, N. Brahimy¹⁰²,
 G. Brandt¹⁸², O. Brandt³², F. Braren⁴⁶, B. Brau¹⁰³, J.E. Brau¹³², W.D. Breaden Madden⁵⁷,
 K. Brendlinger⁴⁶, L. Brenner⁴⁶, R. Brenner¹⁷², S. Bressler¹⁸⁰, B. Brickwedde¹⁰⁰, D.L. Briglin²¹,
 D. Britton⁵⁷, D. Britzger¹¹⁵, I. Brock²⁴, R. Brock¹⁰⁷, G. Brooijmans³⁹, W.K. Brooks^{147d},
 E. Brost¹²¹, J.H. Broughton²¹, P.A. Bruckman de Renstrom⁸⁵, D. Bruncko^{28b}, A. Bruni^{23b},
 G. Bruni^{23b}, L.S. Bruni¹²⁰, S. Bruno^{74a,74b}, B.H. Brunt³², M. Bruschi^{23b}, N. Bruscino¹³⁹,
 P. Bryant³⁷, L. Bryngemark⁹⁷, T. Buanes¹⁷, Q. Buat³⁶, P. Buchholz¹⁵¹, A.G. Buckley⁵⁷,
 I.A. Budagov⁸⁰, M.K. Bugge¹³⁴, F. Bühner⁵², O. Bulekov¹¹², T.J. Burch¹²¹, S. Burdin⁹¹,
 C.D. Burgard¹²⁰, A.M. Burger¹³⁰, B. Burghgrave⁸, J.T.P. Burr⁴⁶, C.D. Burton¹¹,
 J.C. Burzynski¹⁰³, V. Büscher¹⁰⁰, E. Buschmann⁵³, P.J. Bussey⁵⁷, J.M. Butler²⁵, C.M. Buttar⁵⁷,
 J.M. Butterworth⁹⁵, P. Butti³⁶, W. Buttinger³⁶, A. Buzatu¹⁵⁸, A.R. Buzykaev^{122b,122a},
 G. Cabras^{23b,23a}, S. Cabrera Urbán¹⁷⁴, D. Caforio⁵⁶, H. Cai¹⁷³, V.M.M. Cairo¹⁵³, O. Cakir^{4a},
 N. Calace³⁶, P. Calafiura¹⁸, A. Calandri¹⁰², G. Calderini¹³⁶, P. Calfayan⁶⁶, G. Callea⁵⁷,
 L.P. Caloba^{81b}, S. Calvente Lopez⁹⁹, D. Calvet³⁸, S. Calvet³⁸, T.P. Calvet¹⁵⁵, M. Calvetti^{72a,72b},
 R. Camacho Toro¹³⁶, S. Camarda³⁶, D. Camarero Munoz⁹⁹, P. Camarri^{74a,74b}, D. Cameron¹³⁴,
 R. Caminal Armadans¹⁰³, C. Camincher³⁶, S. Campana³⁶, M. Campanelli⁹⁵, A. Camplani⁴⁰,
 A. Campoverde¹⁵¹, V. Canale^{70a,70b}, A. Canesse¹⁰⁴, M. Cano Bret^{60c}, J. Cantero¹³⁰, T. Cao¹⁶¹,
 Y. Cao¹⁷³, M.D.M. Capeans Garrido³⁶, M. Capua^{41b,41a}, R. Cardarelli^{74a}, F. Cardillo¹⁴⁹,
 G. Carducci^{41b,41a}, I. Carli¹⁴³, T. Carli³⁶, G. Carlino^{70a}, B.T. Carlson¹³⁹, L. Carminati^{69a,69b},
 R.M.D. Carney^{45a,45b}, S. Caron¹¹⁹, E. Carquin^{147d}, S. Carrá⁴⁶, J.W.S. Carter¹⁶⁷, M.P. Casado^{14,e},
 A.F. Casha¹⁶⁷, D.W. Casper¹⁷¹, R. Castelijns¹²⁰, F.L. Castillo¹⁷⁴, V. Castillo Gimenez¹⁷⁴,
 N.F. Castro^{140a,140e}, A. Catinaccio³⁶, J.R. Catmore¹³⁴, A. Cattai³⁶, J. Caudron²⁴, V. Cavaliere²⁹,
 E. Cavallaro¹⁴, M. Cavalli-Sforza¹⁴, V. Cavasinni^{72a,72b}, E. Celebi^{12b}, F. Ceradini^{75a,75b},
 L. Cerda Alberich¹⁷⁴, K. Cerny¹³¹, A.S. Cerqueira^{81a}, A. Cerri¹⁵⁶, L. Cerrito^{74a,74b}, F. Cerutti¹⁸,
 A. Cervelli^{23b,23a}, S.A. Cetin^{12b}, Z. Chadi^{35a}, D. Chakraborty¹²¹, S.K. Chan⁵⁹, W.S. Chan¹²⁰,
 W.Y. Chan⁹¹, J.D. Chapman³², B. Chargeishvili^{159b}, D.G. Charlton²¹, T.P. Charman⁹³,
 C.C. Chau³⁴, S. Che¹²⁷, S. Chekanov⁶, S.V. Chekulaev^{168a}, G.A. Chelkov⁸⁰, M.A. Chelstowska³⁶,
 B. Chen⁷⁹, C. Chen^{60a}, C.H. Chen⁷⁹, H. Chen²⁹, J. Chen^{60a}, J. Chen³⁹, S. Chen¹³⁷, S.J. Chen^{15c},
 X. Chen^{15b,aw}, Y. Chen⁸³, Y-H. Chen⁴⁶, H.C. Cheng^{63a}, H.J. Cheng^{15a}, A. Cheplakov⁸⁰,
 E. Cheremushkina¹²³, R. Cherkaoui El Moursli^{35e}, E. Cheu⁷, K. Cheung⁶⁴, T.J.A. Chevaléras¹⁴⁵,
 L. Chevalier¹⁴⁵, V. Chiarella⁵¹, G. Chiarelli^{72a}, G. Chiodini^{68a}, A.S. Chisholm²¹, A. Chitan^{27b},
 I. Chiu¹⁶³, Y.H. Chiu¹⁷⁶, M.V. Chizhov⁸⁰, K. Choi⁶⁶, A.R. Chomont^{73a,73b}, S. Chouridou¹⁶²,
 Y.S. Chow¹²⁰, M.C. Chu^{63a}, X. Chu^{15a,15d}, J. Chudoba¹⁴¹, A.J. Chuinard¹⁰⁴, J.J. Chwastowski⁸⁵,
 L. Chytka¹³¹, D. Cieri¹¹⁵, K.M. Ciesla⁸⁵, D. Cinca⁴⁷, V. Cindro⁹², I.A. Cioară^{27b}, A. Ciocio¹⁸,
 F. Ciroto^{70a,70b}, Z.H. Citron^{180,k}, M. Citterio^{69a}, D.A. Ciubotaru^{27b}, B.M. Ciungu¹⁶⁷,
 A. Clark⁵⁴, M.R. Clark³⁹, P.J. Clark⁵⁰, C. Clement^{45a,45b}, Y. Coadou¹⁰², M. Cokal^{67a,67c},
 A. Coccaro^{55b}, J. Cochran⁷⁹, H. Cohen¹⁶¹, A.E.C. Coimbra³⁶, L. Colasurdo¹¹⁹, B. Cole³⁹,

A.P. Colijn¹²⁰, J. Collot⁵⁸, P. Conde Muiño^{140a,f}, E. Coniavitis⁵², S.H. Connell^{33c},
 I.A. Connolly⁵⁷, S. Constantinescu^{27b}, F. Conventi^{70a,ay}, A.M. Cooper-Sarkar¹³⁵, F. Cormier¹⁷⁵,
 K.J.R. Cormier¹⁶⁷, L.D. Corpe⁹⁵, M. Corradi^{73a,73b}, E.E. Corrigan⁹⁷, F. Corriveau^{104,af},
 A. Cortes-Gonzalez³⁶, M.J. Costa¹⁷⁴, F. Costanza⁵, D. Costanzo¹⁴⁹, G. Cowan⁹⁴, J.W. Cowley³²,
 J. Crane¹⁰¹, K. Cranmer¹²⁵, S.J. Crawley⁵⁷, R.A. Creager¹³⁷, S. Crépé-Renaudin⁵⁸,
 F. Crescioli¹³⁶, M. Cristinziani²⁴, V. Croft¹²⁰, G. Crosetti^{41b,41a}, A. Cueto⁵,
 T. Cuhadar Donszelmann¹⁴⁹, A.R. Cukierman¹⁵³, S. Czekierda⁸⁵, P. Czodrowski³⁶,
 M.J. Da Cunha Sargedas De Sousa^{60b}, J.V. Da Fonseca Pinto^{81b}, C. Da Via¹⁰¹, W. Dabrowski^{84a},
 T. Dado^{28a}, S. Dahbi^{35e}, T. Dai¹⁰⁶, C. Dallapiccola¹⁰³, M. Dam⁴⁰, G. D’amen²⁹,
 V. D’Amico^{75a,75b}, J. Damp¹⁰⁰, J.R. Dandoy¹³⁷, M.F. Daneri³⁰, N.P. Dang^{181,j}, N.S. Dann¹⁰¹,
 M. Danninger¹⁷⁵, V. Dao³⁶, G. Darbo^{55b}, O. Dartsis⁵, A. Dattagupta¹³², T. Daubney⁴⁶,
 S. D’Auria^{69a,69b}, W. Davey²⁴, C. David⁴⁶, T. Davidek¹⁴³, D.R. Davis⁴⁹, I. Dawson¹⁴⁹, K. De⁸,
 R. De Asmundis^{70a}, M. De Beurs¹²⁰, S. De Castro^{23b,23a}, S. De Cecco^{73a,73b}, N. De Groot¹¹⁹,
 P. de Jong¹²⁰, H. De la Torre¹⁰⁷, A. De Maria^{15c}, D. De Pedis^{73a}, A. De Salvo^{73a},
 U. De Sanctis^{74a,74b}, M. De Santis^{74a,74b}, A. De Santo¹⁵⁶, K. De Vasconcelos Corga¹⁰²,
 J.B. De Vivie De Regie⁶⁵, C. Debenedetti¹⁴⁶, D.V. Dedovich⁸⁰, A.M. Deiana⁴²,
 M. Del Gaudio^{41b,41a}, J. Del Peso⁹⁹, Y. Delabat Diaz⁴⁶, D. Delgove⁶⁵, F. Deliot^{145,r},
 C.M. Delitzsch⁷, M. Della Pietra^{70a,70b}, D. Della Volpe⁵⁴, A. Dell’Acqua³⁶, L. Dell’Asta^{74a,74b},
 M. Delmastro⁵, C. Delporte⁶⁵, P.A. Delsart⁵⁸, D.A. DeMarco¹⁶⁷, S. Demers¹⁸³, M. Demichev⁸⁰,
 G. Demontigny¹¹⁰, S.P. Denisov¹²³, D. Denysiuk¹²⁰, L. D’Eramo¹³⁶, D. Derendarz⁸⁵,
 J.E. Derkaoui^{35d}, F. Derue¹³⁶, P. Dervan⁹¹, K. Desch²⁴, C. Deterre⁴⁶, K. Dette¹⁶⁷, C. Deutsch²⁴,
 M.R. Devesa³⁰, P.O. Deviveiros³⁶, A. Dewhurst¹⁴⁴, F.A. Di Bello⁵⁴, A. Di Ciaccio^{74a,74b},
 L. Di Ciaccio⁵, W.K. Di Clemente¹³⁷, C. Di Donato^{70a,70b}, A. Di Girolamo³⁶,
 G. Di Gregorio^{72a,72b}, B. Di Micco^{75a,75b}, R. Di Nardo¹⁰³, K.F. Di Petrillo⁵⁹, R. Di Sipio¹⁶⁷,
 D. Di Valentino³⁴, C. Diaconu¹⁰², F.A. Dias⁴⁰, T. Dias Do Vale^{140a}, M.A. Diaz^{147a},
 J. Dickinson¹⁸, E.B. Diehl¹⁰⁶, J. Dietrich¹⁹, S. Díez Cornell⁴⁶, A. Dimitrievska¹⁸, W. Ding^{15b},
 J. Dingfelder²⁴, F. Dittus³⁶, F. Djama¹⁰², T. Djobava^{159b}, J.I. Djuvsland¹⁷, M.A.B. Do Vale^{81c},
 M. Dobre^{27b}, D. Dodsworth²⁶, C. Doglioni⁹⁷, J. Dolejsi¹⁴³, Z. Dolezal¹⁴³, M. Donadelli^{81d},
 B. Dong^{60c}, J. Donini³⁸, A. D’onofrio⁹³, M. D’Onofrio⁹¹, J. Dopke¹⁴⁴, A. Doria^{70a}, M.T. Dova⁸⁹,
 A.T. Doyle⁵⁷, E. Drechsler¹⁵², E. Dreyer¹⁵², T. Dreyer⁵³, A.S. Drobac¹⁷⁰, Y. Duan^{60b},
 F. Dubinin¹¹¹, M. Dubovsky^{28a}, A. Dubreuil⁵⁴, E. Duchovni¹⁸⁰, G. Duckeck¹¹⁴, A. Ducourthial¹³⁶,
 O.A. Ducu¹¹⁰, D. Duda¹¹⁵, A. Dudarev³⁶, A.C. Dudder¹⁰⁰, E.M. Duffield¹⁸, L. Dufflot⁶⁵,
 M. Dührssen³⁶, C. Dülken¹⁸², M. Dumancic¹⁸⁰, A.E. Dumitriu^{27b}, A.K. Duncan⁵⁷, M. Dunford^{161a},
 A. Duperrin¹⁰², H. Duran Yildiz^{4a}, M. Düren⁵⁶, A. Durglishvili^{159b}, D. Duschinger⁴⁸, B. Dutta⁴⁶,
 D. Duvnjak¹, G.I. Dyckes¹³⁷, M. Dyndal³⁶, S. Dysch¹⁰¹, B.S. Dziedzic⁸⁵, K.M. Ecker¹¹⁵,
 R.C. Edgar¹⁰⁶, M.G. Eggleston⁴⁹, T. Eifert³⁶, G. Eigen¹⁷, K. Einsweiler¹⁸, T. Ekelof¹⁷²,
 H. El Jarrari^{35e}, M. El Kacimi^{35c}, R. El Kosseifi¹⁰², V. Ellajosyula¹⁷², M. Ellert¹⁷²,
 F. Ellinghaus¹⁸², A.A. Elliot⁹³, N. Ellis³⁶, J. Elmsheuser²⁹, M. Elsing³⁶, D. Emelianov¹⁴⁴,
 A. Emerman³⁹, Y. Enari¹⁶³, M.B. Epland⁴⁹, J. Erdmann⁴⁷, A. Ereditato²⁰, M. Errenst³⁶,
 M. Escalier⁶⁵, C. Escobar¹⁷⁴, O. Estrada Pastor¹⁷⁴, E. Etzion¹⁶¹, H. Evans⁶⁶, A. Ezhilov¹³⁸,
 F. Fabbri⁵⁷, L. Fabbri^{23b,23a}, V. Fabiani¹¹⁹, G. Facini⁹⁵, R.M. Faisca Rodrigues Pereira^{140a},
 R.M. Fakhruddinov¹²³, S. Falciano^{73a}, P.J. Falke⁵, S. Falke⁵, J. Faltova¹⁴³, Y. Fang^{15a},
 Y. Fang^{15a}, G. Fanourakis⁴⁴, M. Fanti^{69a,69b}, M. Faraj^{67a,67c,u}, A. Farbin⁸, A. Farilla^{75a},
 E.M. Farina^{71a,71b}, T. Farooque¹⁰⁷, S. Farrell¹⁸, S.M. Farrington⁵⁰, P. Farthouat³⁶, F. Fassi^{35e},
 P. Fassnacht³⁶, D. Fassouliotis⁹, M. Fauci Giannelli⁵⁰, W.J. Fawcett³², L. Fayard⁶⁵,
 O.L. Fedin^{138,p}, W. Fedorko¹⁷⁵, M. Feickert⁴², L. Feligioni¹⁰², A. Fell¹⁴⁹, C. Feng^{60b}, E.J. Feng³⁶,
 M. Feng⁴⁹, M.J. Fenton⁵⁷, A.B. Fenyuk¹²³, J. Ferrando⁴⁶, A. Ferrante¹⁷³, A. Ferrari¹⁷²,
 P. Ferrari¹²⁰, R. Ferrari^{71a}, D.E. Ferreira de Lima^{61b}, A. Ferrer¹⁷⁴, D. Ferrere⁵⁴, C. Ferretti¹⁰⁶,

F. Fiedler¹⁰⁰, A. Filipčić⁹², F. Filthaut¹¹⁹, K.D. Finelli²⁵, M.C.N. Fiolhais^{140a,140c,a}, L. Fiorini¹⁷⁴, F. Fischer¹¹⁴, W.C. Fisher¹⁰⁷, I. Fleck¹⁵¹, P. Fleischmann¹⁰⁶, R.R.M. Fletcher¹³⁷, T. Flick¹⁸², B.M. Flierl¹¹⁴, L. Flores¹³⁷, L.R. Flores Castillo^{63a}, F.M. Follega^{76a,76b}, N. Fomin¹⁷, J.H. Foo¹⁶⁷, G.T. Forcolin^{76a,76b}, A. Formica¹⁴⁵, F.A. Förster¹⁴, A.C. Forti¹⁰¹, A.G. Foster²¹, M.G. Foti¹³⁵, D. Fournier⁶⁵, H. Fox⁹⁰, P. Francavilla^{72a,72b}, S. Francescato^{73a,73b}, M. Franchini^{23b,23a}, S. Franchino^{61a}, D. Francis³⁶, L. Franconi²⁰, M. Franklin⁵⁹, A.N. Fray⁹³, P.M. Freeman²¹, B. Freund¹¹⁰, W.S. Freund^{81b}, E.M. Freundlich⁴⁷, D.C. Frizzell¹²⁹, D. Froidevaux³⁶, J.A. Frost¹³⁵, C. Fukunaga¹⁶⁴, E. Fullana Torregrosa¹⁷⁴, E. Fumagalli^{55b,55a}, T. Fusayasu¹¹⁶, J. Fuster¹⁷⁴, A. Gabrielli^{23b,23a}, A. Gabrielli¹⁸, G.P. Gach^{84a}, S. Gadatsch⁵⁴, P. Gadow¹¹⁵, G. Gagliardi^{55b,55a}, L.G. Gagnon¹¹⁰, C. Galea^{27b}, B. Galhardo^{140a}, G.E. Gallardo¹³⁵, E.J. Gallas¹³⁵, B.J. Gallop¹⁴⁴, G. Galster⁴⁰, R. Gamboa Goni⁹³, K.K. Gan¹²⁷, S. Ganguly¹⁸⁰, J. Gao^{60a}, Y. Gao⁵⁰, Y.S. Gao^{31,m}, C. García¹⁷⁴, J.E. García Navarro¹⁷⁴, J.A. García Pascual^{15a}, C. Garcia-Argos⁵², M. Garcia-Sciveres¹⁸, R.W. Gardner³⁷, N. Garelli¹⁵³, S. Gargiulo⁵², V. Garonne¹³⁴, A. Gaudiello^{55b,55a}, G. Gaudio^{71a}, I.L. Gavrilenko¹¹¹, A. Gavriilyuk¹²⁴, C. Gay¹⁷⁵, G. Gaycken⁴⁶, E.N. Gazis¹⁰, A.A. Geanta^{27b}, C.M. Gee¹⁴⁶, C.N.P. Gee¹⁴⁴, J. Geisen⁵³, M. Geisen¹⁰⁰, M.P. Geisler^{61a}, C. Gemme^{55b}, M.H. Genest⁵⁸, C. Geng¹⁰⁶, S. Gentile^{73a,73b}, S. George⁹⁴, T. Gerasis⁴⁴, L.O. Gerlach⁵³, P. Gessinger-Befurt¹⁰⁰, G. Gessner⁴⁷, S. Ghasemi¹⁵¹, M. Ghasemi Bostanabad¹⁷⁶, A. Ghosh⁶⁵, A. Ghosh⁷⁸, B. Giacobbe^{23b}, S. Giagu^{73a,73b}, N. Giangiacomi^{23b,23a}, P. Giannetti^{72a}, A. Giannini^{70a,70b}, G. Giannini¹⁴, S.M. Gibson⁹⁴, M. Gignac¹⁴⁶, D. Gillberg³⁴, G. Gilles¹⁸², D.M. Gingrich^{3,ax}, M.P. Giordani^{67a,67c}, F.M. Giorgi^{23b}, P.F. Giraud¹⁴⁵, G. Giugliarelli^{67a,67c}, D. Giugni^{69a}, F. Giuli^{74a,74b}, S. Gkaitatzis¹⁶², I. Gkialas^{9,h}, E.L. Gkoukousis¹⁴, P. Gkoutoumis¹⁰, L.K. Gladilin¹¹³, C. Glasman⁹⁹, J. Glatzer¹⁴, P.C.F. Glaysher⁴⁶, A. Glazov⁴⁶, G.R. Gledhill¹³², M. Goblirsch-Kolb²⁶, D. Godin¹¹⁰, S. Goldfarb¹⁰⁵, T. Golling⁵⁴, D. Golubkov¹²³, A. Gomes^{140a,140b}, R. Goncalves Gama⁵³, R. Gonçalo^{140a}, G. Gonella⁵², L. Gonella²¹, A. Gongadze⁸⁰, F. Gonnella²¹, J.L. Gonski⁵⁹, S. González de la Hoz¹⁷⁴, S. Gonzalez-Sevilla⁵⁴, G.R. Gonzalvo Rodriguez¹⁷⁴, L. Goossens³⁶, P.A. Gorbounov¹²⁴, H.A. Gordon²⁹, B. Gorini³⁶, E. Gorini^{68a,68b}, A. Gorišek⁹², A.T. Goshaw⁴⁹, M.I. Gostkin⁸⁰, C.A. Gottardo¹¹⁹, M. Gouighri^{35b}, D. Goujdami^{35c}, A.G. Goussiou¹⁴⁸, N. Govender^{33c}, C. Goy⁵, E. Gozani¹⁶⁰, I. Grabowska-Bold^{84a}, E.C. Graham⁹¹, J. Gramling¹⁷¹, E. Gramstad¹³⁴, S. Grancagnolo¹⁹, M. Grandi¹⁵⁶, V. Gratchev¹³⁸, P.M. Gravila^{27f}, F.G. Gravili^{68a,68b}, C. Gray⁵⁷, H.M. Gray¹⁸, C. Grefe²⁴, K. Gregersen⁹⁷, I.M. Gregor⁴⁶, P. Grenier¹⁵³, K. Grevtsov⁴⁶, C. Grieco¹⁴, N.A. Grieser¹²⁹, J. Griffiths⁸, A.A. Grillo¹⁴⁶, K. Grimm^{31,1}, S. Grinstein^{14,aa}, J.-F. Grivaz⁶⁵, S. Groh¹⁰⁰, E. Gross¹⁸⁰, J. Grosse-Knetter⁵³, Z.J. Grout⁹⁵, C. Grud¹⁰⁶, A. Grummer¹¹⁸, L. Guan¹⁰⁶, W. Guan¹⁸¹, J. Guenther³⁶, A. Guerguichon⁶⁵, J.G.R. Guerrero Rojas¹⁷⁴, F. Guescini¹¹⁵, D. Guest¹⁷¹, R. Gugel⁵², T. Guillemin⁵, S. Guindon³⁶, U. Gul⁵⁷, J. Guo^{60c}, W. Guo¹⁰⁶, Y. Guo^{60a,t}, Z. Guo¹⁰², R. Gupta⁴⁶, S. Gurbuz^{12c}, G. Gustavino¹²⁹, M. Guth⁵², P. Gutierrez¹²⁹, C. Gutsche⁹⁵, C. Guyot¹⁴⁵, C. Gwenlan¹³⁵, C.B. Gwilliam⁹¹, A. Haas¹²⁵, C. Haber¹⁸, H.K. Hadavand⁸, N. Haddad^{35e}, A. Hadeef^{60a}, S. Hageböck³⁶, M. Haleem¹⁷⁷, J. Haley¹³⁰, G. Halladjian¹⁰⁷, G.D. Hallewell¹⁰², K. Hamacher¹⁸², P. Hamal¹³¹, K. Hamano¹⁷⁶, H. Hamdaoui^{35e}, G.N. Hamity¹⁴⁹, K. Han^{60a,z}, L. Han^{60a}, S. Han^{15a}, Y.F. Han¹⁶⁷, K. Hanagaki^{82,x}, M. Hance¹⁴⁶, D.M. Handl¹¹⁴, B. Haney¹³⁷, R. Hankache¹³⁶, E. Hansen⁹⁷, J.B. Hansen⁴⁰, J.D. Hansen⁴⁰, M.C. Hansen²⁴, P.H. Hansen⁴⁰, E.C. Hanson¹⁰¹, K. Hara¹⁶⁹, T. Harenberg¹⁸², S. Harkusha¹⁰⁸, P.F. Harrison¹⁷⁸, N.M. Hartmann¹¹⁴, Y. Hasegawa¹⁵⁰, A. Hasib⁵⁰, S. Hassani¹⁴⁵, S. Haug²⁰, R. Hauser¹⁰⁷, L.B. Havener³⁹, M. Havranek¹⁴², C.M. Hawkes²¹, R.J. Hawkins³⁶, D. Hayden¹⁰⁷, C. Hayes¹⁵⁵, R.L. Hayes¹⁷⁵, C.P. Hays¹³⁵, J.M. Hays⁹³, H.S. Hayward⁹¹, S.J. Haywood¹⁴⁴, F. He^{60a}, M.P. Heath⁵⁰, V. Hedberg⁹⁷, L. Heelan⁸, S. Heer²⁴, K.K. Heidegger⁵², W.D. Heidorn⁷⁹, J. Heilman³⁴, S. Heim⁴⁶, T. Heim¹⁸, B. Heinemann^{46,at}, J.J. Heinrich¹³², L. Heinrich³⁶,

C. Heinz⁵⁶, J. Hejbal¹⁴¹, L. Helary^{61b}, A. Held¹⁷⁵, S. Hellesund¹³⁴, C.M. Helling¹⁴⁶,
 S. Hellman^{45a,45b}, C. Helsens³⁶, R.C.W. Henderson⁹⁰, Y. Heng¹⁸¹, S. Henkelmann¹⁷⁵,
 A.M. Henriques Correia³⁶, G.H. Herbert¹⁹, H. Herde²⁶, V. Herget¹⁷⁷, Y. Hernández Jiménez^{33e},
 H. Herr¹⁰⁰, M.G. Herrmann¹¹⁴, T. Herrmann⁴⁸, G. Herten⁵², R. Hertenberger¹¹⁴, L. Hervas³⁶,
 T.C. Herwig¹³⁷, G.G. Hesketh⁹⁵, N.P. Hessey^{168a}, A. Higashida¹⁶³, S. Higashino⁸²,
 E. Higón-Rodríguez¹⁷⁴, K. Hildebrand³⁷, E. Hill¹⁷⁶, J.C. Hill³², K.K. Hill²⁹, K.H. Hiller⁴⁶,
 S.J. Hillier²¹, M. Hils⁴⁸, I. Hinchliffe¹⁸, F. Hinterkeuser²⁴, M. Hirose¹³³, S. Hirose⁵²,
 D. Hirschbuehl¹⁸², B. Hiti⁹², O. Hladik¹⁴¹, D.R. Hlaluku^{33e}, X. Hoad⁵⁰, J. Hobbs¹⁵⁵, N. Hod¹⁸⁰,
 M.C. Hodgkinson¹⁴⁹, A. Hoecker³⁶, F. Hoenig¹¹⁴, D. Hohn⁵², D. Hohov⁶⁵, T.R. Holmes³⁷,
 M. Holzbock¹¹⁴, L.B.A.H. Hommels³², S. Honda¹⁶⁹, T.M. Hong¹³⁹, A. Hönle¹¹⁵,
 B.H. Hoerberman¹⁷³, W.H. Hopkins⁶, Y. Horii¹¹⁷, P. Horn⁴⁸, L.A. Horyn³⁷, S. Hou¹⁵⁸,
 A. Houmada^{35a}, J. Howarth¹⁰¹, J. Hoya⁸⁹, M. Hrabovsky¹³¹, J. Hrdinka⁷⁷, I. Hristova¹⁹,
 J. Hrivnac⁶⁵, A. Hrynevich¹⁰⁹, T. Hryn'ova⁵, P.J. Hsu⁶⁴, S.-C. Hsu¹⁴⁸, Q. Hu²⁹, S. Hu^{60c},
 D.P. Huang⁹⁵, Y. Huang^{60a}, Y. Huang^{15a}, Z. Hubacek¹⁴², F. Hubaut¹⁰², M. Huebner²⁴,
 F. Huegging²⁴, T.B. Huffman¹³⁵, M. Huhtinen³⁶, R.F.H. Hunter³⁴, P. Huo¹⁵⁵, A.M. Hupe³⁴,
 N. Huseynov^{80,ah}, J. Huston¹⁰⁷, J. Huth⁵⁹, R. Hyneman¹⁰⁶, S. Hyrych^{28a}, G. Iacobucci⁵⁴,
 G. Iakovidis²⁹, I. Ibragimov¹⁵¹, L. Iconomidou-Fayard⁶⁵, Z. Idrissi^{35e}, P. Iengo³⁶, R. Ignazzi⁴⁰,
 O. Igonkina^{120,ac,*}, R. Iguchi¹⁶³, T. Iizawa⁵⁴, Y. Ikegami⁸², M. Ikeno⁸², D. Iliadis¹⁶²,
 N. Ilic^{119,167,af}, F. Iltzsche⁴⁸, G. Introzzi^{71a,71b}, M. Iodice^{75a}, K. Iordanidou^{168a},
 V. Ippolito^{73a,73b}, M.F. Isacson¹⁷², M. Ishino¹⁶³, W. Islam¹³⁰, C. Issever¹³⁵, S. Istin¹⁶⁰, F. Ito¹⁶⁹,
 J.M. Iturbe Ponce^{63a}, R. Iuppa^{76a,76b}, A. Ivina¹⁸⁰, H. Iwasaki⁸², J.M. Izen⁴³, V. Izzo^{70a},
 P. Jacka¹⁴¹, P. Jackson¹, R.M. Jacobs²⁴, B.P. Jaeger¹⁵², V. Jain², G. Jäkel¹⁸², K.B. Jakobi¹⁰⁰,
 K. Jakobs⁵², S. Jakobsen⁷⁷, T. Jakoubek¹⁴¹, J. Jamieson⁵⁷, K.W. Janas^{84a}, R. Jansky⁵⁴,
 J. Janssen²⁴, M. Janus⁵³, P.A. Janus^{84a}, G. Jarlskog⁹⁷, N. Javadov^{80,ah}, T. Javůrek³⁶,
 M. Javurkova⁵², F. Jeanneau¹⁴⁵, L. Jeanty¹³², J. Jejelava^{159a,ai}, A. Jelinkas¹⁷⁸, P. Jenni^{52,b},
 J. Jeong⁴⁶, N. Jeong⁴⁶, S. Jézéquel⁵, H. Ji¹⁸¹, J. Jia¹⁵⁵, H. Jiang⁷⁹, Y. Jiang^{60a}, Z. Jiang^{153,q},
 S. Jiggins⁵², F.A. Jimenez Morales³⁸, J. Jimenez Pena¹¹⁵, S. Jin^{15c}, A. Jinaru^{27b}, O. Jinnouchi¹⁶⁵,
 H. Jivan^{33e}, P. Johansson¹⁴⁹, K.A. Johns⁷, C.A. Johnson⁶⁶, K. Jon-And^{45a,45b}, R.W.L. Jones⁹⁰,
 S.D. Jones¹⁵⁶, S. Jones⁷, T.J. Jones⁹¹, J. Jongmanns^{61a}, P.M. Jorge^{140a}, J. Jovicevic³⁶, X. Ju¹⁸,
 J.J. Junggeburth¹¹⁵, A. Juste Rozas^{14,aa}, A. Kaczmarska⁸⁵, M. Kado^{73a,73b}, H. Kagan¹²⁷,
 M. Kagan¹⁵³, C. Kahra¹⁰⁰, T. Kaji¹⁷⁹, E. Kajomovitz¹⁶⁰, C.W. Kalderon⁹⁷, A. Kaluza¹⁰⁰,
 A. Kamenshchikov¹²³, M. Kaneda¹⁶³, L. Kanjir⁹², Y. Kano¹⁶³, V.A. Kantserov¹¹², J. Kanzaki⁸²,
 L.S. Kaplan¹⁸¹, D. Kar^{33e}, K. Karava¹³⁵, M.J. Kareem^{168b}, S.N. Karpov⁸⁰, Z.M. Karpova⁸⁰,
 V. Kartvelishvili⁹⁰, A.N. Karyukhin¹²³, L. Kashif¹⁸¹, R.D. Kass¹²⁷, A. Kastanas^{45a,45b},
 C. Kato^{60d,60c}, J. Katzy⁴⁶, K. Kawade¹⁵⁰, K. Kawagoe⁸⁸, T. Kawaguchi¹¹⁷, T. Kawamoto¹⁶³,
 G. Kawamura⁵³, E.F. Kay¹⁷⁶, V.F. Kazanin^{122b,122a}, R. Keeler¹⁷⁶, R. Kehoe⁴², J.S. Keller³⁴,
 E. Kellermann⁹⁷, D. Kelsey¹⁵⁶, J.J. Kempster²¹, J. Kendrick²¹, O. Kepka¹⁴¹, S. Kersten¹⁸²,
 B.P. Kerševan⁹², S. Ketabchi Haghighat¹⁶⁷, M. Khader¹⁷³, F. Khalil-Zada¹³, M. Khandoga¹⁴⁵,
 A. Khanov¹³⁰, A.G. Kharlamov^{122b,122a}, T. Kharlamova^{122b,122a}, E.E. Khoda¹⁷⁵, A. Khodinov¹⁶⁶,
 T.J. Khoo⁵⁴, E. Khramov⁸⁰, J. Khubua^{159b}, S. Kido⁸³, M. Kiehn⁵⁴, C.R. Kilby⁹⁴, Y.K. Kim³⁷,
 N. Kimura⁹⁵, O.M. Kind¹⁹, B.T. King^{91,*}, D. Kirchmeier⁴⁸, J. Kirk¹⁴⁴, A.E. Kiryunin¹¹⁵,
 T. Kishimoto¹⁶³, D.P. Kisliuk¹⁶⁷, V. Kitali⁴⁶, O. Kivernyk⁵, T. Klapdor-Kleingrothaus⁵²,
 M. Klassen^{61a}, M.H. Klein¹⁰⁶, M. Klein⁹¹, U. Klein⁹¹, K. Kleinknecht¹⁰⁰, P. Klimek¹²¹,
 A. Klimentov²⁹, T. Klingl²⁴, T. Klioutchnikova³⁶, F.F. Klitzner¹¹⁴, P. Kluit¹²⁰, S. Kluth¹¹⁵,
 E. Kneringer⁷⁷, E.B.F.G. Knoop¹⁰², A. Knue⁵², D. Kobayashi⁸⁸, T. Kobayashi¹⁶³, M. Kobel⁴⁸,
 M. Kocian¹⁵³, P. Kodys¹⁴³, P.T. Koenig²⁴, T. Koffas³⁴, N.M. Köhler³⁶, T. Koi¹⁵³, M. Kolb^{61b},
 I. Koletsou⁵, T. Komarek¹³¹, T. Kondo⁸², N. Kondrashova^{60c}, K. Köneke⁵², A.C. König¹¹⁹,
 T. Kono¹²⁶, R. Konoplich^{125,ao}, V. Konstantinides⁹⁵, N. Konstantinidis⁹⁵, B. Konya⁹⁷,

R. Kopeliansky⁶⁶, S. Koperny^{84a}, K. Korcyl⁸⁵, K. Kordas¹⁶², G. Koren¹⁶¹, A. Korn⁹⁵,
I. Korolkov¹⁴, E.V. Korolkova¹⁴⁹, N. Korotkova¹¹³, O. Kortner¹¹⁵, S. Kortner¹¹⁵, T. Kosek¹⁴³,
V.V. Kostyukhin¹⁶⁶, A. Kotwal⁴⁹, A. Koulouris¹⁰, A. Kourkouveli-Charalampidi^{71a,71b},
C. Kourkouvelis⁹, E. Kourlitis¹⁴⁹, V. Kouskoura²⁹, A.B. Kowalewska⁸⁵, R. Kowalewski¹⁷⁶,
C. Kozakai¹⁶³, W. Kozanecki¹⁴⁵, A.S. Kozhin¹²³, V.A. Kramarenko¹¹³, G. Kramberger⁹²,
D. Krasnopevtsev^{60a}, M.W. Krasny¹³⁶, A. Krasznahorkay³⁶, D. Krauss¹¹⁵, J.A. Kremer^{84a},
J. Kretzschmar⁹¹, P. Krieger¹⁶⁷, F. Krieter¹¹⁴, A. Krishnan^{61b}, K. Krizka¹⁸, K. Kroeninger⁴⁷,
H. Kroha¹¹⁵, J. Kroll¹⁴¹, J. Kroll¹³⁷, J. Krstic¹⁶, U. Kruchonak⁸⁰, H. Krüger²⁴, N. Krumnack⁷⁹,
M.C. Kruse⁴⁹, J.A. Krzysiak⁸⁵, T. Kubota¹⁰⁵, O. Kuchinskaia¹⁶⁶, S. Kудay^{4b}, J.T. Kuechler⁴⁶,
S. Kuehn³⁶, A. Kugel^{61a}, T. Kuhl⁴⁶, V. Kukhtin⁸⁰, R. Kukla¹⁰², Y. Kulchitsky^{108,a1},
S. Kuleshov^{147d}, Y.P. Kulinich¹⁷³, M. Kuna⁵⁸, T. Kunigo⁸⁶, A. Kupco¹⁴¹, T. Kupfer⁴⁷,
O. Kuprash⁵², H. Kurashige⁸³, L.L. Kurchaninov^{168a}, Y.A. Kurochkin¹⁰⁸, A. Kurova¹¹²,
M.G. Kurth^{15a,15d}, E.S. Kuwertz³⁶, M. Kuze¹⁶⁵, A.K. Kvam¹⁴⁸, J. Kvita¹³¹, T. Kwan¹⁰⁴,
A. La Rosa¹¹⁵, L. La Rotonda^{41b,41a}, F. La Ruffa^{41b,41a}, C. Lacasta¹⁷⁴, F. Lacava^{73a,73b},
D.P.J. Lack¹⁰¹, H. Lacker¹⁹, D. Lacour¹³⁶, E. Ladygin⁸⁰, R. Lafaye⁵, B. Laforge¹³⁶, T. Lagouri^{33e},
S. Lai⁵³, S. Lammers⁶⁶, W. Lampl⁷, C. Lampoudis¹⁶², E. Lançon²⁹, U. Landgraf⁵²,
M.P.J. Landon⁹³, M.C. Lanfermann⁵⁴, V.S. Lang⁴⁶, J.C. Lange⁵³, R.J. Langenberg³⁶,
A.J. Lankford¹⁷¹, F. Lanni²⁹, K. Lantzsch²⁴, A. Lanza^{71a}, A. Lapertosa^{55b,55a}, S. Laplace¹³⁶,
J.F. Laporte¹⁴⁵, T. Lari^{69a}, F. Lasagni Manghi^{23b,23a}, M. Lassnig³⁶, T.S. Lau^{63a}, A. Laudrain⁶⁵,
A. Laurier³⁴, M. Lavorgna^{70a,70b}, S.D. Lawlor⁹⁴, M. Lazzaroni^{69a,69b}, B. Le¹⁰⁵, E. Le Guirriec¹⁰²,
M. LeBlanc⁷, T. LeCompte⁶, F. Ledroit-Guillon⁵⁸, A.C.A. Lee⁹⁵, C.A. Lee²⁹, G.R. Lee¹⁷,
L. Lee⁵⁹, S.C. Lee¹⁵⁸, S.J. Lee³⁴, B. Lefebvre^{168a}, M. Lefebvre¹⁷⁶, F. Legger¹¹⁴, C. Leggett¹⁸,
K. Lehmann¹⁵², N. Lehmann¹⁸², G. Lehmann Miotto³⁶, W.A. Leight⁴⁶, A. Leisos^{162,y},
M.A.L. Leite^{81d}, C.E. Leitgeb¹¹⁴, R. Leitner¹⁴³, D. Lellouch^{180,*}, K.J.C. Leney⁴², T. Lenz²⁴,
B. Lenzi³⁶, R. Leone⁷, S. Leone^{72a}, C. Leonidopoulos⁵⁰, A. Leopold¹³⁶, G. Lerner¹⁵⁶, C. Leroy¹¹⁰,
R. Les¹⁶⁷, C.G. Lester³², M. Levchenko¹³⁸, J. Levêque⁵, D. Levin¹⁰⁶, L.J. Levinson¹⁸⁰,
D.J. Lewis²¹, B. Li^{15b}, B. Li¹⁰⁶, C-Q. Li^{60a}, F. Li^{60c}, H. Li^{60a}, H. Li^{60b}, J. Li^{60c}, K. Li¹⁵³,
L. Li^{60c}, M. Li^{15a,15d}, Q. Li^{15a,15d}, Q.Y. Li^{60a}, S. Li^{60d,60c}, X. Li⁴⁶, Y. Li⁴⁶, Z. Li^{60b}, Z. Liang^{15a},
B. Liberti^{74a}, A. Liblong¹⁶⁷, K. Lie^{63c}, C.Y. Lin³², K. Lin¹⁰⁷, T.H. Lin¹⁰⁰, R.A. Linck⁶⁶,
J.H. Lindon²¹, A.L. Lioni⁵⁴, E. Lipeles¹³⁷, A. Lipniacka¹⁷, M. Lisovyi^{61b}, T.M. Liss^{173,av},
A. Lister¹⁷⁵, A.M. Litke¹⁴⁶, J.D. Little⁸, B. Liu⁷⁹, B.L. Liu⁶, H.B. Liu²⁹, H. Liu¹⁰⁶, J.B. Liu^{60a},
J.K.K. Liu¹³⁵, K. Liu¹³⁶, M. Liu^{60a}, P. Liu¹⁸, Y. Liu^{15a,15d}, Y.L. Liu¹⁰⁶, Y.W. Liu^{60a},
M. Livan^{71a,71b}, A. Lleres⁵⁸, J. Llorente Merino¹⁵², S.L. Lloyd⁹³, C.Y. Lo^{63b}, F. Lo Sterzo⁴²,
E.M. Lobodzinska⁴⁶, P. Loch⁷, S. Loffredo^{74a,74b}, T. Lohse¹⁹, K. Lohwasser¹⁴⁹, M. Lokajicek¹⁴¹,
J.D. Long¹⁷³, R.E. Long⁹⁰, L. Longo³⁶, K.A. Looper¹²⁷, J.A. Lopez^{147d}, I. Lopez Paz¹⁰¹,
A. Lopez Solis¹⁴⁹, J. Lorenz¹¹⁴, N. Lorenzo Martinez⁵, M. Losada^{22a}, P.J. Lösel¹¹⁴, A. Lösle⁵²,
X. Lou⁴⁶, X. Lou^{15a}, A. Lounis⁶⁵, J. Love⁶, P.A. Love⁹⁰, J.J. Lozano Bahilo¹⁷⁴, M. Lu^{60a},
Y.J. Lu⁶⁴, H.J. Lubatti¹⁴⁸, C. Luci^{73a,73b}, A. Lucotte⁵⁸, C. Luedtke⁵², F. Luehring⁶⁶, I. Luise¹³⁶,
L. Luminari^{73a}, B. Lund-Jensen¹⁵⁴, M.S. Lutz¹⁰³, D. Lynn²⁹, R. Lysak¹⁴¹, E. Lytken⁹⁷, F. Lyu^{15a},
V. Lyubushkin⁸⁰, T. Lyubushkina⁸⁰, H. Ma²⁹, L.L. Ma^{60b}, Y. Ma^{60b}, G. Maccarrone⁵¹,
A. Macchiolo¹¹⁵, C.M. Macdonald¹⁴⁹, J. Machado Miguens¹³⁷, D. Madaffari¹⁷⁴, R. Madar³⁸,
W.F. Mader⁴⁸, N. Madysa⁴⁸, J. Maeda⁸³, S. Maeland¹⁷, T. Maeno²⁹, M. Maerker⁴⁸,
A.S. Maevskiy¹¹³, V. Magerl⁵², N. Magini⁷⁹, D.J. Mahon³⁹, C. Maidantchik^{81b}, T. Maier¹¹⁴,
A. Maio^{140a,140b,140d}, K. Maj^{84a}, O. Majersky^{28a}, S. Majewski¹³², Y. Makida⁸², N. Makovec⁶⁵,
B. Malaescu¹³⁶, Pa. Malecki⁸⁵, V.P. Maleev¹³⁸, F. Malek⁵⁸, U. Mallik⁷⁸, D. Malon⁶, C. Malone³²,
S. Maltezos¹⁰, S. Malyukov⁸⁰, J. Mamuzic¹⁷⁴, G. Mancini⁵¹, I. Mandić⁹²,
L. Manhaes de Andrade Filho^{81a}, I.M. Maniatis¹⁶², J. Manjarres Ramos⁴⁸, K.H. Mankinen⁹⁷,
A. Mann¹¹⁴, A. Manousos⁷⁷, B. Mansoulie¹⁴⁵, I. Manthos¹⁶², S. Manzoni¹²⁰, A. Marantis¹⁶²,

G. Marceca³⁰, L. Marchese¹³⁵, G. Marchiori¹³⁶, M. Marcisovsky¹⁴¹, C. Marcon⁹⁷,
C.A. Marin Tobon³⁶, M. Marjanovic¹²⁹, Z. Marshall¹⁸, M.U.F. Martensson¹⁷², S. Marti-Garcia¹⁷⁴,
C.B. Martin¹²⁷, T.A. Martin¹⁷⁸, V.J. Martin⁵⁰, B. Martin dit Latour¹⁷, L. Martinelli^{75a,75b},
M. Martinez^{14,aa}, V.I. Martinez Outschoorn¹⁰³, S. Martin-Haugh¹⁴⁴, V.S. Martoiu^{27b},
A.C. Martyniuk⁹⁵, A. Marzin³⁶, S.R. Maschek¹¹⁵, L. Masetti¹⁰⁰, T. Mashimo¹⁶³,
R. Mashinistov¹¹¹, J. Masik¹⁰¹, A.L. Maslennikov^{122b,122a}, L. Massa^{74a,74b}, P. Massarotti^{70a,70b},
P. Mastrandrea^{72a,72b}, A. Mastroberardino^{41b,41a}, T. Masubuchi¹⁶³, D. Matakias¹⁰, A. Matic¹¹⁴,
P. Mättig²⁴, J. Maurer^{27b}, B. Maček⁹², D.A. Maximov^{122b,122a}, R. Mazini¹⁵⁸, I. Maznas¹⁶²,
S.M. Mazza¹⁴⁶, S.P. Mc Kee¹⁰⁶, T.G. McCarthy¹¹⁵, W.P. McCormack¹⁸, E.F. McDonald¹⁰⁵,
J.A. Mcfayden³⁶, G. Mchedlidze^{159b}, M.A. McKay⁴², K.D. McLean¹⁷⁶, S.J. McMahon¹⁴⁴,
P.C. McNamara¹⁰⁵, C.J. McNicol¹⁷⁸, R.A. McPherson^{176,af}, J.E. Mdhului^{33e}, Z.A. Meadows¹⁰³,
S. Meehan³⁶, T. Megy⁵², S. Mehlhase¹¹⁴, A. Mehta⁹¹, T. Meideck⁵⁸, B. Meirose⁴³, D. Melini¹⁷⁴,
B.R. Mellado Garcia^{33e}, J.D. Mellenthin⁵³, M. Melo^{28a}, F. Meloni⁴⁶, A. Melzer²⁴, S.B. Menary¹⁰¹,
E.D. Mendes Gouveia^{140a,140e}, L. Meng³⁶, X.T. Meng¹⁰⁶, S. Menke¹¹⁵, E. Meoni^{41b,41a},
S. Mergelmeyer¹⁹, S.A.M. Merkt¹³⁹, C. Merlassino²⁰, P. Mermod⁵⁴, L. Merola^{70a,70b},
C. Meroni^{69a}, O. Meshkov^{113,111}, J.K.R. Meshreki¹⁵¹, A. Messina^{73a,73b}, J. Metcalfe⁶,
A.S. Mete¹⁷¹, C. Meyer⁶⁶, J. Meyer¹⁶⁰, J.-P. Meyer¹⁴⁵, H. Meyer Zu Theenhausen^{61a}, F. Miano¹⁵⁶,
M. Michetti¹⁹, R.P. Middleton¹⁴⁴, L. Mijović⁵⁰, G. Mikenberg¹⁸⁰, M. Mikestikova¹⁴¹, M. Mikuz⁹²,
H. Mildner¹⁴⁹, M. Milesi¹⁰⁵, A. Milic¹⁶⁷, D.A. Millar⁹³, D.W. Miller³⁷, A. Milov¹⁸⁰,
D.A. Milstead^{45a,45b}, R.A. Mina^{153,q}, A.A. Minaenko¹²³, M. Miñano Moya¹⁷⁴, I.A. Minashvili^{159b},
A.I. Mincer¹²⁵, B. Mindur^{84a}, M. Mineev⁸⁰, Y. Minegishi¹⁶³, L.M. Mir¹⁴, A. Mirto^{68a,68b},
K.P. Mistry¹³⁷, T. Mitani¹⁷⁹, J. Mitrevski¹¹⁴, V.A. Mitsou¹⁷⁴, M. Mittal^{60c}, O. Miu¹⁶⁷,
A. Miucci²⁰, P.S. Miyagawa¹⁴⁹, A. Mizukami⁸², J.U. Mjörnmark⁹⁷, T. Mkrtychyan¹⁸⁴,
M. Mlynarikova¹⁴³, T. Moa^{45a,45b}, K. Mochizuki¹¹⁰, P. Mogg⁵², S. Mohapatra³⁹, R. Moles-Valls²⁴,
M.C. Mondragon¹⁰⁷, K. Mönig⁴⁶, J. Monk⁴⁰, E. Monnier¹⁰², A. Montalbano¹⁵²,
J. Montejo Berlingen³⁶, M. Montella⁹⁵, F. Monticelli⁸⁹, S. Monzani^{69a}, N. Morange⁶⁵,
D. Moreno^{22a}, M. Moreno Llácer³⁶, C. Moreno Martinez¹⁴, P. Morettini^{55b}, M. Morgenstern¹²⁰,
S. Morgenstern⁴⁸, D. Mori¹⁵², M. Morii⁵⁹, M. Morinaga¹⁷⁹, V. Morisbak¹³⁴, A.K. Morley³⁶,
G. Mornacchi³⁶, A.P. Morris⁹⁵, L. Morvaj¹⁵⁵, P. Moschovakos³⁶, B. Moser¹²⁰, M. Mosidze^{159b},
T. Moskalets¹⁴⁵, H.J. Moss¹⁴⁹, J. Moss^{31,n}, E.J.W. Moyses¹⁰³, S. Muanza¹⁰², J. Mueller¹³⁹,
R.S.P. Mueller¹¹⁴, D. Muenstermann⁹⁰, G.A. Mullier⁹⁷, J.L. Munoz Martinez¹⁴,
F.J. Munoz Sanchez¹⁰¹, P. Murin^{28b}, W.J. Murray^{178,144}, A. Murrone^{69a,69b}, M. Muškinja¹⁸,
C. Mwewa^{33a}, A.G. Myagkov^{123,ap}, J. Myers¹³², M. Myska¹⁴², B.P. Nachman¹⁸, O. Nackenhurst⁴⁷,
A.Nag Nag⁴⁸, K. Nagai¹³⁵, K. Nagano⁸², Y. Nagasaka⁶², M. Nagel⁵², J.L. Nagle²⁹, E. Nagy¹⁰²,
A.M. Nairz³⁶, Y. Nakahama¹¹⁷, K. Nakamura⁸², T. Nakamura¹⁶³, I. Nakano¹²⁸, H. Nanjo¹³³,
F. Napolitano^{61a}, R.F. Naranjo Garcia⁴⁶, R. Narayan⁴², I. Naryshkin¹³⁸, T. Naumann⁴⁶,
G. Navarro^{22a}, H.A. Neal^{106,*}, P.Y. Nechaeva¹¹¹, F. Nechansky⁴⁶, T.J. Neep²¹, A. Negri^{71a,71b},
M. Negrini^{23b}, C. Nellist⁵³, M.E. Nelson¹³⁵, S. Nemecek¹⁴¹, P. Nemeti¹²⁵, M. Nessi^{36,d},
M.S. Neubauer¹⁷³, M. Neumann¹⁸², P.R. Newman²¹, Y.S. Ng¹⁹, Y.W.Y. Ng¹⁷¹, B. Ngair^{35e},
H.D.N. Nguyen¹⁰², T. Nguyen Manh¹¹⁰, E. Nibigira³⁸, R.B. Nickerson¹³⁵, R. Nicolaidou¹⁴⁵,
D.S. Nielsen⁴⁰, J. Nielsen¹⁴⁶, N. Nikiforou¹¹, V. Nikolaenko^{123,ap}, I. Nikolic-Audit¹³⁶,
K. Nikolopoulos²¹, P. Nilsson²⁹, H.R. Nindhito⁵⁴, Y. Ninomiya⁸², A. Nisati^{73a}, N. Nishu^{60c},
R. Nisius¹¹⁵, I. Nitsche⁴⁷, T. Nitta¹⁷⁹, T. Nobe¹⁶³, Y. Noguchi⁸⁶, I. Nomidis¹³⁶, M.A. Nomura²⁹,
M. Nordberg³⁶, N. Norjoharuddeen¹³⁵, T. Novak⁹², O. Novgorodova⁴⁸, R. Novotny¹⁴²,
L. Nozka¹³¹, K. Ntekas¹⁷¹, E. Nurse⁹⁵, F.G. Oakham^{34,ax}, H. Oberlack¹¹⁵, J. Ocariz¹³⁶,
A. Ochi⁸³, I. Ochoa³⁹, J.P. Ochoa-Ricoux^{147a}, K. O'Connor²⁶, S. Oda⁸⁸, S. Odaka⁸², S. Oerdek⁵³,
A. Ogrodnik^{84a}, A. Oh¹⁰¹, S.H. Oh⁴⁹, C.C. Ohm¹⁵⁴, H. Oide¹⁶⁵, M.L. Ojeda¹⁶⁷, H. Okawa¹⁶⁹,
Y. Okazaki⁸⁶, Y. Okumura¹⁶³, T. Okuyama⁸², A. Olariu^{27b}, L.F. Oleiro Seabra^{140a},

S.A. Olivares Pino^{147a}, D. Oliveira Damazio²⁹, J.L. Oliver¹, M.J.R. Olsson¹⁷¹, A. Olszewski⁸⁵, J. Olszowska⁸⁵, D.C. O’Neil¹⁵², A.P. O’neill¹³⁵, A. Onofre^{140a,140e}, P.U.E. Onyisi¹¹, H. Oppen¹³⁴, M.J. Oreglia³⁷, G.E. Orellana⁸⁹, D. Orestano^{75a,75b}, N. Orlando¹⁴, R.S. Orr¹⁶⁷, V. O’Shea⁵⁷, R. Ospanov^{60a}, G. Otero y Garzon³⁰, H. Otono⁸⁸, P.S. Ott^{61a}, M. Ouchrif^{35d}, J. Ouellette²⁹, F. Ould-Saada¹³⁴, A. Ouraou¹⁴⁵, Q. Ouyang^{15a}, M. Owen⁵⁷, R.E. Owen²¹, V.E. Ozcan^{12c}, N. Ozturk⁸, J. Pacalt¹³¹, H.A. Pacey³², K. Pachal⁴⁹, A. Pacheco Pages¹⁴, C. Padilla Aranda¹⁴, S. Pagan Griso¹⁸, M. Paganini¹⁸³, G. Palacino⁶⁶, S. Palazzo⁵⁰, S. Palestini³⁶, M. Palka^{84b}, D. Pallin³⁸, I. Panagoulas¹⁰, C.E. Pandini³⁶, J.G. Panduro Vazquez⁹⁴, P. Pani⁴⁶, G. Panizzo^{67a,67c}, L. Paolozzi⁵⁴, C. Papadatos¹¹⁰, K. Papageorgiou^{9,h}, S. Parajuli⁴³, A. Paramonov⁶, D. Paredes Hernandez^{63b}, S.R. Paredes Saenz¹³⁵, B. Parida¹⁶⁶, T.H. Park¹⁶⁷, A.J. Parker³¹, M.A. Parker³², F. Parodi^{55b,55a}, E.W. Parrish¹²¹, J.A. Parsons³⁹, U. Parzefall⁵², L. Pascual Dominguez¹³⁶, V.R. Pascuzzi¹⁶⁷, J.M.P. Pasner¹⁴⁶, E. Pasqualucci^{73a}, S. Passaggio^{55b}, F. Pastore⁹⁴, P. Pasuwan^{45a,45b}, S. Pataraiia¹⁰⁰, J.R. Pater¹⁰¹, A. Pathak^{181,j}, T. Pauly³⁶, B. Pearson¹¹⁵, M. Pedersen¹³⁴, L. Pedraza Diaz¹¹⁹, R. Pedro^{140a}, T. Peiffer⁵³, S.V. Peleganchuk^{122b,122a}, O. Penc¹⁴¹, H. Peng^{60a}, B.S. Peralva^{81a}, M.M. Perego⁶⁵, A.P. Pereira Peixoto^{140a}, D.V. Perepelitsa²⁹, F. Peri¹⁹, L. Perini^{69a,69b}, H. Pernegger³⁶, S. Perrella^{70a,70b}, K. Peters⁴⁶, R.F.Y. Peters¹⁰¹, B.A. Petersen³⁶, T.C. Petersen⁴⁰, E. Petit¹⁰², A. Petridis¹, C. Petridou¹⁶², P. Petroff⁶⁵, M. Petrov¹³⁵, F. Petrucci^{75a,75b}, M. Pettee¹⁸³, N.E. Pettersson¹⁰³, K. Petukhova¹⁴³, A. Peyaud¹⁴⁵, R. Pezoa^{147d}, L. Pezzotti^{71a,71b}, T. Pham¹⁰⁵, F.H. Phillips¹⁰⁷, P.W. Phillips¹⁴⁴, M.W. Phipps¹⁷³, G. Piacquadio¹⁵⁵, E. Pianori¹⁸, A. Picazio¹⁰³, R.H. Pickles¹⁰¹, R. Piegaiia³⁰, D. Pietreanu^{27b}, J.E. Pilcher³⁷, A.D. Pilkington¹⁰¹, M. Pinamonti^{74a,74b}, J.L. Pinfeld³, M. Pitt¹⁶¹, L. Pizzimento^{74a,74b}, M.-A. Pleier²⁹, V. Pleskot¹⁴³, E. Plotnikova⁸⁰, P. Podberezko^{122b,122a}, R. Poettgen⁹⁷, R. Poggi⁵⁴, L. Poggioli⁶⁵, I. Pogrebnyak¹⁰⁷, D. Pohl²⁴, I. Pokharel⁵³, G. Polesello^{71a}, A. Poley¹⁸, A. Policicchio^{73a,73b}, R. Polifka¹⁴³, A. Polini^{23b}, C.S. Pollard⁴⁶, V. Polychronakos²⁹, D. Ponomarenko¹¹², L. Pontecorvo³⁶, S. Popa^{27a}, G.A. Popeneciu^{27d}, L. Portales⁵, D.M. Portillo Quintero⁵⁸, S. Pospisil¹⁴², K. Potamianos⁴⁶, I.N. Potrap⁸⁰, C.J. Potter³², H. Potti¹¹, T. Poulsen⁹⁷, J. Poveda³⁶, T.D. Powell¹⁴⁹, G. Pownall⁴⁶, M.E. Pozo Astigarraga³⁶, P. Pralavorio¹⁰², S. Prell⁷⁹, D. Price¹⁰¹, M. Primavera^{68a}, S. Prince¹⁰⁴, M.L. Proffitt¹⁴⁸, N. Proklova¹¹², K. Prokofiev^{63c}, F. Prokoshin⁸⁰, S. Protopopescu²⁹, J. Proudfoot⁶, M. Przybycien^{84a}, D. Pudzha¹³⁸, A. Puri¹⁷³, P. Puzo⁶⁵, J. Qian¹⁰⁶, Y. Qin¹⁰¹, A. Quadt⁵³, M. Queitsch-Maitland⁴⁶, A. Qureshi¹, M. Racko^{28a}, P. Rados¹⁰⁵, F. Ragusa^{69a,69b}, G. Rahal⁹⁸, J.A. Raine⁵⁴, S. Rajagopalan²⁹, A. Ramirez Morales⁹³, K. Ran^{15a,15d}, T. Rashid⁶⁵, S. Raspopov⁵, D.M. Rauch⁴⁶, F. Rauscher¹¹⁴, S. Rave¹⁰⁰, B. Ravina¹⁴⁹, I. Ravinovich¹⁸⁰, J.H. Rawling¹⁰¹, M. Raymond³⁶, A.L. Read¹³⁴, N.P. Readioff⁵⁸, M. Reale^{68a,68b}, D.M. Rebuffi^{71a,71b}, A. Redelbach¹⁷⁷, G. Redlinger²⁹, K. Reeves⁴³, L. Rehnisch¹⁹, J. Reichert¹³⁷, D. Reikher¹⁶¹, A. Reiss¹⁰⁰, A. Rej¹⁵¹, C. Rembser³⁶, M. Renda^{27b}, M. Rescigno^{73a}, S. Resconi^{69a}, E.D. Resseguie¹³⁷, S. Rettie¹⁷⁵, E. Reynolds²¹, O.L. Rezanova^{122b,122a}, P. Reznicek¹⁴³, E. Ricci^{76a,76b}, R. Richter¹¹⁵, S. Richter⁴⁶, E. Richter-Was^{84b}, O. Ricken²⁴, M. Ridel¹³⁶, P. Rieck¹¹⁵, C.J. Riegel¹⁸², O. Rifki⁴⁶, M. Rijssenbeek¹⁵⁵, A. Rimoldi^{71a,71b}, M. Rimoldi⁴⁶, L. Rinaldi^{23b}, G. Ripellino¹⁵⁴, I. Riu¹⁴, J.C. Rivera Vergara¹⁷⁶, F. Rizatdinova¹³⁰, E. Rizvi⁹³, C. Rizzi³⁶, R.T. Roberts¹⁰¹, S.H. Robertson^{104,af}, M. Robin⁴⁶, D. Robinson³², J.E.M. Robinson⁴⁶, C.M. Robles Gajardo^{147d}, A. Robson⁵⁷, A. Rocchi^{74a,74b}, E. Rocco¹⁰⁰, C. Roda^{72a,72b}, S. Rodriguez Bosca¹⁷⁴, A. Rodriguez Perez¹⁴, D. Rodriguez Rodriguez¹⁷⁴, A.M. Rodríguez Vera^{168b}, S. Roe³⁶, O. Røhne¹³⁴, R. Röhrig¹¹⁵, C.P.A. Roland⁶⁶, J. Roloff⁵⁹, A. Romaniouk¹¹², M. Romano^{23b,23a}, N. Rompotis⁹¹, M. Ronzani¹²⁵, L. Roos¹³⁶, S. Rosati^{73a}, K. Rosbach⁵², G. Rosin¹⁰³, B.J. Rosser¹³⁷, E. Rossi⁴⁶, E. Rossi^{75a,75b}, E. Rossi^{70a,70b}, L.P. Rossi^{55b}, L. Rossini^{69a,69b}, R. Rosten¹⁴, M. Rotaru^{27b}, J. Rothberg¹⁴⁸, D. Rousseau⁶⁵, G. Rovelli^{71a,71b}, A. Roy¹¹, D. Roy^{33e},

A. Rozanov¹⁰², Y. Rozen¹⁶⁰, X. Ruan^{33e}, F. Rubbo¹⁵³, F. Rühr⁵², A. Ruiz-Martinez¹⁷⁴,
 A. Rummeler³⁶, Z. Rurikova⁵², N.A. Rusakovich⁸⁰, H.L. Russell¹⁰⁴, L. Rustige^{38,47},
 J.P. Rutherford⁷, E.M. Rüttinger¹⁴⁹, M. Rybar³⁹, G. Rybkin⁶⁵, E.B. Rye¹³⁴, A. Ryzhov¹²³,
 P. Sabatini⁵³, G. Sabato¹²⁰, S. Sacerdoti⁶⁵, H.F.W. Sadrozinski¹⁴⁶, R. Sadykov⁸⁰,
 F. Safai Tehrani^{73a}, B. Safarzadeh Samani¹⁵⁶, P. Saha¹²¹, S. Saha¹⁰⁴, M. Sahinsoy^{61a}, A. Sahu¹⁸²,
 M. Saimpert⁴⁶, M. Saito¹⁶³, T. Saito¹⁶³, H. Sakamoto¹⁶³, A. Sakharov^{125,ao}, D. Salamani⁵⁴,
 G. Salamanna^{75a,75b}, J.E. Salazar Loyola^{147d}, P.H. Sales De Bruin¹⁷², A. Salnikov¹⁵³, J. Salt¹⁷⁴,
 D. Salvatore^{41b,41a}, F. Salvatore¹⁵⁶, A. Salvucci^{63a,63b,63c}, A. Salzburger³⁶, J. Samarati³⁶,
 D. Sammel⁵², D. Sampsonidis¹⁶², D. Sampsonidou¹⁶², J. Sánchez¹⁷⁴, A. Sanchez Pineda^{67a,67c},
 H. Sandaker¹³⁴, C.O. Sander⁴⁶, I.G. Sanderswood⁹⁰, M. Sandhoff¹⁸², C. Sandoval^{22a},
 D.P.C. Sankey¹⁴⁴, M. Sannino^{55b,55a}, Y. Sano¹¹⁷, A. Sansoni⁵¹, C. Santoni³⁸, H. Santos^{140a,140b},
 S.N. Santpur¹⁸, A. Santra¹⁷⁴, A. Sapronov⁸⁰, J.G. Saraiva^{140a,140d}, O. Sasaki⁸², K. Sato¹⁶⁹,
 F. Sauerburger⁵², E. Sauvan⁵, P. Savard^{167,ax}, N. Savic¹¹⁵, R. Sawada¹⁶³, C. Sawyer¹⁴⁴,
 L. Sawyer^{96,am}, C. Sbarra^{23b}, A. Sbrizzi^{23a}, T. Scanlon⁹⁵, J. Schaarschmidt¹⁴⁸, P. Schacht¹¹⁵,
 B.M. Schachtner¹¹⁴, D. Schaefer³⁷, L. Schaefer¹³⁷, J. Schaeffer¹⁰⁰, S. Schaepe³⁶, U. Schäfer¹⁰⁰,
 A.C. Schaffer⁶⁵, D. Schaile¹¹⁴, R.D. Schamberger¹⁵⁵, N. Scharmberg¹⁰¹, V.A. Schegelsky¹³⁸,
 D. Scheirich¹⁴³, F. Schenck¹⁹, M. Schernau¹⁷¹, C. Schiavi^{55b,55a}, S. Schier¹⁴⁶, L.K. Schildgen²⁴,
 Z.M. Schillaci²⁶, E.J. Schioppa³⁶, M. Schioppa^{41b,41a}, K.E. Schleicher⁵², S. Schlenker³⁶,
 K.R. Schmidt-Sommerfeld¹¹⁵, K. Schmieden³⁶, C. Schmitt¹⁰⁰, S. Schmitt⁴⁶, S. Schmitz¹⁰⁰,
 J.C. Schmoeckel⁴⁶, U. Schnoor⁵², L. Schoeffel¹⁴⁵, A. Schoening^{61b}, P.G. Scholer⁵², E. Schopf¹³⁵,
 M. Schott¹⁰⁰, J.F.P. Schouwenberg¹¹⁹, J. Schovancova³⁶, S. Schramm⁵⁴, F. Schroeder¹⁸²,
 A. Schulte¹⁰⁰, H-C. Schultz-Coulon^{61a}, M. Schumacher⁵², B.A. Schumm¹⁴⁶, Ph. Schune¹⁴⁵,
 A. Schwartzman¹⁵³, T.A. Schwarz¹⁰⁶, Ph. Schwemling¹⁴⁵, R. Schwienhorst¹⁰⁷, A. Sciandra¹⁴⁶,
 G. Sciolla²⁶, M. Scodreggio⁴⁶, M. Scornajenghi^{41b,41a}, F. Scuri^{72a}, F. Scutti¹⁰⁵, L.M. Scyboz¹¹⁵,
 C.D. Sebastiani^{73a,73b}, P. Seema¹⁹, S.C. Seidel¹¹⁸, A. Seiden¹⁴⁶, B.D. Seidlitz²⁹, T. Seiss³⁷,
 J.M. Seixas^{81b}, G. Sekhniaidze^{70a}, K. Sekhon¹⁰⁶, S.J. Sekula⁴², N. Semprini-Cesari^{23b,23a},
 S. Sen⁴⁹, S. Senkin³⁸, C. Serfon⁷⁷, L. Serin⁶⁵, L. Serkin^{67a,67b}, M. Sessa^{60a}, H. Severini¹²⁹,
 T. Šfiligoj⁹², F. Sforza^{55b,55a}, A. Sfyrta⁵⁴, E. Shabalina⁵³, J.D. Shahinian¹⁴⁶, N.W. Shaikh^{45a,45b},
 D. Shaked Renous¹⁸⁰, L.Y. Shan^{15a}, R. Shang¹⁷³, J.T. Shank²⁵, M. Shapiro¹⁸, A. Sharma¹³⁵,
 A.S. Sharma¹, P.B. Shatalov¹²⁴, K. Shaw¹⁵⁶, S.M. Shaw¹⁰¹, A. Shcherbakova¹³⁸, M. Shehade¹⁸⁰,
 Y. Shen¹²⁹, N. Sherafati³⁴, A.D. Sherman²⁵, P. Sherwood⁹⁵, L. Shi^{158,au}, S. Shimizu⁸²,
 C.O. Shimmin¹⁸³, Y. Shimogama¹⁷⁹, M. Shimojima¹¹⁶, I.P.J. Shipsey¹³⁵, S. Shirabe⁸⁸,
 M. Shiyakova^{80,ad}, J. Shlomi¹⁸⁰, A. Shmeleva¹¹¹, M.J. Shochet³⁷, J. Shojaii¹⁰⁵, D.R. Shope¹²⁹,
 S. Shrestha¹²⁷, E.M. Shrif^{33e}, E. Shulga¹⁸⁰, P. Sicho¹⁴¹, A.M. Sickles¹⁷³, P.E. Sidebo¹⁵⁴,
 E. Sideras Haddad^{33e}, O. Sidiropoulou³⁶, A. Sidoti^{23b,23a}, F. Siegert⁴⁸, Dj. Sijacki¹⁶,
 M.Jr. Silva¹⁸¹, M.V. Silva Oliveira^{81a}, S.B. Silverstein^{45a}, S. Simion⁶⁵, E. Simioni¹⁰⁰,
 R. Simoniello¹⁰⁰, S. Simsek^{12b}, P. Sinervo¹⁶⁷, V. Sinetkii^{113,111}, N.B. Sinev¹³², M. Sioli^{23b,23a},
 I. Siral¹⁰⁶, S.Yu. Sivoklov¹¹³, J. Sjölin^{45a,45b}, E. Skorda⁹⁷, P. Skubic¹²⁹, M. Slawinska⁸⁵,
 K. Sliwa¹⁷⁰, R. Slovak¹⁴³, V. Smakhtin¹⁸⁰, B.H. Smart¹⁴⁴, J. Smiesko^{28a}, N. Smirnov¹¹²,
 S.Yu. Smirnov¹¹², Y. Smirnov¹¹², L.N. Smirnova^{113,v}, O. Smirnova⁹⁷, J.W. Smith⁵³,
 M. Smizanska⁹⁰, K. Smolek¹⁴², A. Smykiewicz⁸⁵, A.A. Snesev¹¹¹, H.L. Snoek¹²⁰,
 I.M. Snyder¹³², S. Snyder²⁹, R. Sobie^{176,af}, A. Soffer¹⁶¹, A. Sogaard⁵⁰, F. Sohns⁵³,
 C.A. Solans Sanchez³⁶, E.Yu. Soldatov¹¹², U. Soldevila¹⁷⁴, A.A. Solodkov¹²³, A. Soloshenko⁸⁰,
 O.V. Solovyanov¹²³, V. Solovyev¹³⁸, P. Sommer¹⁴⁹, H. Son¹⁷⁰, W. Song¹⁴⁴, W.Y. Song^{168b},
 A. Sopczak¹⁴², F. Sopkova^{28b}, C.L. Sotiropoulou^{72a,72b}, S. Sottocornola^{71a,71b}, R. Soualah^{67a,67c,g},
 A.M. Soukharev^{122b,122a}, D. South⁴⁶, S. Spagnolo^{68a,68b}, M. Spalla¹¹⁵, M. Spangenberg¹⁷⁸,
 F. Spano⁹⁴, D. Sperlich⁵², T.M. Spieker^{61a}, R. Spighi^{23b}, G. Spigo³⁶, M. Spina¹⁵⁶, D.P. Spiteri⁵⁷,
 M. Spousta¹⁴³, A. Stabile^{69a,69b}, B.L. Stamas¹²¹, R. Stamen^{61a}, M. Stamenkovic¹²⁰,

E. Stanecka⁸⁵, B. Stanislaus¹³⁵, M.M. Stanitzki⁴⁶, M. Stankaityte¹³⁵, B. Stapf¹²⁰,
 E.A. Starchenko¹²³, G.H. Stark¹⁴⁶, J. Stark⁵⁸, S.H. Stark⁴⁰, P. Staroba¹⁴¹, P. Starovoitov^{61a},
 S. Stärz¹⁰⁴, R. Staszewski⁸⁵, G. Stavropoulos⁴⁴, M. Stegler⁴⁶, P. Steinberg²⁹, A.L. Steinhebel¹³²,
 B. Stelzer¹⁵², H.J. Stelzer¹³⁹, O. Stelzer-Chilton^{168a}, H. Stenzel⁵⁶, T.J. Stevenson¹⁵⁶,
 G.A. Stewart³⁶, M.C. Stockton³⁶, G. Stoicea^{27b}, M. Stolarski^{140a}, S. Stonjek¹¹⁵, A. Straessner⁴⁸,
 J. Strandberg¹⁵⁴, S. Strandberg^{45a,45b}, M. Strauss¹²⁹, P. Strizeneč^{28b}, R. Ströhmer¹⁷⁷,
 D.M. Strom¹³², R. Stroynowski⁴², A. Strubig⁵⁰, S.A. Stucci²⁹, B. Stugu¹⁷, J. Stupak¹²⁹,
 N.A. Styles⁴⁶, D. Su¹⁵³, S. Suchek^{61a}, V.V. Sulin¹¹¹, M.J. Sullivan⁹¹, D.M.S. Sultan⁵⁴,
 S. Sultansoy^{4c}, T. Sumida⁸⁶, S. Sun¹⁰⁶, X. Sun³, K. Suruliz¹⁵⁶, C.J.E. Suster¹⁵⁷, M.R. Sutton¹⁵⁶,
 S. Suzuki⁸², M. Svatos¹⁴¹, M. Swiatlowski³⁷, S.P. Swift², T. Swirski¹⁷⁷, A. Sydorenko¹⁰⁰,
 I. Sykora^{28a}, M. Sykora¹⁴³, T. Sykora¹⁴³, D. Ta¹⁰⁰, K. Tackmann^{46,ab}, J. Taenzer¹⁶¹,
 A. Taffard¹⁷¹, R. Tafirout^{168a}, H. Takai²⁹, R. Takashima⁸⁷, K. Takeda⁸³, T. Takeshita¹⁵⁰,
 E.P. Takeva⁵⁰, Y. Takubo⁸², M. Talby¹⁰², A.A. Talyshv^{122b,122a}, N.M. Tamir¹⁶¹, J. Tanaka¹⁶³,
 M. Tanaka¹⁶⁵, R. Tanaka⁶⁵, S. Tapia Araya¹⁷³, S. Tapprogge¹⁰⁰,
 A. Tarek Abouelfadl Mohamed¹³⁶, S. Tarem¹⁶⁰, K. Tariq^{60b}, G. Tarna^{27b,c}, G.F. Tartarelli^{69a},
 P. Tas¹⁴³, M. Tasevsky¹⁴¹, T. Tashiro⁸⁶, E. Tassi^{41b,41a}, A. Tavares Delgado^{140a,140b},
 Y. Tayalati^{35e}, A.J. Taylor⁵⁰, G.N. Taylor¹⁰⁵, W. Taylor^{168b}, A.S. Tee⁹⁰, R. Teixeira De Lima¹⁵³,
 P. Teixeira-Dias⁹⁴, H. Ten Kate³⁶, J.J. Teoh¹²⁰, S. Terada⁸², K. Terashi¹⁶³, J. Terron⁹⁹,
 S. Terzo¹⁴, M. Testa⁵¹, R.J. Teuscher^{167,af}, S.J. Thais¹⁸³, T. Theveneaux-Pelzer⁴⁶, F. Thiele⁴⁰,
 D.W. Thomas⁹⁴, J.O. Thomas⁴², J.P. Thomas²¹, A.S. Thompson⁵⁷, P.D. Thompson²¹,
 L.A. Thomsen¹⁸³, E. Thomson¹³⁷, E.J. Thorpe⁹³, Y. Tian³⁹, R.E. Ticse Torres⁵³,
 V.O. Tikhomirov^{111,aq}, Yu.A. Tikhonov^{122b,122a}, S. Timoshenko¹¹², P. Tipton¹⁸³, S. Tisserant¹⁰²,
 K. Todome^{23b,23a}, S. Todorova-Nova⁵, S. Todt⁴⁸, J. Tojo⁸⁸, S. Tokár^{28a}, K. Tokushuku⁸²,
 E. Tolley¹²⁷, K.G. Tomiwa^{33e}, M. Tomoto¹¹⁷, L. Tompkins^{153,q}, B. Tong⁵⁹, P. Tornambe¹⁰³,
 E. Torrence¹³², H. Torres⁴⁸, E. Torró Pastor¹⁴⁸, C. Tosciri¹³⁵, J. Toth^{102,ae}, D.R. Tovey¹⁴⁹,
 A. Traeet¹⁷, C.J. Treado¹²⁵, T. Trefzger¹⁷⁷, F. Tresoldi¹⁵⁶, A. Tricoli²⁹, I.M. Trigger^{168a},
 S. Trincaz-Duvoid¹³⁶, W. Trischuk¹⁶⁷, B. Trocmé⁵⁸, A. Trofymov¹⁴⁵, C. Troncon^{69a},
 M. Trovatelli¹⁷⁶, F. Trovato¹⁵⁶, L. Truong^{33c}, M. Trzebinski⁸⁵, A. Trzupek⁸⁵, F. Tsai⁴⁶,
 J.C-L. Tseng¹³⁵, P.V. Tsiarshka^{108,al}, A. Tsirigotis¹⁶², N. Tsirintanis⁹, V. Tsiskaridze¹⁵⁵,
 E.G. Tskhadadze^{159a}, M. Tsopoulou¹⁶², I.I. Tsukerman¹²⁴, V. Tsulaia¹⁸, S. Tsuno⁸²,
 D. Tsybychev¹⁵⁵, Y. Tu^{63b}, A. Tudorache^{27b}, V. Tudorache^{27b}, T.T. Tulbure^{27a}, A.N. Tuna⁵⁹,
 S. Turchikhin⁸⁰, D. Turgeman¹⁸⁰, I. Turk Cakir^{4b,w}, R.J. Turner²¹, R.T. Turra^{69a}, P.M. Tuts³⁹,
 S. Tzamarias¹⁶², E. Tzovara¹⁰⁰, G. Uccielli⁴⁷, K. Uchida¹⁶³, I. Ueda⁸², M. Ughetto^{45a,45b},
 F. Ukegawa¹⁶⁹, G. Unal³⁶, A. Undrus²⁹, G. Unel¹⁷¹, F.C. Ungaro¹⁰⁵, Y. Unno⁸², K. Uno¹⁶³,
 J. Urban^{28b}, P. Urquijo¹⁰⁵, G. Usai⁸, Z. Uysal^{12d}, L. Vacavant¹⁰², V. Vacek¹⁴², B. Vachon¹⁰⁴,
 K.O.H. Vadla¹³⁴, A. Vaidya⁹⁵, C. Valderanis¹¹⁴, E. Valdes Santurio^{45a,45b}, M. Valente⁵⁴,
 S. Valentineti^{23b,23a}, A. Valero¹⁷⁴, L. Valéry⁴⁶, R.A. Vallance²¹, A. Vallier³⁶, J.A. Valls Ferrer¹⁷⁴,
 T.R. Van Daalen¹⁴, P. Van Gemmeren⁶, I. Van Vulpen¹²⁰, M. Vanadia^{74a,74b}, W. Vandelli³⁶,
 A. Vaniachine¹⁶⁶, D. Vannicola^{73a,73b}, R. Vari^{73a}, E.W. Varnes⁷, C. Varni^{55b,55a}, T. Varol¹⁵⁸,
 D. Varouchas⁶⁵, K.E. Varvell¹⁵⁷, M.E. Vasile^{27b}, G.A. Vasquez¹⁷⁶, J.G. Vasquez¹⁸³, F. Vazeille³⁸,
 D. Vazquez Furelos¹⁴, T. Vazquez Schroeder³⁶, J. Veatch⁵³, V. Vecchio^{75a,75b}, M.J. Veen¹²⁰,
 L.M. Veloce¹⁶⁷, F. Veloso^{140a,140c}, S. Veneziano^{73a}, A. Ventura^{68a,68b}, N. Venturi³⁶,
 A. Verbytskyi¹¹⁵, V. Vercesi^{71a}, M. Verducci^{72a,72b}, C.M. Vergel Infante⁷⁹, C. Vergis²⁴,
 W. Verkerke¹²⁰, A.T. Vermeulen¹²⁰, J.C. Vermeulen¹²⁰, M.C. Vetterli^{152,ax}, N. Viaux Maira^{147d},
 M. Vicente Barreto Pinto⁵⁴, T. Vickey¹⁴⁹, O.E. Vickey Boeriu¹⁴⁹, G.H.A. Viehhauser¹³⁵,
 L. Vigani^{61b}, M. Villa^{23b,23a}, M. Villaplana Perez^{69a,69b}, E. Vilucchi⁵¹, M.G. Vinciter³⁴,
 G.S. Virdee²¹, A. Vishwakarma⁴⁶, C. Vittori^{23b,23a}, I. Vivarelli¹⁵⁶, M. Vogel¹⁸², P. Vokac¹⁴²,
 S.E. von Buddenbrock^{33e}, E. Von Toerne²⁴, V. Vorobel¹⁴³, K. Vorobev¹¹², M. Vos¹⁷⁴,

J.H. Vossebeld⁹¹, M. Vozak¹⁰¹, N. Vranjes¹⁶, M. Vranjes Milosavljevic¹⁶, V. Vrba¹⁴²,
M. Vreeswijk¹²⁰, R. Vuillermet³⁶, I. Vukotic³⁷, P. Wagner²⁴, W. Wagner¹⁸², J. Wagner-Kuhr¹¹⁴,
S. Wahdan¹⁸², H. Wahlberg⁸⁹, V.M. Walbrecht¹¹⁵, J. Walder⁹⁰, R. Walker¹¹⁴, S.D. Walker⁹⁴,
W. Walkowiak¹⁵¹, V. Wallangen^{45a,45b}, A.M. Wang⁵⁹, C. Wang^{60c}, C. Wang^{60b}, F. Wang¹⁸¹,
H. Wang¹⁸, H. Wang³, J. Wang¹⁵⁷, J. Wang^{61b}, P. Wang⁴², Q. Wang¹²⁹, R.-J. Wang¹⁰⁰,
R. Wang^{60a}, R. Wang⁶, S.M. Wang¹⁵⁸, W.T. Wang^{60a}, W. Wang^{15c,ag}, W.X. Wang^{60a,ag},
Y. Wang^{60a,an}, Z. Wang^{60c}, C. Wanotayaroj⁴⁶, A. Warburton¹⁰⁴, C.P. Ward³², D.R. Wardrope⁹⁵,
N. Warrack⁵⁷, A. Washbrook⁵⁰, A.T. Watson²¹, M.F. Watson²¹, G. Watts¹⁴⁸, B.M. Waugh⁹⁵,
A.F. Webb¹¹, S. Webb¹⁰⁰, C. Weber¹⁸³, M.S. Weber²⁰, S.A. Weber³⁴, S.M. Weber^{61a},
A.R. Weidberg¹³⁵, J. Weingarten⁴⁷, M. Weirich¹⁰⁰, C. Weiser⁵², P.S. Wells³⁶, T. Wenaus²⁹,
T. Wengler³⁶, S. Wenig³⁶, N. Vermes²⁴, M.D. Werner⁷⁹, M. Wessels^{61a}, T.D. Weston²⁰,
K. Whalen¹³², N.L. Whallon¹⁴⁸, A.M. Wharton⁹⁰, A.S. White¹⁰⁶, A. White⁸, M.J. White¹,
D. Whiteson¹⁷¹, B.W. Whitmore⁹⁰, W. Wiedenmann¹⁸¹, M. Wielers¹⁴⁴, N. Wieseotte¹⁰⁰,
C. Wiglesworth⁴⁰, L.A.M. Wiik-Fuchs⁵², F. Wilk¹⁰¹, H.G. Wilkens³⁶, L.J. Wilkins⁹⁴,
H.H. Williams¹³⁷, S. Williams³², C. Willis¹⁰⁷, S. Willocq¹⁰³, J.A. Wilson²¹, I. Wingerter-Seez⁵,
E. Winkels¹⁵⁶, F. Winklmeier¹³², O.J. Winston¹⁵⁶, B.T. Winter⁵², M. Wittgen¹⁵³, M. Wobisch⁹⁶,
A. Wolf¹⁰⁰, T.M.H. Wolf¹²⁰, R. Wolff¹⁰², R. Wölker¹³⁵, J. Wollrath⁵², M.W. Wolter⁸⁵,
H. Wolters^{140a,140c}, V.W.S. Wong¹⁷⁵, N.L. Woods¹⁴⁶, S.D. Worm²¹, B.K. Wosiek⁸⁵,
K.W. Woźniak⁸⁵, K. Wraight⁵⁷, S.L. Wu¹⁸¹, X. Wu⁵⁴, Y. Wu^{60a}, T.R. Wyatt¹⁰¹, B.M. Wynne⁵⁰,
S. Xella⁴⁰, Z. Xi¹⁰⁶, L. Xia¹⁷⁸, X. Xiao¹⁰⁶, I. Xiotidis¹⁵⁶, D. Xu^{15a}, H. Xu^{60a,c}, L. Xu²⁹, T. Xu¹⁴⁵,
W. Xu¹⁰⁶, Z. Xu^{60b}, Z. Xu¹⁵³, B. Yabsley¹⁵⁷, S. Yacoob^{33a}, K. Yajima¹³³, D.P. Yallup⁹⁵,
D. Yamaguchi¹⁶⁵, Y. Yamaguchi¹⁶⁵, A. Yamamoto⁸², M. Yamatani¹⁶³, T. Yamazaki¹⁶³,
Y. Yamazaki⁸³, Z. Yan²⁵, H.J. Yang^{60c,60d}, H.T. Yang¹⁸, S. Yang⁷⁸, X. Yang^{60b,58}, Y. Yang¹⁶³,
W.-M. Yao¹⁸, Y.C. Yap⁴⁶, Y. Yasu⁸², E. Yatsenko^{60c,60d}, J. Ye⁴², S. Ye²⁹, I. Yeletsikh⁸⁰,
M.R. Yexley⁹⁰, E. Yigitbasi²⁵, K. Yorita¹⁷⁹, K. Yoshihara¹³⁷, C.J.S. Young³⁶, C. Young¹⁵³,
J. Yu⁷⁹, R. Yuan^{60b,i}, X. Yue^{61a}, S.P.Y. Yuen²⁴, M. Zaazoua^{35e}, B. Zabinski⁸⁵, G. Zacharis¹⁰,
E. Zaffaroni⁵⁴, J. Zahreddine¹³⁶, A.M. Zaitsev^{123,ap}, T. Zakareishvili^{159b}, N. Zakharchuk³⁴,
S. Zambito⁵⁹, D. Zanzi³⁶, D.R. Zaripovas⁵⁷, S.V. Zeißner⁴⁷, C. Zeitnitz¹⁸², G. Zemaityte¹³⁵,
J.C. Zeng¹⁷³, O. Zenin¹²³, T. Ženiš^{28a}, D. Zerwas⁶⁵, M. Zgubič¹³⁵, D.F. Zhang^{15b}, G. Zhang^{15b},
H. Zhang^{15c}, J. Zhang⁶, L. Zhang^{15c}, L. Zhang^{60a}, M. Zhang¹⁷³, R. Zhang²⁴, X. Zhang^{60b},
Y. Zhang^{15a,15d}, Z. Zhang^{63a}, Z. Zhang⁶⁵, P. Zhao⁴⁹, Y. Zhao^{60b}, Z. Zhao^{60a}, A. Zhemchugov⁸⁰,
Z. Zheng¹⁰⁶, D. Zhong¹⁷³, B. Zhou¹⁰⁶, C. Zhou¹⁸¹, M.S. Zhou^{15a,15d}, M. Zhou¹⁵⁵, N. Zhou^{60c},
Y. Zhou⁷, C.G. Zhu^{60b}, H.L. Zhu^{60a}, H. Zhu^{15a}, J. Zhu¹⁰⁶, Y. Zhu^{60a}, X. Zhuang^{15a},
K. Zhukov¹¹¹, V. Zhulanov^{122b,122a}, D. Zieminska⁶⁶, N.I. Zimine⁸⁰, S. Zimmermann⁵²,
Z. Zinonos¹¹⁵, M. Ziolkowski¹⁵¹, L. Živković¹⁶, G. Zobernig¹⁸¹, A. Zoccoli^{23b,23a}, K. Zoch⁵³,
T.G. Zorbas¹⁴⁹, R. Zou³⁷, L. Zwalinski³⁶

¹ Department of Physics, University of Adelaide, Adelaide; Australia

² Physics Department, SUNY Albany, Albany NY; U.S.A.

³ Department of Physics, University of Alberta, Edmonton AB; Canada

⁴ Department of Physics^(a), Ankara University, Ankara; Istanbul Aydin University^(b), Istanbul;
Division of Physics^(c), TOBB University of Economics and Technology, Ankara; Turkey

⁵ LAPP, Université Grenoble Alpes, Université Savoie Mont Blanc, CNRS/IN2P3, Annecy; France

⁶ High Energy Physics Division, Argonne National Laboratory, Argonne IL; U.S.A.

⁷ Department of Physics, University of Arizona, Tucson AZ; U.S.A.

⁸ Department of Physics, University of Texas at Arlington, Arlington TX; U.S.A.

⁹ Physics Department, National and Kapodistrian University of Athens, Athens; Greece

¹⁰ Physics Department, National Technical University of Athens, Zografou; Greece

¹¹ Department of Physics, University of Texas at Austin, Austin TX; U.S.A.

¹² Bahcesehir University^(a), Faculty of Engineering and Natural Sciences, Istanbul; Istanbul Bilgi

- University^(b), Faculty of Engineering and Natural Sciences, Istanbul; Department of Physics^(c), Bogazici University, Istanbul; Department of Physics Engineering^(d), Gaziantep University, Gaziantep; Turkey
- ¹³ Institute of Physics, Azerbaijan Academy of Sciences, Baku; Azerbaijan
- ¹⁴ Institut de Física d'Altes Energies (IFAE), Barcelona Institute of Science and Technology, Barcelona; Spain
- ¹⁵ Institute of High Energy Physics^(a), Chinese Academy of Sciences, Beijing; Physics Department^(b), Tsinghua University, Beijing; Department of Physics^(c), Nanjing University, Nanjing; University of Chinese Academy of Science (UCAS)^(d), Beijing; China
- ¹⁶ Institute of Physics, University of Belgrade, Belgrade; Serbia
- ¹⁷ Department for Physics and Technology, University of Bergen, Bergen; Norway
- ¹⁸ Physics Division, Lawrence Berkeley National Laboratory and University of California, Berkeley CA; U.S.A.
- ¹⁹ Institut für Physik, Humboldt Universität zu Berlin, Berlin; Germany
- ²⁰ Albert Einstein Center for Fundamental Physics and Laboratory for High Energy Physics, University of Bern, Bern; Switzerland
- ²¹ School of Physics and Astronomy, University of Birmingham, Birmingham; United Kingdom
- ²² Facultad de Ciencias y Centro de Investigaciones^(a), Universidad Antonio Nariño, Bogotá; Departamento de Física^(b), Universidad Nacional de Colombia, Bogotá, Colombia; Colombia
- ²³ INFN Bologna and Università' di Bologna^(a), Dipartimento di Fisica; INFN Sezione di Bologna^(b); Italy
- ²⁴ Physikalisches Institut, Universität Bonn, Bonn; Germany
- ²⁵ Department of Physics, Boston University, Boston MA; U.S.A.
- ²⁶ Department of Physics, Brandeis University, Waltham MA; U.S.A.
- ²⁷ Transilvania University of Brasov^(a), Brasov; Horia Hulubei National Institute of Physics and Nuclear Engineering^(b), Bucharest; Department of Physics^(c), Alexandru Ioan Cuza University of Iasi, Iasi; National Institute for Research and Development of Isotopic and Molecular Technologies^(d), Physics Department, Cluj-Napoca; University Politehnica Bucharest^(e), Bucharest; West University in Timisoara^(f), Timisoara; Romania
- ²⁸ Faculty of Mathematics^(a), Physics and Informatics, Comenius University, Bratislava; Department of Subnuclear Physics^(b), Institute of Experimental Physics of the Slovak Academy of Sciences, Kosice; Slovak Republic
- ²⁹ Physics Department, Brookhaven National Laboratory, Upton NY; U.S.A.
- ³⁰ Departamento de Física, Universidad de Buenos Aires, Buenos Aires; Argentina
- ³¹ California State University, CA; U.S.A.
- ³² Cavendish Laboratory, University of Cambridge, Cambridge; United Kingdom
- ³³ Department of Physics^(a), University of Cape Town, Cape Town;^(b) iThemba Labs, Western Cape; Department of Mechanical Engineering Science^(c), University of Johannesburg, Johannesburg; University of South Africa^(d), Department of Physics, Pretoria; School of Physics^(e), University of the Witwatersrand, Johannesburg; South Africa
- ³⁴ Department of Physics, Carleton University, Ottawa ON; Canada
- ³⁵ Faculté des Sciences Ain Chock^(a), Réseau Universitaire de Physique des Hautes Energies — Université Hassan II, Casablanca; Faculté des Sciences^(b), Université Ibn-Tofail, Kénitra; Faculté des Sciences Semlalia^(c), Université Cadi Ayyad, LPHEA-Marrakech; Faculté des Sciences^(d), Université Mohamed Premier and LPTPM, Oujda; Faculté des sciences^(e), Université Mohammed V, Rabat; Morocco
- ³⁶ CERN, Geneva; Switzerland
- ³⁷ Enrico Fermi Institute, University of Chicago, Chicago IL; U.S.A.
- ³⁸ LPC, Université Clermont Auvergne, CNRS/IN2P3, Clermont-Ferrand; France
- ³⁹ Nevis Laboratory, Columbia University, Irvington NY; U.S.A.
- ⁴⁰ Niels Bohr Institute, University of Copenhagen, Copenhagen; Denmark
- ⁴¹ Dipartimento di Fisica^(a), Università della Calabria, Rende; INFN Gruppo Collegato di Cosenza^(b),

- Laboratori Nazionali di Frascati; Italy
- 42 Physics Department, Southern Methodist University, Dallas TX; U.S.A.
- 43 Physics Department, University of Texas at Dallas, Richardson TX; U.S.A.
- 44 National Centre for Scientific Research “Demokritos”, Agia Paraskevi; Greece
- 45 Department of Physics^(a), Stockholm University; Oskar Klein Centre^(b), Stockholm; Sweden
- 46 Deutsches Elektronen-Synchrotron DESY, Hamburg and Zeuthen; Germany
- 47 Lehrstuhl für Experimentelle Physik IV, Technische Universität Dortmund, Dortmund; Germany
- 48 Institut für Kern- und Teilchenphysik, Technische Universität Dresden, Dresden; Germany
- 49 Department of Physics, Duke University, Durham NC; U.S.A.
- 50 SUPA — School of Physics and Astronomy, University of Edinburgh, Edinburgh; United Kingdom
- 51 INFN e Laboratori Nazionali di Frascati, Frascati; Italy
- 52 Physikalisches Institut, Albert-Ludwigs-Universität Freiburg, Freiburg; Germany
- 53 II. Physikalisches Institut, Georg-August-Universität Göttingen, Göttingen; Germany
- 54 Département de Physique Nucléaire et Corpusculaire, Université de Genève, Genève; Switzerland
- 55 Dipartimento di Fisica^(a), Università di Genova, Genova; INFN Sezione di Genova^(b); Italy
- 56 II. Physikalisches Institut, Justus-Liebig-Universität Giessen, Giessen; Germany
- 57 SUPA — School of Physics and Astronomy, University of Glasgow, Glasgow; United Kingdom
- 58 LPSC, Université Grenoble Alpes, CNRS/IN2P3, Grenoble INP, Grenoble; France
- 59 Laboratory for Particle Physics and Cosmology, Harvard University, Cambridge MA; U.S.A.
- 60 Department of Modern Physics and State Key Laboratory of Particle Detection and Electronics^(a), University of Science and Technology of China, Hefei; Institute of Frontier and Interdisciplinary Science and Key Laboratory of Particle Physics and Particle Irradiation (MOE)^(b), Shandong University, Qingdao; School of Physics and Astronomy^(c), Shanghai Jiao Tong University, KLPPAC-MoE, SKLPPC, Shanghai; Tsung-Dao Lee Institute^(d), Shanghai; China
- 61 Kirchhoff-Institut für Physik^(a), Ruprecht-Karls-Universität Heidelberg, Heidelberg; Physikalisches Institut^(b), Ruprecht-Karls-Universität Heidelberg, Heidelberg; Germany
- 62 Faculty of Applied Information Science, Hiroshima Institute of Technology, Hiroshima; Japan
- 63 Department of Physics^(a), Chinese University of Hong Kong, Shatin, N.T., Hong Kong; Department of Physics^(b), University of Hong Kong, Hong Kong; Department of Physics and Institute for Advanced Study^(c), Hong Kong University of Science and Technology, Clear Water Bay, Kowloon, Hong Kong; China
- 64 Department of Physics, National Tsing Hua University, Hsinchu; Taiwan
- 65 IJCLab, Université Paris-Saclay, CNRS/IN2P3, 91105, Orsay; France
- 66 Department of Physics, Indiana University, Bloomington IN; U.S.A.
- 67 INFN Gruppo Collegato di Udine^(a), Sezione di Trieste, Udine; ICTP^(b), Trieste; Dipartimento Politecnico di Ingegneria e Architettura^(c), Università di Udine, Udine; Italy
- 68 INFN Sezione di Lecce^(a); Dipartimento di Matematica e Fisica^(b), Università del Salento, Lecce; Italy
- 69 INFN Sezione di Milano^(a); Dipartimento di Fisica^(b), Università di Milano, Milano; Italy
- 70 INFN Sezione di Napoli^(a); Dipartimento di Fisica^(b), Università di Napoli, Napoli; Italy
- 71 INFN Sezione di Pavia^(a); Dipartimento di Fisica^(b), Università di Pavia, Pavia; Italy
- 72 INFN Sezione di Pisa^(a); Dipartimento di Fisica E. Fermi^(b), Università di Pisa, Pisa; Italy
- 73 INFN Sezione di Roma^(a); Dipartimento di Fisica^(b), Sapienza Università di Roma, Roma; Italy
- 74 INFN Sezione di Roma Tor Vergata^(a); Dipartimento di Fisica^(b), Università di Roma Tor Vergata, Roma; Italy
- 75 INFN Sezione di Roma Tre^(a); Dipartimento di Matematica e Fisica^(b), Università Roma Tre, Roma; Italy
- 76 INFN-TIFPA^(a); Università degli Studi di Trento^(b), Trento; Italy
- 77 Institut für Astro- und Teilchenphysik, Leopold-Franzens-Universität, Innsbruck; Austria
- 78 University of Iowa, Iowa City IA; U.S.A.
- 79 Department of Physics and Astronomy, Iowa State University, Ames IA; U.S.A.
- 80 Joint Institute for Nuclear Research, Dubna; Russia

- 81 *Departamento de Engenharia Elétrica^(a), Universidade Federal de Juiz de Fora (UFJF), Juiz de Fora; Universidade Federal do Rio De Janeiro COPPE/EE/IF^(b), Rio de Janeiro; Universidade Federal de São João del Rei (UFSJ)^(c), São João del Rei; Instituto de Física^(d), Universidade de São Paulo, São Paulo; Brazil*
- 82 *KEK, High Energy Accelerator Research Organization, Tsukuba; Japan*
- 83 *Graduate School of Science, Kobe University, Kobe; Japan*
- 84 *AGH University of Science and Technology^(a), Faculty of Physics and Applied Computer Science, Krakow; Marian Smoluchowski Institute of Physics^(b), Jagiellonian University, Krakow; Poland*
- 85 *Institute of Nuclear Physics Polish Academy of Sciences, Krakow; Poland*
- 86 *Faculty of Science, Kyoto University, Kyoto; Japan*
- 87 *Kyoto University of Education, Kyoto; Japan*
- 88 *Research Center for Advanced Particle Physics and Department of Physics, Kyushu University, Fukuoka ; Japan*
- 89 *Instituto de Física La Plata, Universidad Nacional de La Plata and CONICET, La Plata; Argentina*
- 90 *Physics Department, Lancaster University, Lancaster; United Kingdom*
- 91 *Oliver Lodge Laboratory, University of Liverpool, Liverpool; United Kingdom*
- 92 *Department of Experimental Particle Physics, Jožef Stefan Institute and Department of Physics, University of Ljubljana, Ljubljana; Slovenia*
- 93 *School of Physics and Astronomy, Queen Mary University of London, London; United Kingdom*
- 94 *Department of Physics, Royal Holloway University of London, Egham; United Kingdom*
- 95 *Department of Physics and Astronomy, University College London, London; United Kingdom*
- 96 *Louisiana Tech University, Ruston LA; U.S.A.*
- 97 *Fysiska institutionen, Lunds universitet, Lund; Sweden*
- 98 *Centre de Calcul de l'Institut National de Physique Nucléaire et de Physique des Particules (IN2P3), Villeurbanne; France*
- 99 *Departamento de Física Teórica C-15 and CIAFF, Universidad Autónoma de Madrid, Madrid; Spain*
- 100 *Institut für Physik, Universität Mainz, Mainz; Germany*
- 101 *School of Physics and Astronomy, University of Manchester, Manchester; United Kingdom*
- 102 *CPPM, Aix-Marseille Université, CNRS/IN2P3, Marseille; France*
- 103 *Department of Physics, University of Massachusetts, Amherst MA; U.S.A.*
- 104 *Department of Physics, McGill University, Montreal QC; Canada*
- 105 *School of Physics, University of Melbourne, Victoria; Australia*
- 106 *Department of Physics, University of Michigan, Ann Arbor MI; U.S.A.*
- 107 *Department of Physics and Astronomy, Michigan State University, East Lansing MI; U.S.A.*
- 108 *B.I. Stepanov Institute of Physics, National Academy of Sciences of Belarus, Minsk; Belarus*
- 109 *Research Institute for Nuclear Problems of Byelorussian State University, Minsk; Belarus*
- 110 *Group of Particle Physics, University of Montreal, Montreal QC; Canada*
- 111 *P.N. Lebedev Physical Institute of the Russian Academy of Sciences, Moscow; Russia*
- 112 *National Research Nuclear University MEPhI, Moscow; Russia*
- 113 *D.V. Skobeltsyn Institute of Nuclear Physics, M.V. Lomonosov Moscow State University, Moscow; Russia*
- 114 *Fakultät für Physik, Ludwig-Maximilians-Universität München, München; Germany*
- 115 *Max-Planck-Institut für Physik (Werner-Heisenberg-Institut), München; Germany*
- 116 *Nagasaki Institute of Applied Science, Nagasaki; Japan*
- 117 *Graduate School of Science and Kobayashi-Maskawa Institute, Nagoya University, Nagoya; Japan*
- 118 *Department of Physics and Astronomy, University of New Mexico, Albuquerque NM; U.S.A.*
- 119 *Institute for Mathematics, Astrophysics and Particle Physics, Radboud University Nijmegen/Nikhef, Nijmegen; Netherlands*
- 120 *Nikhef National Institute for Subatomic Physics and University of Amsterdam, Amsterdam; Netherlands*
- 121 *Department of Physics, Northern Illinois University, DeKalb IL; U.S.A.*

- ¹²² *Budker Institute of Nuclear Physics and NSU^(a), SB RAS, Novosibirsk; Novosibirsk State University Novosibirsk^(b); Russia*
- ¹²³ *Institute for High Energy Physics of the National Research Centre Kurchatov Institute, Protvino; Russia*
- ¹²⁴ *Institute for Theoretical and Experimental Physics named by A.I. Alikhanov of National Research Centre “Kurchatov Institute”, Moscow; Russia*
- ¹²⁵ *Department of Physics, New York University, New York NY; U.S.A.*
- ¹²⁶ *Ochanomizu University, Otsuka, Bunkyo-ku, Tokyo; Japan*
- ¹²⁷ *Ohio State University, Columbus OH; U.S.A.*
- ¹²⁸ *Faculty of Science, Okayama University, Okayama; Japan*
- ¹²⁹ *Homer L. Dodge Department of Physics and Astronomy, University of Oklahoma, Norman OK; U.S.A.*
- ¹³⁰ *Department of Physics, Oklahoma State University, Stillwater OK; U.S.A.*
- ¹³¹ *Palacký University, RCPTM, Joint Laboratory of Optics, Olomouc; Czech Republic*
- ¹³² *Institute for Fundamental Science, University of Oregon, Eugene, OR; U.S.A.*
- ¹³³ *Graduate School of Science, Osaka University, Osaka; Japan*
- ¹³⁴ *Department of Physics, University of Oslo, Oslo; Norway*
- ¹³⁵ *Department of Physics, Oxford University, Oxford; United Kingdom*
- ¹³⁶ *LPNHE, Sorbonne Université, Université de Paris, CNRS/IN2P3, Paris; France*
- ¹³⁷ *Department of Physics, University of Pennsylvania, Philadelphia PA; U.S.A.*
- ¹³⁸ *Konstantinov Nuclear Physics Institute of National Research Centre “Kurchatov Institute”, PNPI, St. Petersburg; Russia*
- ¹³⁹ *Department of Physics and Astronomy, University of Pittsburgh, Pittsburgh PA; U.S.A.*
- ¹⁴⁰ *Laboratório de Instrumentação e Física Experimental de Partículas — LIP^(a), Lisboa; Departamento de Física^(b), Faculdade de Ciências, Universidade de Lisboa, Lisboa; Departamento de Física^(c), Universidade de Coimbra, Coimbra; Centro de Física Nuclear da Universidade de Lisboa^(d), Lisboa; Departamento de Física^(e), Universidade do Minho, Braga; Departamento de Física Teórica y del Cosmos^(f), Universidad de Granada, Granada (Spain); Dep Física and CEFITEC of Faculdade de Ciências e Tecnologia^(g), Universidade Nova de Lisboa, Caparica; Instituto Superior Técnico^(h), Universidade de Lisboa, Lisboa; Portugal*
- ¹⁴¹ *Institute of Physics of the Czech Academy of Sciences, Prague; Czech Republic*
- ¹⁴² *Czech Technical University in Prague, Prague; Czech Republic*
- ¹⁴³ *Charles University, Faculty of Mathematics and Physics, Prague; Czech Republic*
- ¹⁴⁴ *Particle Physics Department, Rutherford Appleton Laboratory, Didcot; United Kingdom*
- ¹⁴⁵ *IRFU, CEA, Université Paris-Saclay, Gif-sur-Yvette; France*
- ¹⁴⁶ *Santa Cruz Institute for Particle Physics, University of California Santa Cruz, Santa Cruz CA; U.S.A.*
- ¹⁴⁷ *Departamento de Física^(a), Pontificia Universidad Católica de Chile, Santiago; Universidad Andres Bello^(b), Department of Physics, Santiago; Instituto de Alta Investigación^(c), Universidad de Tarapacá; Departamento de Física^(d), Universidad Técnica Federico Santa María, Valparaíso; Chile*
- ¹⁴⁸ *Department of Physics, University of Washington, Seattle WA; U.S.A.*
- ¹⁴⁹ *Department of Physics and Astronomy, University of Sheffield, Sheffield; United Kingdom*
- ¹⁵⁰ *Department of Physics, Shinshu University, Nagano; Japan*
- ¹⁵¹ *Department Physik, Universität Siegen, Siegen; Germany*
- ¹⁵² *Department of Physics, Simon Fraser University, Burnaby BC; Canada*
- ¹⁵³ *SLAC National Accelerator Laboratory, Stanford CA; U.S.A.*
- ¹⁵⁴ *Physics Department, Royal Institute of Technology, Stockholm; Sweden*
- ¹⁵⁵ *Departments of Physics and Astronomy, Stony Brook University, Stony Brook NY; U.S.A.*
- ¹⁵⁶ *Department of Physics and Astronomy, University of Sussex, Brighton; United Kingdom*
- ¹⁵⁷ *School of Physics, University of Sydney, Sydney; Australia*
- ¹⁵⁸ *Institute of Physics, Academia Sinica, Taipei; Taiwan*
- ¹⁵⁹ *E. Andronikashvili Institute of Physics^(a), Iv. Javakishvili Tbilisi State University, Tbilisi; High*

- Energy Physics Institute^(b), Tbilisi State University, Tbilisi; Georgia
- ¹⁶⁰ Department of Physics, Technion, Israel Institute of Technology, Haifa; Israel
- ¹⁶¹ Raymond and Beverly Sackler School of Physics and Astronomy, Tel Aviv University, Tel Aviv; Israel
- ¹⁶² Department of Physics, Aristotle University of Thessaloniki, Thessaloniki; Greece
- ¹⁶³ International Center for Elementary Particle Physics and Department of Physics, University of Tokyo, Tokyo; Japan
- ¹⁶⁴ Graduate School of Science and Technology, Tokyo Metropolitan University, Tokyo; Japan
- ¹⁶⁵ Department of Physics, Tokyo Institute of Technology, Tokyo; Japan
- ¹⁶⁶ Tomsk State University, Tomsk; Russia
- ¹⁶⁷ Department of Physics, University of Toronto, Toronto ON; Canada
- ¹⁶⁸ TRIUMF^(a), Vancouver BC; Department of Physics and Astronomy^(b), York University, Toronto ON; Canada
- ¹⁶⁹ Division of Physics and Tomonaga Center for the History of the Universe, Faculty of Pure and Applied Sciences, University of Tsukuba, Tsukuba; Japan
- ¹⁷⁰ Department of Physics and Astronomy, Tufts University, Medford MA; U.S.A.
- ¹⁷¹ Department of Physics and Astronomy, University of California Irvine, Irvine CA; U.S.A.
- ¹⁷² Department of Physics and Astronomy, University of Uppsala, Uppsala; Sweden
- ¹⁷³ Department of Physics, University of Illinois, Urbana IL; U.S.A.
- ¹⁷⁴ Instituto de Física Corpuscular (IFIC), Centro Mixto Universidad de Valencia — CSIC, Valencia; Spain
- ¹⁷⁵ Department of Physics, University of British Columbia, Vancouver BC; Canada
- ¹⁷⁶ Department of Physics and Astronomy, University of Victoria, Victoria BC; Canada
- ¹⁷⁷ Fakultät für Physik und Astronomie, Julius-Maximilians-Universität Würzburg, Würzburg; Germany
- ¹⁷⁸ Department of Physics, University of Warwick, Coventry; United Kingdom
- ¹⁷⁹ Waseda University, Tokyo; Japan
- ¹⁸⁰ Department of Particle Physics, Weizmann Institute of Science, Rehovot; Israel
- ¹⁸¹ Department of Physics, University of Wisconsin, Madison WI; U.S.A.
- ¹⁸² Fakultät für Mathematik und Naturwissenschaften, Fachgruppe Physik, Bergische Universität Wuppertal, Wuppertal; Germany
- ¹⁸³ Department of Physics, Yale University, New Haven CT; U.S.A.
- ¹⁸⁴ Yerevan Physics Institute, Yerevan; Armenia
- ^a Also at Borough of Manhattan Community College, City University of New York, New York NY; U.S.A.
- ^b Also at CERN, Geneva; Switzerland
- ^c Also at CPPM, Aix-Marseille Université, CNRS/IN2P3, Marseille; France
- ^d Also at Département de Physique Nucléaire et Corpusculaire, Université de Genève, Genève; Switzerland
- ^e Also at Departament de Física de la Universitat Autònoma de Barcelona, Barcelona; Spain
- ^f Also at Departamento de Física, Instituto Superior Técnico, Universidade de Lisboa, Lisboa; Portugal
- ^g Also at Department of Applied Physics and Astronomy, University of Sharjah, Sharjah; United Arab Emirates
- ^h Also at Department of Financial and Management Engineering, University of the Aegean, Chios; Greece
- ⁱ Also at Department of Physics and Astronomy, Michigan State University, East Lansing MI; U.S.A.
- ^j Also at Department of Physics and Astronomy, University of Louisville, Louisville, KY; U.S.A.
- ^k Also at Department of Physics, Ben Gurion University of the Negev, Beer Sheva; Israel
- ^l Also at Department of Physics, California State University, East Bay; U.S.A.

- ^m Also at Department of Physics, California State University, Fresno; U.S.A.
- ⁿ Also at Department of Physics, California State University, Sacramento; U.S.A.
- ^o Also at Department of Physics, King's College London, London; United Kingdom
- ^p Also at Department of Physics, St. Petersburg State Polytechnical University, St. Petersburg; Russia
- ^q Also at Department of Physics, Stanford University, Stanford CA; U.S.A.
- ^r Also at Department of Physics, University of Adelaide, Adelaide; Australia
- ^s Also at Department of Physics, University of Fribourg, Fribourg; Switzerland
- ^t Also at Department of Physics, University of Michigan, Ann Arbor MI; U.S.A.
- ^u Also at Dipartimento di Matematica, Informatica e Fisica, Università di Udine, Udine; Italy
- ^v Also at Faculty of Physics, M.V. Lomonosov Moscow State University, Moscow; Russia
- ^w Also at Giresun University, Faculty of Engineering, Giresun; Turkey
- ^x Also at Graduate School of Science, Osaka University, Osaka; Japan
- ^y Also at Hellenic Open University, Patras; Greece
- ^z Also at IJCLab, Université Paris-Saclay, CNRS/IN2P3, 91405, Orsay; France
- ^{aa} Also at Institutio Catalana de Recerca i Estudis Avancats, ICREA, Barcelona; Spain
- ^{ab} Also at Institut für Experimentalphysik, Universität Hamburg, Hamburg; Germany
- ^{ac} Also at Institute for Mathematics, Astrophysics and Particle Physics, Radboud University Nijmegen/Nikhef, Nijmegen; Netherlands
- ^{ad} Also at Institute for Nuclear Research and Nuclear Energy (INRNE) of the Bulgarian Academy of Sciences, Sofia; Bulgaria
- ^{ae} Also at Institute for Particle and Nuclear Physics, Wigner Research Centre for Physics, Budapest; Hungary
- ^{af} Also at Institute of Particle Physics (IPP), Vancouver; Canada
- ^{ag} Also at Institute of Physics, Academia Sinica, Taipei; Taiwan
- ^{ah} Also at Institute of Physics, Azerbaijan Academy of Sciences, Baku; Azerbaijan
- ^{ai} Also at Institute of Theoretical Physics, Iliia State University, Tbilisi; Georgia
- ^{aj} Also at Instituto de Física Teórica, IFT-UAM/CSIC, Madrid; Spain
- ^{ak} Also at Istanbul University, Dept. of Physics, Istanbul; Turkey
- ^{al} Also at Joint Institute for Nuclear Research, Dubna; Russia
- ^{am} Also at Louisiana Tech University, Ruston LA; U.S.A.
- ^{an} Also at LPNHE, Sorbonne Université, Université de Paris, CNRS/IN2P3, Paris; France
- ^{ao} Also at Manhattan College, New York NY; U.S.A.
- ^{ap} Also at Moscow Institute of Physics and Technology State University, Dolgoprudny; Russia
- ^{aq} Also at National Research Nuclear University MEPhI, Moscow; Russia
- ^{ar} Also at Physics Department, An-Najah National University, Nablus; Palestine
- ^{as} Also at Physics Dept, University of South Africa, Pretoria; South Africa
- ^{at} Also at Physikalisches Institut, Albert-Ludwigs-Universität Freiburg, Freiburg; Germany
- ^{au} Also at School of Physics, Sun Yat-sen University, Guangzhou; China
- ^{av} Also at The City College of New York, New York NY; U.S.A.
- ^{aw} Also at The Collaborative Innovation Center of Quantum Matter (CICQM), Beijing; China
- ^{ax} Also at TRIUMF, Vancouver BC; Canada
- ^{ay} Also at Università di Napoli Parthenope, Napoli; Italy

* Deceased